Investigation into the influence of electrode material on the IEC Inclined Plane test procedure (IEC 60587) when applied for Direct Current (DC) voltages

by
Raphael Swinny

Thesis presented in partial fulfilment of the requirements for the degree
Master of Engineering (Electrical) in the Faculty of Engineering
at Stellenbosch University

Supervisor: Mr J.C. Bekker

Co-supervisor: Dr. W.L. Vosloo

March 2021

Plagiarism Declaration

Plagiarism is the use of ideas, material and other intellectual property of another's work and to present it as my own.

I agree that plagiarism is a punishable offence because it constitutes theft.

I also understand that direct translations are plagiarism.

Accordingly, all quotations and contributions from any source whatsoever (including the internet) have been cited fully. I understand that the reproduction of text without quotation marks (even when the source is cited) is plagiarism.

I declare that the work contained in this assignment is my original work and that I have not previously (in its entirety or in part) submitted it for grading in another project / thesis / dissertation.

Name: Raphael Swinny

Date: March 2021

Acknowledgements

I would like to extend my sincere gratitude to:

- My supervisor, Mr Nelius Bekker, for the continuous support, weekly meetings and commitment shown towards the completion of my thesis.
- My co-supervisor, Dr Wallace Vosloo, for the technical guidance during this research and years of mentorship over the past two decades.
- Dr J.P.Holtzhausen, for valuable contributions in terms of document review and technical editing.
- My colleagues Mr R. Watson, Mr T.D. Mvayo and Dr M. Tomlinson for assistance in conducting the research.
- My wife Claudia, and children Tristan, Connor and Blake, for the constant love and support.
- My parents Harold and Emily Swinny, for the many sacrifices made.

Abstract

The inclined plane test (IPT) for testing the tracking and erosion resistance of polymer insulating materials is well established for AC conditions. Numerous researchers have used the standard AC test procedure and adapted it for DC application by applying both polarities of DC. Most researchers identify the amplitude and polarity of the applied DC voltage, conductivity and flow rate of contaminant, material properties of the samples under test, and erosion of the steel electrodes under DC energization as critical factors affecting the outcome of the tests.

This research investigated the extent and effect of steel electrode erosion under DC energization, making use of the IEC 60587 test procedure, adapted for DC application. AC and DC inclined plane tests were conducted using standard steel electrodes as specified by IEC 60587. In addition, special carbon glass electrodes, with dimensions similar to that of the standard steel electrodes, were introduced into the test to ascertain whether this type of electrode material would eliminate/reduce the impact of steel electrode erosion. Tests were conducted at 4.5kV AC and ± DC, at a contaminant flow rate of 0.6 ml/min, using standard HTV Silicone Rubber samples with 51 % weight ATH filler.

Results confirmed substantial erosion of the steel electrodes particularly under DC + energisation. The substitution of carbon glass for steel as an electrode material overcame the problem of electrode erosion, however tests conducted using the carbon glass electrodes were found to be much more aggressive in terms of material degradation. This is attributed to the reduced thermal conductivity of the carbon glass electrodes. Lastly, contaminant flow rate was found to be one of the biggest factors affecting the repeatability of the IPT, whether conducted under AC or DC.

Opsomming

Die skuinsvlak-toets (*inclined plane test*) vir die toets van die bestandheid van polimere wat as isoleermateriale gebruik word ten opsigte van spoorvorming en erosie is reeds goed gevestig vir wisselspanning (WS). Baie navorsers het die standaard WS-toetsprosedure aangepas en gebruik vir die toets met gelykspanning (GS) van albei polariteite. Die meeste navorsers het die amplitude en polariteit van die aangelegde GS-spanning, die konduktiwiteit en vloeitempo van die vloeistof, materiaal-eienskappe van die toetsmonsters en die erosie van die staal-elektrodes onder GS-spanning geïdentifiseer as kritiese faktore wat die toetsresultaat beïnvloed.

Hierdie navorsing ondersoek die omvang en graad van die erosie van die staalelektrodes met GS-spanning deur die IEC 60587 toetsprosedure, aangepas vir GS, te gebruik. Die WS en GS skuinsvlaktoetse is uitgevoer met standaard staalelektrodes soos deur IEC 60587 gespesifiseer. Verder is koolstofglas-elektrodes met soortgelyke afmetings as die standaard staalelektrodes tydens die toets gebruik ten einde vas te stel of die materiaal-tipe die effek van staalektrodes uitskakel of verminder. Toetse is uitgevoer teen 4.5 kV WS en ± DC met ’n vloeitempo van 0.6 ml/min en standaard HTV silikoonrubber toetsmonsters met 51 % per gewig ATH-vuller.

Die resultate het beduidende erosie van die staalelektrodes bevestig, veral met GS+ spanning. Die vervanging van die staalektrodes met koolstofglas het die probleem van die erosie van die elektrodes opgelos, maar dit is bevind dat die toetse met die glas elektrodes meer aggressiewe afbreking van die materiaal tot gevolg gehad het. Dit word toegeskryf aan die laer termiese konduktiwiteit van die koolstofglas elektrodes. Verder is bevind dat die vloeitempo van die kontaminant een van die belangrikste faktore is wat die herhaalbaarheid van WS- en GS-skuinsvlaktoetse is.

Table of Contents

List of Figures

List of Tables

Nomenclature

AC	Alternating Current
ANSI	American National Standards Institute
ASTM	American Society for Testing and Materials
ATH	Aluminium Tri-Hydrate
CENELEC	European Committee for Electrotechnical Standardisation
Cigre	Conseil Internationale des Grandes Reseaux Electriques (*International Council for Large Electric Systems*)
DBA	Dry band Arcing
DC	Direct Current
EPDM	Ethylene Propylene Diene Monomer
ESKOM	South African Power Utility, formerly “ESCOM” for Electricity Supply Commission
ESP	Enhanced Silicone Polymer
EVA	Ethylene-Vinyl Acetate
FTIR	Fourier Transform Infrared Spectroscopy
HC	Hydrophobicity Classification
HTV-SR	High Temperature Vulcanized Silicone Rubber
HV	High Voltage
HVAC	High Voltage Alternating Current
HVDC	High Voltage Direct Current
IEC	International Electrotechnical Commission
IPT	Inclined Plane Test
KIPTS	Koeberg Insulator Pollution Test Station
NCI	Non-Ceramic Insulator
OLCA	Online Leakage Current Analyser
rms	Root Mean Square
RRT	Round Robin Test

RTV	Room Temperature Vulcanized
SCD	Specific Creepage Distance
SEM	Scanning Electrode Microscope
SR	Silicone Rubber
TC	Technical Committee
TGA	Thermal Gravimetric Analysis
Triton-X	Wetting agent
USA	United States of America
USCD	Unified Specific Creepage Distance
UV	Ultra Violet

1 INTRODUCTION

1.1. Background

High Voltage (HV) insulators form the backbone of electrical Transmission and Distribution networks. They fulfil two primary roles, i.e. to mechanically support the live conductors as well as to provide an insulating medium between the live conductors and the grounded structure. In general, an HV insulator consists of two metal end fittings joined by a dielectric insulating medium. Figure 1-1 shows the various insulator types that have been in existence, some since the dawn of electricity.

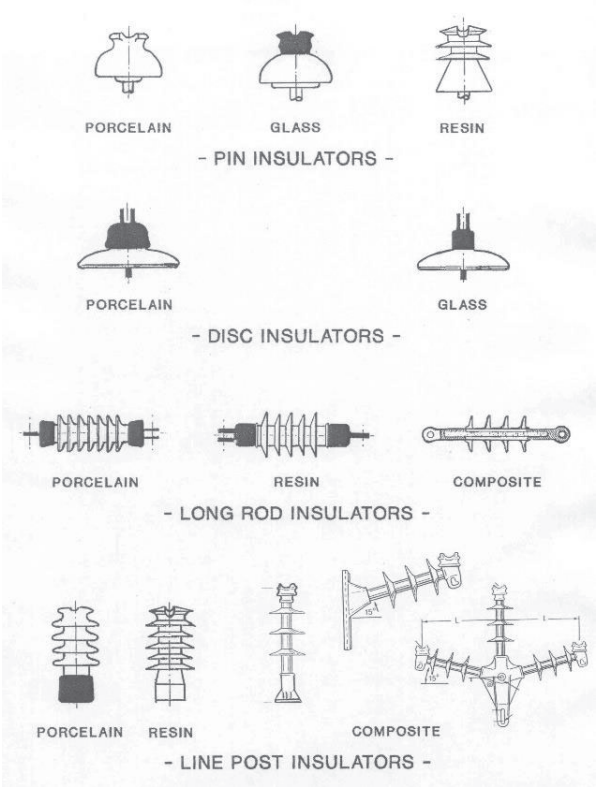

Figure 1-1: Various forms of HV insulators (picture courtesy of W. Vosloo).

The electrical performance of the insulating medium is dependent on how well it can withstand the various environmental stresses, e.g. Ultra Violet (UV) radiation, precipitation, humidity, pollution, temperature, ozone, lightning, etc., that it is exposed to.

The first insulators that were produced were made from toughened porcelain and glass [1]. These insulators were in existence for many years and would generally last the lifetime of the electrical network due to the inert nature of the dielectric medium. During the 1960's, with the onset of

materials technologies, a new range of non-ceramic insulators (NCI) became available [1]. These included Cycloaliphatic resins and polymeric formulations such as Silicone Rubber (SR), Ethylene Propylene Diene Monomer (EPDM), Enhanced Silicone Polymer (ESP) and Ethylene Vinyl Acetate (EVA) to name a few. Ceramic insulators, although inert and not prone to material degradation, do not perform well under polluted conditions due to the hydrophilic nature of their surfaces. Certain NCI on the other hand, particularly SR, are hydrophobic and are generally able to limit leakage current extremely well under wet polluted conditions. In addition to their perceived improved leakage current performance, NCI have a greater mechanical strength to weight ratio and are thus easier to transport and install. They are much less prone to vandalism as well as construction damage when handled properly. NCI are however prone to material degradation, especially when exposed to the combination of electrical stresses and adverse environmental conditions. This could eventually lead to poor electrical performance and premature ageing of the insulator, resulting in the need for replacement.

Many testing methodologies and specifications are currently in existence to prove both the mechanical and electrical integrity of HV insulators. These include laboratory-based tests as well as natural ageing and pollution performance tests. The ultimate aim of these tests is to ensure that products installed on HV networks are fit for purpose and match the expected lifetime of the complete network.

1.2. IEC Test Procedures, Specifications and Guides

The IEC (International Electrotechnical Commission), founded in 1906, is one of the world's largest organizations dealing with the preparation and publication of International Standards for all electrical, electronic and related technologies [2]. Representatives from worldwide industries, power utilities, manufacturers, testing laboratories and government departments are drawn together in the various technical committees and working groups with the objective of developing appropriate international standards and specifications. Other international organizations that produce similar standards include

the American National Standards Institute (ANSI) and the European Committee for Electrotechnical Standardisation (CENELEC). The IEC has a close working relationship with the International Council on Large Electric Systems (Cigre), with many Cigre documents eventually evolving into IEC guidelines. Within the South African utility, i.e. Eskom, most specifications relating to HV Insulators are based on IEC specifications and guidelines.

IEC Technical Committee (TC) 36 was established in 1949 with a specific focus on the standardisation of specifications, guidelines and test methods for HV equipment including bushings, insulators for overhead lines and substations and their couplings [3]. This serves to ensure that HV insulators conform to set dimensions and quality levels. In addition, and more importantly, test standards aim to ensure that insulators in service meet the required electrical performance levels and are able to withstand the harsh environmental conditions that many are exposed to, without premature ageing of the housing material. For both ceramic and composite insulators, three categories of tests exist, i.e. type, sample and routine. Type tests are conducted to ensure that the designed product conforms to the requirements of the end-users' specification. Sample tests are done on certain production units to ensure that insulators off the production line are in conformance to the units that were type tested. Routine tests are conducted on every unit produced to confirm production quality. For composite insulators, a further category known as design tests is utilized. Design tests focus on the ability of the composite material to withstand tracking and erosion, ageing under accelerated weathering conditions, degree of flammability and resistance to moisture ingress of both the housing material as well as the core. Tests also focus on the strength of the core and the integrity of all interfaces. IEC 62217 describes in detail the applicable design, type, sample and routine tests that composite insulators should undergo [4]. In addition to IEC 62217, there are test procedures that deal with specific areas of testing such as IEC 60507 [5], IEC 61109 [6], IEC 61302 [7] and IEC 60587 [8].

1.3. Testing of HV Insulators for HVDC Application

With the advancements in High Voltage Direct Current (HVDC) technology, HVDC transmission is not only feasible but in many cases the preferred solution due to greater transmission capacity as well as lower electrical losses. The electrical stresses that an insulator is exposed to are different under DC as opposed to AC. The effect of polarity and pollution catch affects the overall insulator performance and therefore influences the choice of insulator material and design parameters [9]. It is thus important that composite insulators for HVDC power lines undergo suitable testing to ensure that they are able to withstand the stresses that they are exposed to. In Africa, composite insulators have been installed on the Cabora Bassa – Apollo ± 533 kV line for over 25 years, with good experience to date [10]. Similar experiences have been noted internationally on HVDC lines in the USA and New Zealand [11].

Various AC performance and ageing tests have been adapted for DC testing by applying a DC voltage. These include the 1000hr salt fog test, rotating wheel dip test, 5000hr ageing test as well DC tests conducted at natural outdoor test stations such as the Koeberg Insulator Pollution Test Station (KIPTS). These tests have been conducted with a fair degree of repeatability and are reviewed in detail in Chapter 2 .

One test that has not shown repeatability when performed under DC conditions is the Inclined Plane Test (IPT) neither when the IEC 60587 nor the ASTM D2303 standard is applied. This test evaluates a composite's materials susceptibility to tracking and erosion. Tracking, as per definition within the IEC 60587 standard, is the progressive degradation of the surface of a solid insulating material by local discharges to form conducting or partially conducting paths. The tracked paths are conducting, therefore, they have the effect of reducing the effective creepage distance of the insulation, resulting in reduced leakage current performance. Erosion, which is defined as loss of insulation material as a result of leakage current or electrical discharges, also reduces the effective creepage distance of a material. Erosion can also result in exposure of the fibreglass core and subsequent insulator failure.

Numerous researchers have made use of the standard IPT procedure but adapted it for DC application by applying both polarities DC [12-17]. Critical factors listed by most researchers affecting the outcome of the tests include the amplitude and polarity of the applied DC voltage, the pollution severity as well as flow rate of the contaminant, the material properties of the samples under test and the erosion of the steel electrodes under DC energisation. Each of these aspects will be studied in detail in Chapter 2. This project will focus on investigating the extent of erosion of the steel electrodes under DC energisation.

1.4. Hypothesis and Research Questions

The hypothesis for this study is that an alternative electrode material in the form of carbon glass will provide the same test performance in the IPT under AC energisation as normal steel electrodes would, but will not be susceptible to cathodic erosion under DC energisation.

For this project the use of carbon glass electrodes, conforming to the same dimensions as standard steel electrodes, will be investigated. The tests will be conducted under the same test conditions as specified under IEC 60587 to determine whether carbon glass electrodes can be used as an alternative to steel electrodes, thus increasing the repeatability of the test under DC conditions.

In particular, the following research questions will be addressed through performing a detailed literature study as well as conducting laboratory tests:

- What is the extent of electrode erosion under DC energisation during the IPT?
- What is the effect of electrode erosion on material performance under DC energisation during the IPT?
- How can electrode erosion in the IPT be eliminated?
- To what extent will the repeatability of the DC IPT improve if the electrode erosion is eliminated?
- What other test parameters influence the repeatability of the DC IPT?

1.5. Structure of Thesis

This thesis consists of six chapters.

In **Chapter 1**, a brief background is given in terms of the development of composite insulators and the need for appropriate test procedures for both AC and DC voltages. The hypothesis and research questions are also outlined.

In **Chapter 2**, the literature survey focusses on in-service experience and laboratory research conducted to date on the testing of composite insulator materials under DC energisation.

In **Chapter 3**, the test methodology is outlined.

In **Chapter 4**, a description of the equipment that was either developed or procured to implement the test methodology is given.

In **Chapter 5**, the results of the various inclined plane AC and DC tests are described and discussed.

Chapter 6 concludes the thesis with a summary of findings and recommendations for future work.

2 LITERATURE REVIEW

2.1. Overview

The literature survey focusses on research conducted to date on the performance of HV insulators under DC energisation in various environments. The chapter commences by looking at the in-service performance of HV insulators installed on HVDC lines from various utilities. Thereafter, a review of HVDC tests conducted at various natural aging test stations is presented. Results of laboratory tests, including the 1000 hr salt fog test and the rotating wheel dip test, adapted for DC application, are discussed. The standard AC IEC 60587 inclined plane test procedure is discussed briefly, where after factors affecting the outcomes of the DC adapted test are discussed in detail. This includes the effect of voltage amplitude and polarity, the effect of filler percentage on material performance, the effect of contaminant flow rate and the effect of electrode performance during the IPT. Lastly, a summary of the results of a round-robin test done by Cigre working group D1.27 is presented.

2.2. Ageing of HV Insulators under DC energisation in natural environments

Sections 2.2.1 and 2.2.2 below provide a summary of data gathered by various researchers on the performance of composite insulators under DC energisation in natural environments, including in-service and outdoor test station experience.

2.2.1 Field Experience of HV Insulators Under DC Energisation

Cigre Working Group 03 of study committee 22 commissioned a study to gather data on composite insulators installed on HVDC lines [11]. Feedback was obtained from four utilities; Transpower from New Zealand and three from the United States of America (USA). At the time, approximately 800 silicone rubber and EPDM composite insulators had been installed on ± 270 kV and ± 400 kV DC lines of these utilities, with the first units being installed in 1976. Transpower reported good overall performance, however significant corrosion of end fittings was noted. USA utilities noted flashovers on EPDM units in heavily polluted areas, but reasonable performance on the silicone rubber units. At the time, it represented 16 years of service experience for composite insulators under HVDC.

Seifert et al presented a comprehensive review of the performance of silicone rubber insulators installed on various HVDC lines, particularly the Cabora Bassa – Apollo ± 533 kV line between South Africa and Mozambique, the ± 500 kV Pacific Intertie in Western USA and ± 270 kV lines in New Zealand [10]. The performance of the insulators installed on all of these lines was found to be good over a period of approximately 25 years. Samples removed from the field showed little damage and good hydrophobicity, however most lines were located in areas of light and medium pollution severity. Seifert sought to compare the results of laboratory ageing tests with field experience and adapted the IEC 601109 5000hr laboratory ageing test by applying a DC voltage. Similar profiled insulators to those installed in the field were used and similar ageing mechanisms were found. Seifert also performed an adapted inclined plane test using IEC 60587, however the yielded results contradicted the exceptional performance obtained during field service under HVDC. Seifert noted that the effect of hydrophobicity has a major impact on silicone rubber performance under HVDC. More recently, Windmar conducted evaluations of 6 different types of DC-energized composite insulators removed from the field [18]. These insulators had been installed over a period of 17 years mostly within light and medium pollution areas. No signs of degradation were observed, and all samples showed excellent hydrophobicity. Windmar also noted that pollution deposition was found to be uniform across the surface of the insulators.

2.2.2 DC Experience with Outdoor Test Stations

Outdoor test stations allow for the testing of insulators under natural environmental conditions. Although natural pollution tests generally take much longer than laboratory-based tests, the results generated are seen to provide a more realistic understanding of the material ageing and pollution performance of HV insulators in specific climatic and pollution zones. Sorqvist reported on the performance of EPDM and SR insulators that were energized at ±300kV DC at the Anneberg outdoor test station in Sweden for a period of 7 years [19]. The test station is located approximately 10km from the coast. The environment is stated as being relatively clean with the main pollutant being marine salt brought in from the coast during heavy winds. Sorqvist showed that even under DC

energisation, ATH filled SR insulators maintained hydrophobicity and showed much lower leakage currents than the hydrophilic EPDM units. Gustavsson et al made use of the same test station to study the effect of ATH and silicone oil on SR performance under DC energisation over a period of 32 months [20]. The effect of insulator geometry was minimized by making use of cylindrical test samples. Results showed that, in general, hydrophobicity was maintained for all samples under test, except during periods of high wetting. Samples having high ratios of ATH in the filler always showed less overall erosion. It was highlighted that the highest degree of erosion occurred at the ends of the samples close to the grounded electrode. Gustavsson states that the data indicates that the level of electric stress together with the type of voltage applied has a greater influence on insulator performance than material formulation. The addition of silicone oil limited leakage current activity. The filler level did not assist in limiting leakage current but had an effect on the extent of material degradation. In both the above studies, no mention is made of the effect of polarity on material performance.

Mouton compared the performance of identically profiled EPDM, HTV SR and RTV SR insulators under HVAC and HVDC excitation when energized in a severe marine environment [21]. The RTV SR was in the form of an RTV SR coating applied to a porcelain insulator of identical profile to the EPDM and HTV SR units. Tests were conducted at the Koeberg Insulator Pollution Test Station (KIPTS) in South Africa over a period of 12 months. The results obtained were referenced to bare porcelain and glass. The AC test voltage was 12.7 kV_{rms} phase-to-ground with the applied DC test voltage being the same. From a material ageing perspective, Mouton states that HTV SR performs better than EPDM under all excitation voltages. The most degradation was found to occur under DC - energisation on both materials, however a higher degree of erosion was noted on EPDM. Notwithstanding the above, only light erosion was noted with no samples failing the KIPTS test criteria which states that no erosion greater than 2mm should occur [22]. Mouton noted corrosion of the end fittings under DC energisation of all the samples tested except for the glass units. This is shown in Figure 2-1 and Figure 2-2. The HTV SR units showed light end-fitting corrosion with the remaining units displaying moderate

corrosion. Under DC +, corrosion was observed on the live end fitting, whereas under DC -, corrosion was noted on the ground end fitting.

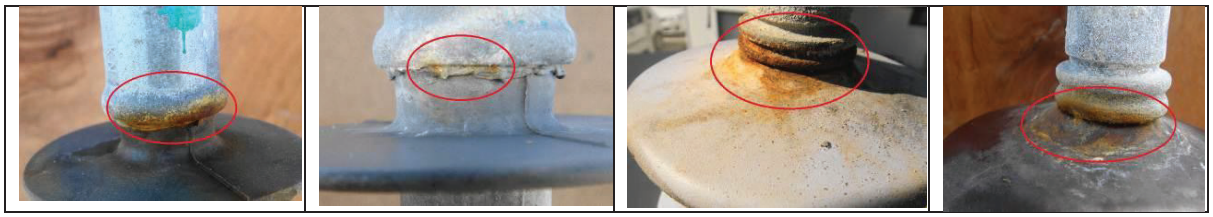

Figure 2-1: Corrosion of earth end fitting under DC - energisation [21].

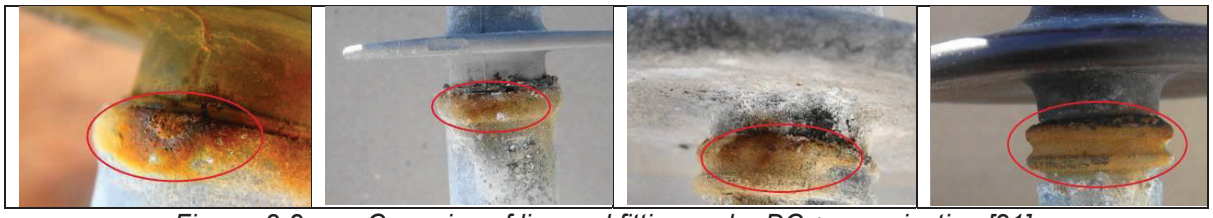

Figure 2-2: Corrosion of live end fitting under DC + energisation [21].

Corrosion of the end fittings is as a result of electrolysis. Glass cap and pin insulators are equipped with a sacrificial zinc sleeve, which prohibits cap and pin corrosion. It could be expected that the by-products of corrosion would have an effect on the leakage current performance of insulators under DC - energisation, as the earth end is positioned on top, allowing for run-off of contaminants over the material surface. In general, HTV SR test samples showed superior leakage current performance to EPDM for all excitation voltages. This is attributed in part to the hydrophobic characteristics of SR, with the SR test samples remaining hydrophobic for large parts of the test cycle. Mouton however could not draw conclusive results in terms of which polarity had a more severe effect on the various material types.

Elombo conducted further testing at KIPTS using HTV SR insulators from the same manufacturer but with varying creepage lengths [23]. Samples with Unified Specific Creepage Distances (USCD) of 87, 75, 58, 46 and 29 mm/kV were tested. A glass cap and pin disk insulator with a USCD of 42 mm/kV was used as a reference. Samples were energized under AC and ±DC, with similar voltage levels to those used by Mouton [21]. Elombo reported that on the SR units, leakage currents were found to be higher on the units energized with DC +, whilst on the glass, leakage currents were higher under DC - energisation. For the SR insulators, more flashovers were recorded under DC + (on the short units),

whereas with the glass, most flashovers happened under DC - energisation. In general, it was noted that reduced creepage resulted in reduced pollution performance. However, in terms of material ageing, less erosion was noted on the short insulator for both AC and DC energisation. This phenomenon has been noted at KIPTS previously [24]. It is postulated that shorter creepage insulators are prone to higher leakage currents with mobile dry band arcing (DBA). Higher creepage insulators tend to have lower leakage currents, with stable DBA allowing for deeper erosion at specific areas.

Windmar et al reported on the performance of composite insulators energized in a natural environment over a period of 4 years at the Swedish Transmission Research Institute (STRI) outdoor test station [18]. Energized insulators showed extensive blackening with the measured pollution levels on the DC energized units being twice that of AC energized units. No tracking or erosion was noted on either the AC or DC energized units, with good hydrophobicity being maintained as well on all samples under test.

2.3. Laboratory testing under DC energisation

Sections 2.3.1 and 2.3.2 provide a summary of data gathered by various researchers on the performance of composite insulators under DC energisation laboratory tests, including the 1000 hr salt fog test and the rotating wheel dip test.

2.3.1 DC 1000HR Salt Fog Test

The 1000hr salt fog test, performed according to the IEC 62217 standard (second edition 2012, section 9.3.3), is a tracking and erosion test conducted on production line sample insulators [4]. Two test specimens are required per test, one energized in the horizontal position and the other in the vertical position. The AC power frequency test voltage is set such that the specific creepage distance of the test specimens equals 20 mm/kV. A sample is considered to pass if no signs of tracking, no signs of puncture and no erosion greater than 3mm are detected at the end of the test.

Gorur et al tested HTV SR and EPDM rod samples in a fog chamber, making use of both low and high conductivity salt fog [25]. Tests were done using ±DC and were compared to AC results obtained in a

previous study. The test samples had varying degrees of filler material, i.e. ATH and Silica. Under DC - , the anode experienced erosion and an electrode mass loss of up to 5% was recorded in a 100hr period. Electrodes made of aluminium, stainless steel, brass and copper were utilised but all eroded and caused early flashover, especially under high conductivity fog. Erosion deposits were noted on all test samples. Gorur et al noted that for AC and DC +, the time to failure was similar during both the low and high conductivity tests, however the time to failure under DC - was a factor of 4 shorter. Under low conductivity fog, SR outperformed EPDM in terms of tracking time. However, under high conductivity fog, EPDM samples performed better than SR. It is noted that filler type and percentage play a crucial role in the ability of a material to withstand tracking and erosion. ATH ($Al(OH)_3$) has the ability, under heating (such as that experienced during DBA) to decompose into alumina and water (water of hydration), making ATH an effective flame retardant, increasing the material's resistance to tracking and erosion. Gorur et al also noted that the mechanism by which fillers impart tracking and erosion resistance was the same for AC and DC. Correlation of leakage current to tracking and erosion showed that, if leakage current is kept below a certain threshold value, good material performance could be expected, even at relatively high electric stress values.

Numerous researchers made use of salt fog tests to determine, amongst others, the difference in withstand capability of composite insulators energised under AC and ± DC [26-28]. In general, the withstand capability for both SR and EPDM was lower for ± DC than for AC. In certain instances, the DC- withstand voltage was found to be 70% of the AC withstand voltage

2.3.2 DC Rotating Wheel Dip Test

Prior to 2012, the IEC 62217 standard listed three tracking and erosion tests, i.e. the 1000 hr salt fog test, the 5000 hr ageing test and the rotating wheel dip test. IEC TC 36 made the decision to standardize on the 1000 hr salt fog test within IEC 62217. The rotating wheel dip test and the 5000 hr ageing test was removed from IEC 62217 and included in a new technical report i.e. IEC TR 62730 – HV Polymeric Insulators for Indoor and Outdoor use, Tracking and Erosion Testing by Wheel Test and

5000 hr Test. The tests described in IEC TR 62730 are AC test standards and as yet no standard has been published for DC application.

Yu et al adapted the standard tracking wheel test by applying both polarities DC to SR insulator samples for a period of 1000 hrs [29]. It was observed that hydrophobicity played a distinct role in the level of leakage current recorded. In the beginning of the test, good hydrophobicity limited leakage current to values below 10 mA. This only lasted for approximately two days where after hydrophobicity decreased substantially and the level of leakage current was then determined by the material properties of the insulator. Leakage current values of up to 150 mA were recorded near the end of the test. Greater degradation was noted under DC.

Limbo et al compared the performance of EPDM rubber and HTV SR when energized under AC and DC ± using the tracking wheel test [30]. Samples were energized at positive and negative 13.6 kV DC with the AC test voltage being 13.6 kV_{rms}. DC + had the most severe effect on both EPDM and SR, with final peak leakage currents for DC + being 37 % and 41 % higher than DC - for the two materials, respectively. HTV SR exhibited more severe degradation than EPDM, even though hydrophobicity of the SR was found to be relatively good (HC 1 – 3 as per STRI hydrophobicity classification criteria [31]). EPDM, as expected, lost all hydrophobicity for the duration of the test.

Holtzhausen together with Limbo went further by testing 6 insulators of varying material composition and creepage, including EPDM rubber, three variations of HTV SR (two material variations and one increased creepage length), RTV coated porcelain and bare porcelain [32]. All samples had a USCD of 28 mm/kV, except for the longer SR with a USCD of 35mm/kV. The EPDM unit recorded similar levels of leakage current for both AC and DC ±. For the two variations of SR, one recorded slightly higher levels of leakage current than the EPDM unit. The other one however had drastically higher leakage currents and suffered severe degradation. The higher creepage SR insulator had acceptable AC performance, but failed on both polarities DC. Interestingly the bare porcelain insulator showed the best leakage current performance out of all the samples on test. The coated porcelain performed

poorly with severe degradation and high leakage current being recorded. Another interesting observation during all the tests was the occurrence of brown deposits on all of the insulators, this being attributed to corrosion of the end fittings. And energy dispersive X-ray spectroscopy analysis (EDS) done on the brown residue showed it to be iron oxide, which the authors state could have had an influence on the results.

2.4. The IEC 60587 Inclined Plane test procedure and key factors for consideration when applied for DC voltages

2.4.1 Overview

This section provides an overview of the IEC 60587 standard together with research conducted using the IEC 60587 standard with the aim of identifying key parameters for DC application. The IEC 60587 standard provides a test method known as the Inclined Plane Test (IPT). The IPT is well established and is used worldwide as a means to gauge a material's resistance to tracking and erosion when energized under AC voltage in polluted conditions. It is a laboratory-based test, and with a maximum duration of six hours, it provides a quick, repeatable means to gauge the integrity of composite housing materials when subjected to severe electrical and pollution stresses. Most test arrangements allow for the testing of five samples simultaneously, allowing one to relatively rank the performance of various materials. The test was first introduced in 1986, with an update being provided in 2007.

2.4.2 Standard AC Test Procedure

The standard prescribes two test methods i.e. the constant tracking voltage method and the stepwise tracking voltage method. Both these methods prescribe the test voltage at power frequency ranging from 45 Hz to 65 Hz, in effect AC voltage. The standard prescribes that for the test, flat insulator samples of approximately 50 x 120 mm, with a thickness of 6mm, be installed on an inclined plane at an angle of 45 ^{0} from the horizontal, and energized under the flow of a liquid contaminant. Figure 2-3 shows a circuit diagram of a standard inclined plane test setup.

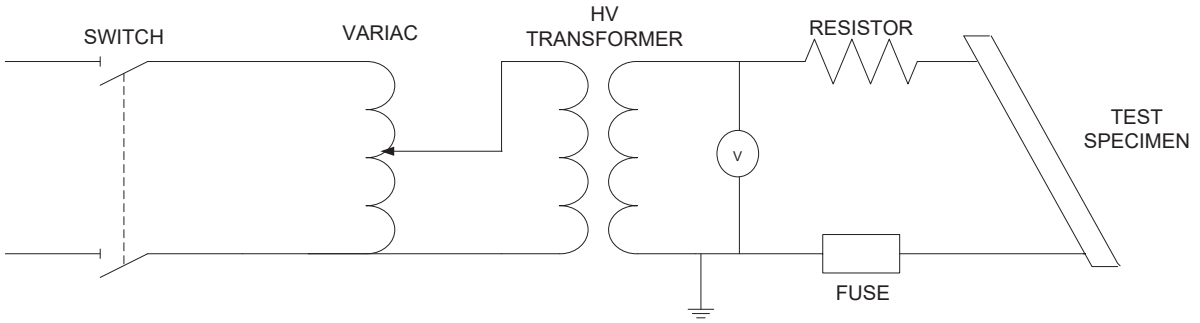

Figure 2-3: Standard Inclined Plane Circuit Diagram.

The standard requires a power supply up to 6 kV_{rms} with a rated current of at least 0.1 A_{rms} for each specimen on test. The constant tracking voltage method, which is the method most widely used, suggests rms test voltages of either 2.5 kV, 3.5 kV or 4.5 kV.

The insulator samples are energized via two electrodes, spaced 50 mm from each other. The standard prescribes that all electrodes, fixtures and any other assembly apparatus be made of stainless steel (grade 302). Figure 2-4 shows a standard electrode geometry. Electrodes should be at least 0.5mm thick.

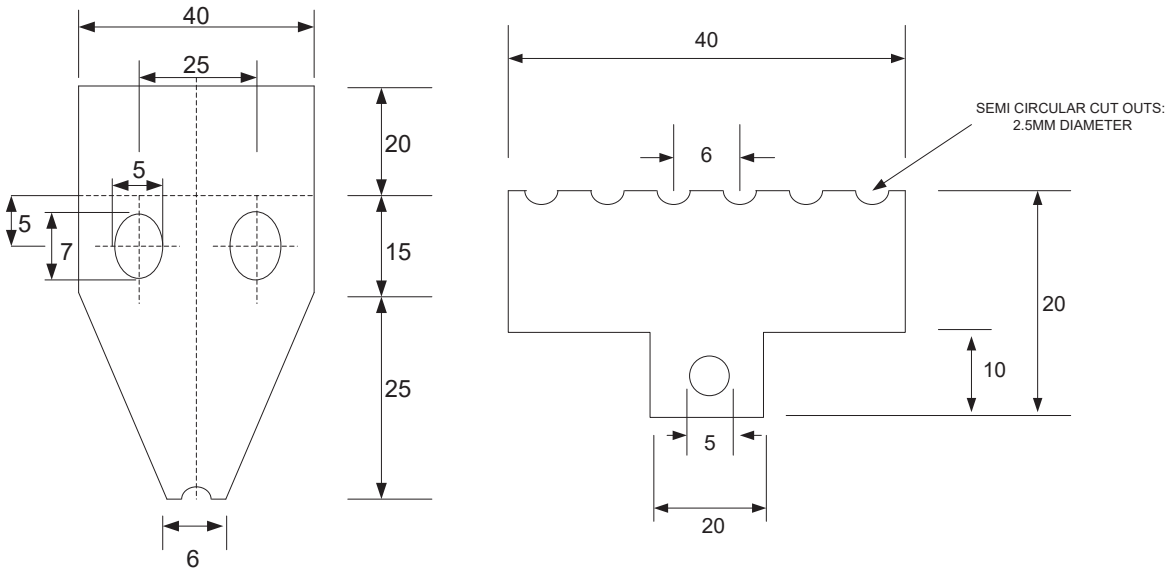

Figure 2-4: Top (left) and bottom (right) electrodes for inclined plane test.

To facilitate the conduction of leakage current across the test sample surface, a contaminant is required to flow at a fixed rate, over the insulator surface between the two electrodes. The flow of the contaminant varies depending on the voltage that the samples are energized at. The contaminant

should consist of 0.1 % ± 0.002 % mass NH4Cl (ammonium chloride) and 0.02 % ± 0.002 % mass isooctylphenoxypolyethoxyethanol in distilled or de-ionized water. The contaminant should have a resistivity of 3.95 Ωm ± 0.05 Ωm at 23 ^{0}C. Filter paper clamped between the test specimen and the electrode acts as a reservoir for the contaminant, with the objective being a uniform flow between the top and bottom electrodes before the test voltage is applied.

There are two methods of voltage application. The first method, namely the constant tracking voltage is the preferred method. This method prescribes that, with the contaminant flowing uniformly at a specified rate, the voltage is applied and raised to either 2.5 kV, 3.5 kV or 4.5 kV. The applied voltage is then kept constant for 6 hours. The constant tracking voltage is termed as the highest voltage withstood by the specimen for 6 hours without failure.

The second method, i.e. the stepwise tracking voltage, requires voltage application at a selected value for 1 hour, then increases of 250 V for each subsequent hour until failure occurs. As the voltage is increased, the standard specifies an increase of the contaminant flow rate as well as the resistance value of the series resistor. The stepwise tracking voltage is the highest voltage withstood by the specimen for 1 hour without failure.

Two failure criteria are defined by IEC 60587 viz :

1. Leakage current across the specimen exceeds 60 mA or the specimen exhibits a hole due to erosion or the specimen ignites.
2. Tracking on the specimen reaches a distance of 25 mm from the lower electrode or the specimen exhibits a hole due to excessive erosion or the specimen ignites.

Two internationally recognized IPT procedures exist i.e. IEC 60587 and ASTM D2303 [33]. The ASTM standard differs in approach in that there are two test methods for tracking, i.e. initial tracking voltage method and time to track method, and a separate method using a constant voltage, i.e. outlined in annexure A of the standard, for erosion determination. Even though these two standards differ

somewhat in approach, the data obtained from either standard can be considered to be technically equivalent. Research from both standards is documented in the literature review, however the laboratory tests conducted for this study will be done according to IEC 60587.

Sections 2.4.3 to 2.4.6 look at the effects that key parameters such as voltage (amplitude and polarity), filler material, contaminant flow rate and electrode material have on the outcomes of IPT tests under both AC and DC energisation.

2.4.3 Effect of Voltage Amplitude and Polarity

In an attempt to determine an equivalent positive and negative DC voltage for DC IPT application, Ghunem et al established a coefficient of variation that could be applied in order to determine the IPT equivalent DC test voltage in relation to AC [34]. The establishment of the coefficient was done using the ASTM D2303 test procedure, employing the initial tracking voltage test method. Here the starting test voltage is applied for 60 minutes, and increased by 250 V every hour thereafter. At least three voltage steps are required for a successful test. Failure criteria include tracking more than 25 mm, erosion through more than half the sample thickness or ignition of the test specimen. Five RTV Silicone Rubber formulations comprising 30 wt% silica filler were used as test specimens, with the test being conducted three times. The starting rms voltages for AC, DC + and DC - were set at 3.25 kV $_{rms}$, 2.25 kV and 2.5 kV, respectively. These values were based on the known severity of DC in relation to AC and to ensure that the test would progress through the required steps. The contaminant flow rate utilized was 0.3 ml/min. Results showed the initial tracking voltage for AC, DC + and DC - to be 3.75 – 4 kV $_{rms}$, +2.5 – 2.75 kV and -3.25 kV, respectively. Utilizing this method Ghunem et al thus state that for the specific test material and specific test conditions, the DC + and DC - equivalent for the AC test voltage is 66% and 86% respectively. Further work by Ghunem et al using 3 variations of silicone rubber (0%, 20% and 30% filler weight) resulted in average variation coefficients of 67% and 84% for DC + and DC – respectively [35]. As such, subsequent IPT work done by these researchers made use of +2.25 kV and

-3.0 kV as being equivalent to 3.5 kV_{rms} AC when testing at a contaminant flow rate of 0.3 ml/min [36, 37].

Cherney et al documents round robin tests that were conducted in five laboratories according to ASTM D2303 with the main objective being to standardize on the equivalent DC test voltages in relation to AC [38]. Similar values of 67% and 87% were achieved when testing 5 identical silicone rubber samples, with a maximum deviation of 11% being recorded. The authors suggest that in future the test voltage values be rounded to 70% and 90% of the AC test voltage for DC + and DC – respectively. It is important to note that these results are based on tests conducted using the ASTM D2303 test procedure on one type of material with a specific filler type and filler percentage.

Several other researchers have conducted DC tests using an adapted version of the IEC 60587 IPT procedure. In choosing equivalent DC voltages, some researchers adopted the methodology of calculating the area under half the period of an AC wave (also known as the average voltage) in order to determine the DC equivalent voltage.

$$Vave = \frac{2Vp}{\pi} = 0.637\,Vp \qquad (2.1)$$

Using equation (2.1) Bruce et al conducted DC IPT tests at the DC equivalent voltage of 2.5 kV_{rms} and 3.5 kV_{rms} [16, 17]. This equated to DC voltages of ± 2.25 kV and ± 3.15 kV. Heger et al adopted a slightly different approach, using the rms voltage values for both AC and DC ± [15, 39]. Comparative tests were conducted on silicone rubber samples using 4.0 kV_{rms} AC and ± 4.0 kV DC. The basis for this approach is the argument that erosion of composite insulator material is an energy driven process as shown by Crespo – Sandoval et al and that the use of rms values for both AC and DC provides an equal basis on which to evaluate the polarity effect of AC vs DC [40].

The general consensus throughout all literature is that DC + is more damaging than its negative equivalent, however tracking time seems to be the shortest under DC -.

2.4.4 Effect of filler percentage on performance of Composite Materials under AC and DC Energisation

Bulk filler materials such as ATH and Silica assist in providing tracking and erosion resistance for NCI. ATH is known to degrade at approximately 200 ^{0} C, forming aluminium oxide and water vapour which is often termed water of hydration. The formation of water vapour under high temperatures as would be experienced during DBA, assists in reducing the surface temperature of the material, leading to reduced erosion of the base compound. Silica on the other hand finds its effectiveness in how strongly it bonds to the base polymer. The high mechanical strength of the bond between the Silica filler and the base polymer results in reduced material erosion.

Meyer et al investigated the effect of filler type and filler particle size on the performance of SR using the ASTM D2303 IPT [41, 42]. SR samples comprising of 10%, 30% and 50% weight concentration as well as filler particle sizes of 1.5, 5 and 10 µm were tested for each of the filler types. It was observed that at low filler concentration (10% weight), ATH filled samples performed slightly better than the Silica filled samples. At higher concentrations, no notable difference in performance between the two filler types was noted. Meyer showed that increased filler concentration led to increased thermal conductivity of the material. In terms of filler particle size, the most optimum particle size in relation to thermal conductivity was found to be 5 µm for both ATH and Silica. The results of this work showed that a higher thermal conductivity resulted in reduced material erosion.

Kumagai and Yoshimura studied the effect of filler percentage on the tracking and erosion resistance of HTV SR using the standard IEC 60587 IPT [43]. SR samples ranging in filler percentage from 0 to 60% weight ATH, with an average particle diameter of 1 µm, were tested at AC voltages of 3.0, 3.5, 4.5 and 5.0 kV. Peak leakage current pulses as well as SR surface temperatures (using an infrared thermovision system) were measured. It was observed that for samples with 10 to 40% weight ATH, a test voltage of 4.5 kV resulted in the quickest time to failure. For samples with 40% weight, it was observed that one in five samples had tracking and erosion within the test limit of six hours for test voltages 3.0, 3.5 and 5.0 kV. However, at 4.5 kV, four in five samples showed severe tracking and

erosion. Kumagai observed that there was a certain value of leakage current that seemed to be most efficient in producing tracking and erosion on samples with 40% weight filler or less during the IPT. Samples with more than 40% weight filler withstood tracking and erosion at all the test voltages, indicating 40% weight to be the lower limit in terms of filler percentage for the SR materials under test. Kumagai also observed the occurrence of thermal spots, which he defined as spots at which the surface temperature of the test sample exceeds 400 ^{0}C. These spots were characterized by lifetime, ranging from 0 to 1, 1 to 5, 5 to 20 and 20 to 100 s. A direct correlation was observed between the rate at which thermal spots appeared and the number of leakage current pulses measured. At lower filler percentages, the occurrence of thermal spots resulted in tracking and erosion. At filler percentages of 40% and higher, the appearance of thermal spots did not lead to tracking and erosion, indicating the ability of ATH filler, when loaded at the correct concentration, to prevent thermal degradation under DBA.

Ghunem et al investigated the effect of ATH and Silica in reducing erosion of SR under DC [35]. Tests were conducted using DC +, which produced the highest degree of stable DBA in previous work by the researchers. Surface temperature and time to erosion (TE) were used as measurement parameters. Test samples comprising HTV SR with 25 % and 58 % weight ATH filler, as well as RTV SR with 30 % weight Silica and ATH were analysed. The results showed that for the HTV samples, DBA was intermittent at surface temperatures below 200 ^{0} C, with little erosion present. It is suggested that thermal conductivity plays a crucial role in reducing the formation of stable DBA. Stable DBA in samples with 25 % weight ATH occurred considerably sooner at 80 minutes, as opposed to 115 minutes for the 50 % weight samples. The role of filler type was investigated by observing the TE of the RTV samples filled with ATH and Silica. ATH filled samples showed a TE of approximately 70 minutes vs 50 minutes for Silica filled samples. The water of hydration is seen to play a key role in suppressing the temperature rise on the surface of ATH filled SR, resulting in a delayed TE when compared with Silica filled samples.

Ghunem et al investigated the relative performance of both EPDM and SR samples under DC energisation in the IPT [44]. Commercially available samples filled with 25% weight ATH filler were energized under both polarities DC according to the ASTM D 2303 test procedure, making use of both the initial tracking voltage (ITV) and constant voltage test methods. For the constant voltage tests, Ghunem made use of equivalent test voltages of + 2.25kV and -3 kV. Two distinct failure mechanisms were noted, with the EPDM failing due to tracking and the SR due to erosion. Erosion also occurred on the EPDM samples but to a lesser degree than the SR. Ignition of the test sample occurred with both materials. This could have been due to the low percentage of filler, and subsequent reduced flame retardency, for both materials. The measured leakage current showed more periods of non-conduction for SR, indicating stable DBA prior to SR failure. For EPDM, intermittent leakage current pulses were found to be dominant. Ghunem stated that supplementary ionization as a result of oligomers given off during the decomposition of the SR surface could play a role in the increased DBA, especially under DC +.

Heger et al investigated the relative performance of RTV coated porcelain, HTV SR (two variations) and EPDM when exposed to both AC and DC voltages using the IPT [39]. Tests were conducted at an AC voltage of 4 kV_{rms} and ± 4kV DC. SR based materials showed minor erosion during the AC tests. EPDM showed severe erosion under AC energisation. Under DC + energisation, HTV SR based material showed a vast increase in erosion, with both the two samples failing the test. The RTV coated porcelain sample showed greatest erosion under DC -. The EPDM sample showed reduced erosion when compared to its performance under AC. Under DC - similar results were observed, with EPDM having similar performance to when energized under DC + and having better performance than when energized under AC. Heger states that the performance in terms of erosion of various SR based materials during the IPT is largely dependent on voltage type and polarity, whereas EPDM seems to exhibit a greater independence.

2.4.5 Effect of Contaminant Flow Rate during IPT

Vosloo et al showed that the leakage current flowing across the surface of an insulator is largely determined by the resistance of the electrolytic pollution layer according to the following equation [1]:

$$R_{pol} = \frac{\rho\, L_{CD}}{A} \qquad 2.2$$

Where:

R_{pol} : resistance of surface electrolytic pollution layer in MΩ

P : volume resistivity of electrolytic pollution layer in MΩ.mm

L_{CD} : insulator creepage distance in mm

A : cross sectional area of electrolytic pollution layer

In the context of the IPT, IEC 60587 specifies that standard samples measuring 50 x 120 mm are utilized, hence the L_{CD} is always kept constant. Similarly, the contaminant is specified to have a resistivity of 3.95 Ωm at 23 ^{0}C. Hence the only variable is the cross-sectional area of the electrolytic pollution layer, determined by the flow rate of the contaminant. Increasing the flow rate results in an increased cross-sectional area, leading to a decrease in surface resistance and subsequent increased surface leakage current.

As discussed in section 2.4.4, tracking and erosion occurs as a result of stable DBA and the associated heating effects thereof. For the IPT, there is an optimum flow rate that will result in the most tracking and erosion. A flow rate that is too high will result in high leakage current, leading to flashover, but will not allow for drying of the insulator surface and associated DBA. A flow rate that is too low will not be able to sustain the leakage current required to cause damage. This is confirmed by Bruce et al [16]. IEC 06587 specifies flow rates for each test voltage. For example, at an AC test voltage of 3.5 kV_{rms}, a flow rate of 0.3 ml/min should be utilized. Questions remain however in terms of the correct flow rate to be used under DC, especially considering the polarity effect.

As seen in section 2.4.3, there are different views in terms of what the DC equivalent test voltage should be for the IPT. This in turn has led to different flow rates being applied for the various voltage levels. Ghunem et al made use of a standard flow rate but varied the DC test voltages to account for the effects of polarity [34]. This resulted in a flow rate of 0.3 ml/min being used for AC 3.5 kV_{rms}, + 2.25 kV and -3.0 kV DC. Bruce et al applied the recommended AC flow rates to the DC equivalent voltages, making use of a flow rate of 0.3 ml/min at ± 3.15 kV DC (the deemed equivalent DC voltage to 3.5 kV_{rms}) [16]. Heger et al chose identical rms voltage magnitudes for both their AC and DC tests, and as such made use of identical flow rates for AC and DC [39].

2.4.6 Electrode Performance during AC and DC IPT Tests

Due to the harshness of the IPT, erosion of the steel electrodes over the duration of a few AC tests is known to occur and these have to be replaced on a regular basis. However, many researchers have noted increased electrode erosion under DC energisation, and this can be attributed to the process of electrolysis.

Under DC +, the top steel electrode becomes actively anodic (positive) while the earth electrode at the bottom is forced to become 'partially' or 'temporarily' cathodic in relation to the top electrode. The chemical reaction taking place at the top steel electrode (anode) is:

$$Fe(s) \quad Fe^{2+}(aq) + 2e^{-} \qquad 2.3$$

This results in a decrease in electrode mass due to Fe moving into the contaminant solution. The cathodic reaction at the bottom electrode is as follows:

$$2H_2O(l) + 2e^{-} \quad H_2(g) + 2OH^{-}(aq) \qquad 2.4$$

The cathode in this case does not physically participate in the reaction.

Under DC -, the top steel electrode now becomes cathodic but does not physically partake in the reaction. The bottom earth electrode becomes 'partially' anodic and Fe moves into the contaminant

solution. The erosion, and mass loss, should not be as aggressive as under DC + as the bottom electrode is 'partially' anodic due to its earth characteristics.

Important variables affecting the degree of electrolysis include:

- Electrode composition
- Electrolyte composition (including pH, ionic strength, etc.)
- Voltage and Current levels
- Temperature of the system
- Arrangement of the anode, cathode and contaminant

Bruce et al observed substantial erosion of the top positive electrode (anode) under DC energisation. During DC + tests, mass loss in the region of 10 to 35 mg was noted on the top electrode, with the bottom grounded electrode (cathode) increasing in mass [17]. This can be attributed to the formation of iron oxide (Fe_2O_3) on the ground electrode. Dark discolouration of the grounded electrode was also noted. During DC - tests, the bottom electrode exhibited mass loss as well, however it was found to be less with a maximum loss of 18 mg being recorded.

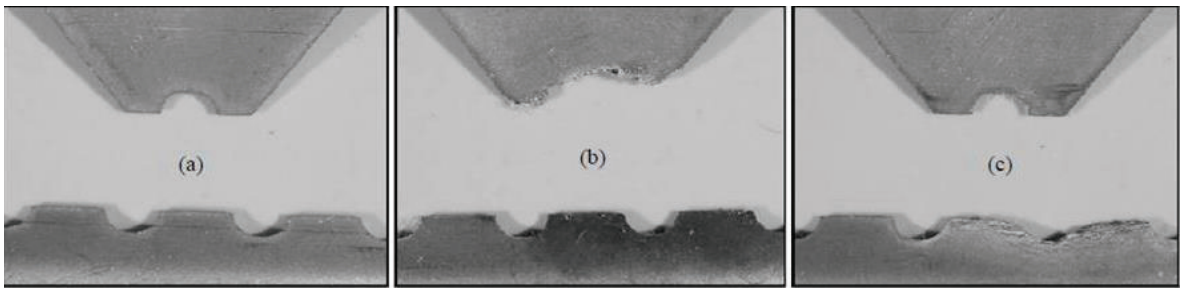

Figure 2-5: Steel electrodes used during DC IPT (a) before testing, (b) after 6 hr +2.7 kV DC test and (c) after 6 hr -2.7 kV DC test [17]

The contaminant always flows from the top electrode to the bottom, therefore, it is reasonable to assume that during the positive DC test, erosion of the top electrode as a result of electrolysis, and the resultant ion migration into the contaminant, results in increased contaminant conductivity. Under negative DC energisation, even though electrode erosion occurs to a lesser extent, the contaminant flowing over the material surface under test is not affected. The assumption then is that

under DC IPT testing, one of the reasons why the positive test is that much more severe than the negative test is due to increased contaminant conductivity under positive energisation.

Gorur et al tested HTV-SR and EPDM samples in a fog chamber under DC energisation, where electrode erosion resulting in weight loss of between 1 and 5 % of total weight was observed [25]. Various electrode materials were utilized, including aluminium, stainless steel, brass and copper. All experienced varying degrees of erosion resulting in premature flashover due to contamination of the contaminant as a result of electrode erosion. Gorur noted that the use of carbon electrodes resulted in decreased incidents of flashover with no electrode erosion being observed.

2.5. Cigre Working Group D1:27 Round Robin Tests

One of the objectives of the Cigre Working Group D1:27 (Material Properties for New and Non-ceramic Insulation) was to look at the feasibility of using the standard AC inclined plane test for the evaluation of polymeric insulating materials resistance to tracking and erosion under DC conditions. In order to achieve this outcome, a Round Robin Test (RRT) was conducted at four laboratories i.e. Zittau (Germany), ABB (Sweden), NGK (Japan) and Seves (France) over a period of 5 years between 2009 and 2014. The test specification defined for this RRT was based on the AC test parameters as defined in IEC 60587 but also included input from a Chinese Standard for 500kV DC long rod composite insulators - DL/T-810 (2002) wherein test parameters for a DC inclined plane tracking and erosion test were outlined [45]. The Cigre TB 611 lists one of the major issues encountered during these tests as being the erosion of the steel electrodes due to electrolysis under DC energisation [46]. This erosion was reported by all the participants in the study. The conclusion from the RRT tests conducted was that the results from the various test laboratories were not satisfactory to allow for standardisation and further investigation with improved test and equipment specification is required. Specific factors mentioned in the final report that still need to be investigated include flow rate of the contaminant, electrode corrosion, electrode surface roughness, stability of the power source and composition of the electrolyte.

2.6. Summary of Literature Review

The literature review shows that in general, composite insulators, particularly SR, have shown relatively good in-service experience when energised under HVDC. Data gathered from various utilities worldwide, shows minimal material degradation and good hydrophobicity for SR insulators installed in a range of pollution environments over an installed period of up to 25 years [11, 10, 18]. What has also been consistently noted is substantial end-fitting corrosion for HV insulators energised under HVDC.

Results of various tests conducted at natural ageing tests stations, where the performance of various formulations of SR and some EPDM insulators were energised under both AC and DC voltages, show in general that HTV SR provides good pollution performance with minimal material erosion [19]. Materials with higher filler concentration in the form of ATH showed better resistance to tracking and erosion, but had less of an effect in limiting leakage currents [20]. Most SR materials tested displayed good hydrophobicity throughout the test period. Corrosion of end-fittings was again noted on samples tested within natural ageing test stations [21].

Research from laboratory based tracking and erosion tests in the form of the 1000 hr salt fog test, the rotating wheel dip test and the IPT, conducted using both AC and DC voltages, was reviewed. Results from a 1000 hr salt fog test showed substantial erosion of aluminium, stainless steel, brass and copper electrodes under DC energisation, resulting in early flashover [25]. It was also noted that filler type and percentage played a crucial role in the ability of the material to withstand tracking and erosion. In addition, the mechanism by which fillers impart tracking and erosion resistance was found to be the same for AC and DC.

Results from the DC rotating wheel dip test showed that in the beginning, hydrophobicity was good and leakage current was limited to under 10 mA. However, within 100 hrs(of the prescribed 1000 hrs), hydrophobicity reduced drastically leading to increased leakage currents and greater degradation [29]. Similarly to the 1000 hr salt fog test, corrosion of the end-fittings was observed

during the tracking wheel test, with brown deposits being observed on samples at the end of the test [32].

A review of the IPT adapted for DC application showed that the factors influencing the outcome of the test include the amplitude of the applied voltage, the filler material utilised, contaminant flow rate and the erosion of the steel electrodes.

The philosophy employed by certain researchers was to determine an equivalent ± DC voltage that would result in the equivalent material performance as that would be experienced under AC energisation. This was based on tests using a specific filler percentage and flow rate. For work done by both Ghunem et al [37] and Cherney et al [38], coefficients of 67 % and 84 % were found for DC + and DC – respectively, as a percentage of the standard AC test voltage. This was eventually rounded off to 70 % and 90 % for DC + and DC –, respectively. Hence if tests were conducted at AC voltages of 3.5 kV_{rms}, the equivalent DC + and DC – voltages utilised would be 2.45 kV for DC + and 3.15 kV for DC - . Bruce et al determined the equivalent voltage by calculating the area under half the period of an AC wave (also known as the average voltage), and for 3.5kV_{rms}, utilised 3.15 kV for both polarities DC [17]. Heger et al utilised the rms values for both AC and DC, arguing that the erosion of composite insulator material is an energy driven process and the use of rms values for both AC and DC provides an equal basis on which to evaluate the polarity effect of AC vs DC [15, 40]. For this work, the same philosophy was employed, with test voltages of 4.5 kV_{rms} AC and ± 4.5 kV DC being utilised.

The research reviewed shows that in general HTV SR materials utilizing ATH as filler, with a filler percentage greater than 40 % performed best during both the AC and DC versions of the IPT [41, 43]. For this work, HTV SR samples with a filler percentage of 50 % were utilised.

The standard AC IPT procedure prescribes contaminant flow rates for the various test voltages. As there are differing views in terms of the equivalent DC test voltage in relation to AC, certain researchers applied varying flow rates in relation to their chosen test voltages. For this work,

equivalent AC and DC test voltages were utilised, hence identical contaminant flow rates of 0.6 ml/min were utilised for both the AC and DC tests.

Numerous researchers reported extensive erosion of steel electrodes under DC energisation during the IPT [16, 17]. This was particularly evident for the top live electrode under DC + energisation and for a range of various electrode materials such as aluminium, stainless steel, brass and copper [25]. These observations were confirmed by a RRT done by Cigre working group D1.27. The results published in Cigre TB 611 emphasise the erosion of steel electrodes as being a major impediment to ensuring repeatability of the DC IPT. Work done by Gorur et al showed that the use of carbon electrodes, as a substitute for steel, resulted in decreased incidents of flashover and that no electrode erosion was observed. For this work, carbon glass electrodes have been utilised in conjunction with standard steel electrodes in order to gauge the effect of electrode erosion on the outcome of the DC IPT.

3 RESEARCH METHODOLOGY

3.1. Overview

This chapter describes the testing methodology that was designed in order to answer the research questions and achieve the research objective as outlined in Chapter 1. This is discussed under the following headings:

- Choice of test procedure, test methods and test parameters
- Choice of electrode material
- Choice of insulator material
- Choice of Contaminant
- Electrode material combinations for AC and DC tests
- Procedure for reliability and repeatability of test programme

3.2. Choice of Test Procedure, Test Methods and Test Parameters

As discussed in section 2.2.2, two internationally recognised inclined plane test procedures exist for the testing of composite insulator materials susceptibility to tracking and erosion, these being the IEC 60587 standard and the ASTM D2303 standard. Both standards specify testing parameters and criteria for AC energisation. In South Africa, the energy utility Eskom bases most specifications relating to HV Insulators on IEC specifications and guidelines. Hence, for the purposes of this research, the IEC 60587 standard was utilised for AC testing and adapted for both polarities DC energisation as well.

The IEC 60587 standard allows for two methods of testing to be utilised:

- Method 1: constant tracking voltage, and
- Method 2: stepwise tracking voltage

With method 1, a fixed voltage is maintained for the full duration of the test, which is stipulated as 6 hours. With method 2, a starting voltage is selected and maintained for the first hour, where after the voltage is increased in steps of 250 V for each subsequent hour, until failure occurs. Method 2 requires that the contaminant flow rate, as well as the resistance value of the series resistor, be steadily

increased with the increase in voltage. For the purpose of this work, method 1 was utilised so as to ensure uniformity of test voltage level and contaminant flow rate for all tests conducted.

The standard recommends test voltages of either 2.5, 3.5 or 4.5 kV, at associated flow rates of 0.15, 0.3 and 0.6 ml/min, respectively. For this work, a test voltage of 4.5 kV_{rms} for AC and both polarities DC, at an associated contaminant flow rate of 0.6ml/min, was chosen. These test parameters were deemed to be best suited to highlight the effect of electrolysis and resultant electrode erosion under DC energisation.

IEC 60587 lists two failure criterion, i.e:

- Criterion A: Leakage current in excess of 60 mA for longer than 2 seconds, or the specimen exhibits a hole due to intensive erosion or the specimen ignites
- Criterion B Tracking in excess of 25 mm from the lower electrode, or the specimen shows a hole due to intensive erosion or the specimen ignites.

For this work, results were evaluated against both criterion.

3.3. Choice of Electrode Material

The main objectives of the study were to show that steel electrode erosion occurs under DC energisation during the inclined plane test, to quantify the effect that this has on material performance and then to investigate if the use of a substitute electrode would result in improved repeatability of the test. AC and DC inclined plane tests were conducted using standard steel electrodes as specified by IEC 60587. In addition, special carbon glass electrodes, with dimensions similar to that of the standard steel electrodes, were procured and introduced into the test to ascertain whether this type of electrode material would eliminate/reduce the impact of steel electrode erosion. According to the manufacturer, carbon glass as a material possesses extreme corrosion resistance, exhibits high hardness and strength, is extremely resistant to thermal shock and has good electrical conductivity. It was thus considered to be a suitable alternative electrode material. Steel and carbon glass electrodes used for this research can be seen in Figures 3-1 and 3-2.

3.3.1 Steel Electrodes

The steel electrodes, shown in Figure 3-1, were manufactured, as per the standard, from grade 302 stainless steel. They were 0.5 mm thick and weighed on average 14 and 4 grams for the top and bottom electrodes, respectively.

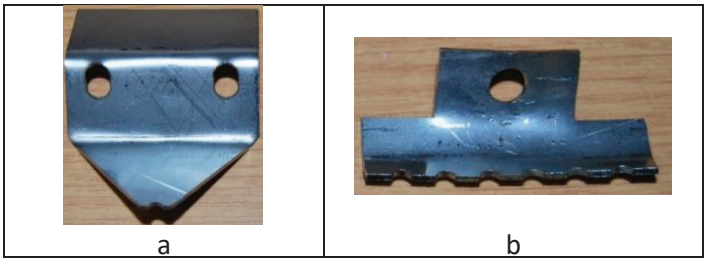

Figure 3-1: Stainless steel top (a) and bottom (b) electrodes.

3.3.2 Carbon Glass Electrodes

The carbon glass electrodes, shown in Figure 3-2, were manufactured to specification by Sigradur in Germany. It was important that the shape of the carbon glass electrodes be as close as possible to that of the steel electrodes. Slight adjustments were required in terms of mounting of the glass electrodes. On average both the top and bottom electrodes weighed roughly 0.5 grams.

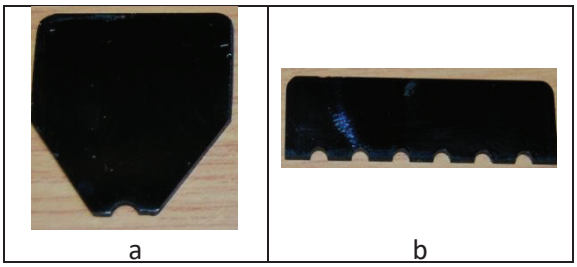

Figure 3-2: Carbon glass top and bottom electrodes.

3.4. Choice of Insulator Material

In order to minimise variability, a single formulation of commercially available HTV silicone rubber was tested. Table 3-1 lists the complete chemical composition of the material, with Aluminium Trihydrate (ATH) filler and Siloxane Polymer making up the largest portion of the material at 51% and 36% respectively. Figure 3-3 shows a standard test sample. The dimensions of the test samples were 120 x 50 x 6 mm (as per IEC 60587 requirements) and weighed approximately 57 grams.

Table 3-1: HTV SR sample composition.

Material	% Composition
Siloxane Polymer	36
Fumed Silica Reinforcement	10
Aluminium Trihydrate (Surface Treated)	51
Pigment	0.3
Process Additives	2
Antifungal Oxide	0.7
TOTAL	**100**

Figure 3-3: HTV SR test sample.

3.5. Choice of Contaminant

A combination of ammonium chloride (0.1 % ± 0.002 by mass) and Triton X-100, which acts as a wetting agent, was utilised to ensure a contaminant conductivity of 2.53 mS/cm ± 0.03 @ 23°C (resistivity of 3.95 Ωm)

3.6. Electrode Material Combinations for AC and DC Tests

The inclined plane test apparatus utilised had capacity for testing five samples simultaneously, however for direct comparison of performance between the steel and carbon glass electrodes, it was decided from the outset that only two stages would be utilised per test. Table 3-2 shows the sequence of electrode configuration that was utilised for each voltage type. A total of nine tests were conducted, i.e. three AC, three DC+ and three DC-.

Table 3-2: Electrode combinations for AC and DC tests.

Test No.	Voltage Type	Sample 1 Electrode	Sample 2 electrode
1	AC	Steel	Steel
2	AC	Steel	Glass
3	AC	Glass	Glass
4	DC+	Steel	Steel
5	DC+	Steel	Glass
6	DC+	Glass	Glass
7	DC-	Steel	Steel
8	DC-	Steel	Glass
9	DC-	Glass	Glass

3.7. Procedure for Reliability and Repeatability of Test Programme

For each of the tests listed in Table 3-2, a detailed systematic process was followed to ensure reliability and repeatability of the test programme. The form used for recording the data for each test can be found in Annexure 1. The form also provides an outline of the procedure followed pre-test, during the test and post-test. The remainder of this section discuss some of the most important aspects of the form, e.g., details of the measurements that were done and recorded as well as test parameters that were documented.

3.7.1 Pre-testing

Prior to the start of each test, the date was recorded. The contaminant conductivity was checked to ensure compliance to the specification and recorded. The temperature and humidity within the mobile test laboratory were measured and recorded. The type of voltage to be used, i.e. AC, DC+ or DC-, as well as actual measured amplitude was recorded for each test.

Each test sample was marked with a unique number (date and test position) on the back. The test surface of each sample was cleaned using ethyl alcohol to remove all debris. Thereafter each sample was weighed and photographed prior to installation, and the weight and photo number recorded.

For each test, the correct electrode type was identified according to Table 3-2. The electrodes were then weighed and photographed prior to installation and the weight and photo number recorded. For each sample on test, a filter paper reservoir consisting of 8 layers of filter paper was cut according to the template set out in IEC 60587. Prior to energisation, the peristaltic pumps were turned on to initiate contaminant flow. This allowed for the contaminant flow to be checked for consistency and uniformity prior to samples being energised.

From a safety perspective, all interlocking mechanisms were checked prior to energisation. For DC tests, the capacitor bank utilised was equipped with a discharge switch, connected to ground via a resistor and it was important to verify that the switch was open prior to energisation.

3.7.2 During test

The start time of the test was noted. The test voltage was switched on and adjusted via a variac located on the control panel, until the required test voltage was reached. This voltage was measured using a Fluke multimeter attached to a voltage probe connected to the HV supply.

Detailed field notes were recorded whilst testing was in progress. To enhance the visual observation with regards to leakage current activity, contaminant flow and material degradation as well as to provide an accurate time stamp for the various observations that were noted during the test process, video recordings were made. Each test was video recorded as follows:

- The first hour was recorded in 3 x 20 minute intervals.
- At commencement of the 3rd hour, 1 x 20-minute recording was conducted.
- At commencement of the 5th hour, 1 x 20-minute recording was conducted.

At the start of each test, the leakage current logger was checked to ensure that all leakage current data was being recorded. At the end of the test, the supply voltage was switched off and the test apparatus made safe. The end time of the test was noted.

3.7.3 Post test

Samples were carefully removed from the test apparatus and detailed photographs were taken to illustrate damage. Samples were weighed and weights and photo numbers recorded. Electrodes were carefully removed and weighed and photographed and the weights and photo numbers recorded. Test samples and electrodes were stored in separate airtight labelled containers for further analysis.

3.8. Summary

This chapter described the processes that were followed in conducting AC and both polarities DC inclined plane tests according to the IEC 60587 test procedure, with the introduction of a new electrode material in form of carbon glass.

4 TEST EQUIPMENT

4.1. Overview

A five-stage inclined plane mobile test laboratory, housed within a 6 m container, was procured in order to address the research questions outlined in chapter 1. The complete test rig was placed within an Eskom substation, powered via a 220 V supply from a relay room and connected to the general substation earth mat. The original test rig was supplied with an integrated 220 V/6 kV AC/DC transformer unit as seen in Figure 4-1 below.

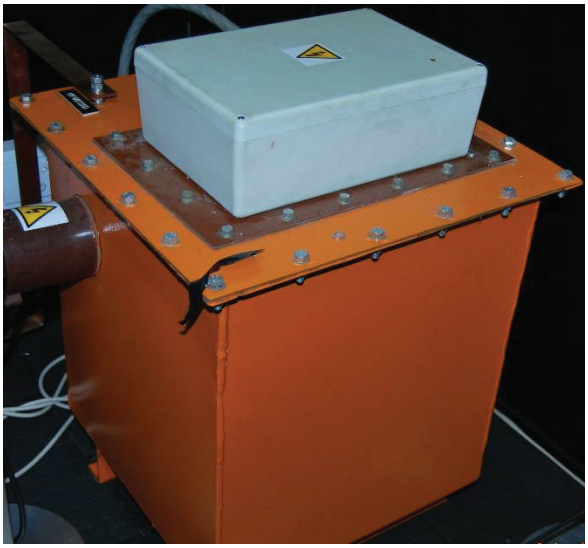

Figure 4-1: 220 V/6 kV AC/DC Transformer.

This transformer unit housed a bridge rectifier circuit that would be engaged via the selection of various link combinations to provide DC voltage. During commissioning, this transformer and bridge rectifier combination was found to be incapable of meeting the full load volt drop criteria of ± 5% specified by IEC 60587. Hence, before any testing could commence, an adequate voltage supply had to be acquired and this involved the sourcing of an alternate transformer and the design and construction of a suitable DC rectifier.

This chapter focusses predominantly on the processes employed to design, construct and test the revised voltage source. In addition, measuring equipment that was utilised is also discussed.

4.2. AC Power Supply and DC Rectifier Circuit

A schematic diagram of the test set-up including two transformers and the full-bridge DC rectifier circuit is shown in Figure 4-2.

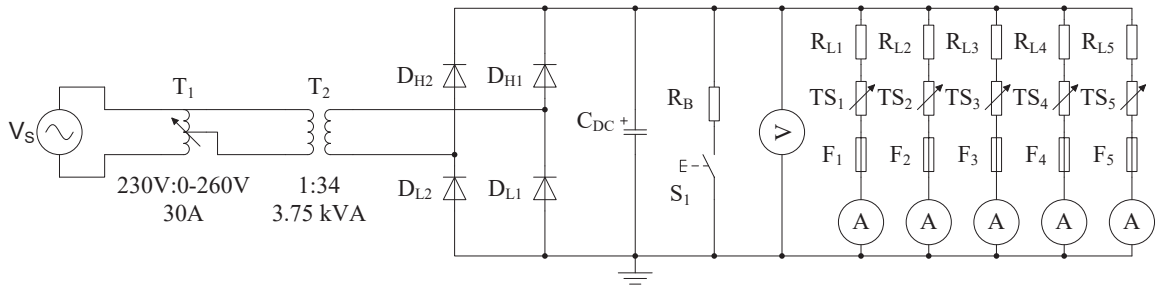

Figure 4-2: Transformer and DC rectifier circuit diagram.

Power to the test rig was supplied by a 230 VAC, 50 Hz wall socket indicated by V_s. The supply was passed through a single-phase variable transformer T_1 with a variable output of 0-260 V and a maximum output current of 30 A. The output from the variable transformer fed a 3.75 kVA step-up transformer T_2 with a 1:34 winding ratio and a maximum output voltage rating of 7.5 kV. Each of the five test bays consisted of a 33 kΩ limiting resistor $R_{L(n)}$ in series with the test sample TS_n and a 63 mA fuse F_n for protection, as per IEC 60587 specification [8].

At a test voltage of 4.5 kV, and with a current limiting resistor of 33 kΩ in series with the test sample, the current requirements to drive five test bays under simultaneous short circuit or flashover conditions are $136\ mA\ \times 5 = 680\ mA$. The total power of the load was

$$P_{load} = V \times I$$
$$= 4.5\ kV\ \times 680\ mA$$
$$= 3.06\ kVA$$

which was within the 3.75 kVA power rating limit of the step-up transformer. With a winding ratio of 1:34, the load current of five test bays on the low-voltage side of the step-up transformer was 23.12 A at a test voltage of 4.5 kV and was also within the 30 A current limit of the variable transformer. This met the requirements for AC testing.

Short circuit AC tests were conducted to determine the volt drop under flashover conditions using both one and two test bays. This was done by removing the test sample from the network and connecting the HV supply to ground via the 33 kΩ limiting resistor. The results of these tests are shown in Table 4-1.

Table 4-1: Recorded volt drop at full load AC.

No of Bays	V_{nl} (v)	V_{fl} (v)	I_L (mA)	V_d (%)
1	4511	4322	159	4.2
2	4515	4311	314	4.5

IEC 60587 stipulates that each stage must have the capacity to provide 100 mA within the required volt drop limitations. The two stage short circuit test showed that with a load current of 314 mA, the volt drop would be within specification, thus proving that the test configurations would meet the AC test requirements for three stages. Certain limitations prevented further testing to determine the short circuit volt drop for 3 or more stages. This was not seen as a limiting factor, as the test methodology decided upon only required the use of 2 stages.

For DC testing, a full bridge rectifier was designed and built in accordance to Figure 4-2. The rectifier consisted of four high-voltage diode modules in a full-bridge configuration where D_{H1} and D_{H2} denote the high-side diodes and D_{L1} and D_{L2} denote the low-side diodes. Each diode module consisted of a string of ten diodes connected in series with their accompanying snubber capacitors and balancing resistors as shown in Figure 4-3 (a).

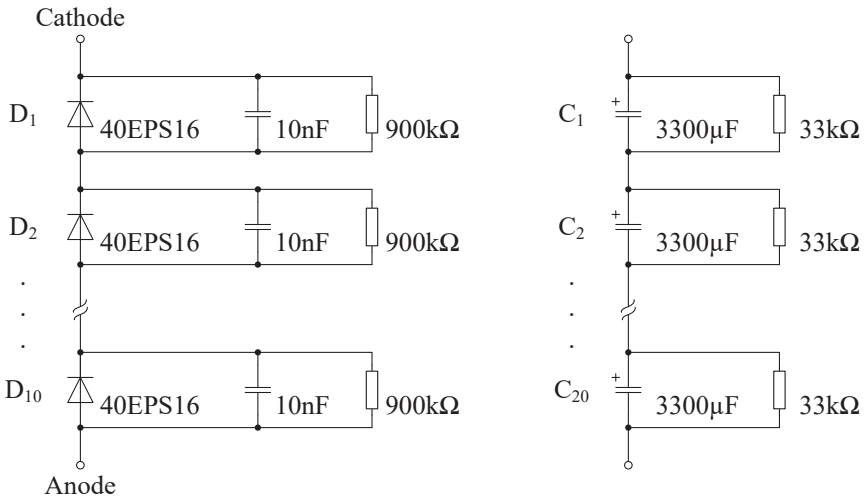

Figure 4-3: High voltage diode modules (a) and High voltage capacitors (b).

Each diode module was rated for a reverse blocking voltage of 16 kV. The test chamber was designed for a maximum test voltage of 6 kV_{AC} (8.48 kV_{peak}). In the full-bridge configuration each diode module should withstand the peak applied voltage of 8.48 kV, which leaves a wide safety margin. In the forward bias mode, the diode module was rated for a maximum forward voltage of 11.4 V at the rated current of 40 A. In this application each test bay was protected by a 63 mA fuse. which amounted to a maximum total current of 315 mA under worst case conditions. The diode module was therefore more than sufficient to handle the required current capabilities during a fault condition.

The high-voltage DC-bus capacitor C_{DC} was rated for 165 µF, 9 kV. The capacitor consisted of twenty smaller 3300 µF, 450 V electrolytic capacitors that were series stacked as shown in Figure 4-3 (b). To ensure that the voltage across the capacitors remains balanced, 33 kΩ resistors were placed in shunt with each capacitor. A discharge resistor R_B and discharge switch S_1 was placed in shunt with C_{DC} as a safety mechanism to discharge the capacitor when the test chamber was not in operation. The voltage measurement was taken across the DC-bus capacitor. The completed rectifier and capacitor bank is shown in Figure 4-4.

Figure 4-4: Completed DC rectifier and capacitor bank.

The voltage ripple on the DC-bus is dependent on the load current and is obtained by the following equation

$$V_{pp} \approx \frac{I_{load}}{2fC},$$

where I_{load} is the load current, f is the line frequency and C is the DC-bus capacitance. The maximum ripple component is calculated for three scenarios where a 4.5 kV DC voltage is applied:

For five test bays the peak-to-peak ripple voltage, when a maximum test current of 136 mA is present at each bay, is

$$V_{pp(5\ test\ bays)} = \frac{I_{load}}{2fC}$$

$$= \frac{680\ mA}{2 \times 50 \times 165\ \mu F}$$

$$= 41\ V$$

which constitutes a ripple component of 0.9 %. For two test bays the peak-to-peak ripple voltage, when a maximum test current of 272 mA is present at each bay is 17 V, which constitutes a ripple component of 0.37%. For one test bay, the calculated ripple component was 0.18 % (8 V).

Short circuit DC tests, similar to those done for AC, were conducted to determine the volt drop under flashover conditions using both one and two test bays. The measured results are shown in table 4-2.

Table 4-2: Recorded volt drop at full load DC.

No of Bays	V_{nl} (v)	V_{fl} (v)	I_L (mA)	V_d (%)
1	4530	4480	131	1.1
2	4550	4450	251	2.2

4.3. Measuring and Recording Equipment

The following equipment was utilised to assist in capturing the test conditions and data that was produced whilst conducting the various tests:

- An Online Leakage Current Analyser (OLCA) and various sensors to capture leakage currents across the surface of the test samples and environmental data within the test laboratory.
- A Tektronix high voltage probe (P6015A) connected to a Fluke multimeter to measure the HV supply voltage.
- A Nikon D5600 digital SLR camera to record photos of degradation and videos of leakage current activity on the surface the test samples
- A Citizen CX301 precision balance to weigh both the test material and electrodes prior to and after each test
- A GMH 3410 digital conductivity meter to measure contaminant conductivity
- A 5 ml syringe to measure contaminant flow rate.

Each of these instruments are discussed in more detail below.

4.3.1 Online Leakage Current Logger and Associated Sensors

One of the failure criteria for the IPT is leakage current across the surface of the test sample in excess of 60 mA for longer than 2 seconds. As such, a device to continuously monitor and record the test sample leakage current was required. The Online Leakage Current Analyser (OLCA), shown in Figure 4-5, is a device that was designed and manufactured for research conducted at KIPTS [47]. It is a data acquisition system that has the ability to receive input from 9 individual leakage current sensors as well as a combined temperature and humidity probe, a wind speed and direction sensor, a rain gauge and a UVB Ultraviolet sensor. For the purposes of this work, only the leakage current sensors, shown

in Figure 4-6, and the combined temperature and humidity probe, shown in Figure 4-7, were utilised. The AC and DC leakage current sensors make use of high accuracy hall effect transducers which are galvanically isolated up to 6kV and have a bandwith of 0 to 10 kHz. The logger samples at 2 kHz continuously and saves the following time stamped parameters every 10 minutes:

- Highest positive and negative peak values of leakage current
- Positive and negative leakage current pulse counters
- Positive and negative average value of leakage current
- The RMS value of leakage current
- Maximum leakage current waveform per test cycle

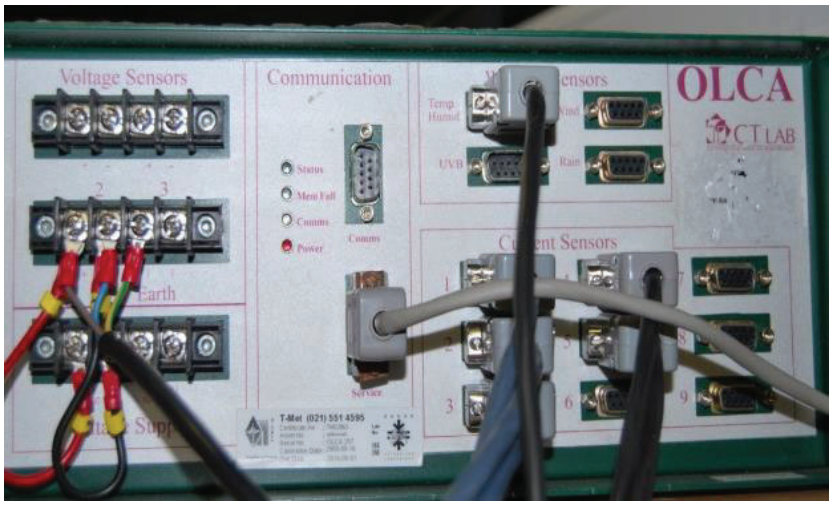

Figure 4-5: Photograph of OLCA logger.

Figure 4-6: Photograph of Leakage current sensor.

Figure 4-7: Temperature and humidity sensor.

Data stored on the hard drive of the OLCA can be extracted to a database for further analysis using the OLCA software. For this work, only the rms leakage current values for the various tests were analysed and reported on in chapter 5.

4.3.2 Tektronix High Voltage Probe

In order to measure the exact voltage applied the test samples, a Tektronix P6015A ground-referenced 100 MΩ, 3.0 pF high voltage probe with 1000X attenuation was utilised. This was used in conjunction with a Tektronix TDS3014C Digital Phosphor Oscilloscope as well as a standard Fluke multimeter.

4.3.3 Nikon D5600 Digital Camera

It was critically important that detailed visual observations in relation to damage and degradation on both the material samples as well as the electrodes be accurately documented and recorded. In order to achieve this, a Nikon D5600 digital SLR camera. Besides the high resolution still photos that are possible with this camera, it is also capable of producing full HD 20-minute video recordings at 60 frames per second, which allowed for detailed visual observations of leakage current activity of the surface of the test samples throughout various stages of the test cycle.

4.3.4 Precision Scale

In order to measure minute weight difference pre and post-test, an accurate scale with sufficient resolution was required. A Citizen CX301 precision balance, shown in Figure 4-8, with a weight capacity of 300 grams and a resolution of 0.0001 grams, was utilised to measure the weight difference of the SR test samples as well as the steel and carbon glass electrodes, before and after each test.

Figure 4-8: Precision scale for weighing of test samples and electrodes.

4.3.5 Conductivity Meter

Prior to each test, the resistivity of the contaminant was checked to ensure that it conformed to the requirement of 3.95 Ωm at 23 ^{0}C. This was done using a Greisinger GMH 3410 digital conductivity meter, shown in Figure 4-9 below.

Figure 4-9: Conductivity meter.

4.3.6 Measuring Flow Rate

Table 1 of IEC 60587 stipulates that for a test voltage of 4.5 kV, a contaminant flow rate of 0.6 ml/min is required. Measurement of the flow rate was done by noting the time taken to fill a 5 ml syringe. A flow rate of 0.6 ml/min was confirmed for the purposes of this test.

5 RESULTS

5.1. Overview

This chapter outlines the results obtained from AC, DC + and DC – inclined plane tests conducted according to IEC 60587, using the standard AC test procedure adapted for DC application. The constant tracking voltage method was utilised, at a test voltage of 4.5kV, and a contaminant flow rate of 0.6 ml/min, for both AC and DC tests.

Results are presented in the following order for AC, DC + and DC –:

- Visual observations in relation to HTV SR material degradation, Dry Band Arcing (DBA) across the surface of the test sample, electrode damage and contaminant flow.
- Measured leakage current.
- Mass loss (gain) on electrodes and SR test samples.

A single formulation of HTV SR material, with a 51 % filler content, was utilised for all the tests. For the purpose of this study, tests were conducted using both standard steel electrodes, as prescribed by IEC 60587, as well as carbon glass electrodes. Two samples were tested at a time, which allowed for various configurations of steel/glass electrode combinations to be tested for each of the voltage types.

Results are evaluated in relation to failure criteria defined by IEC 60587 and listed below:

- Leakage current across the specimen exceeds 60 mA or the specimen exhibits a hole due to erosion or the material ignites.
- Tracking on the specimen reaches a distance of 25 mm from the lower electrode or the specimen exhibits a hole due to excessive erosion or the specimen ignites.

5.2. AC Test Results

5.2.1 Visual Observations

Visuals observations of material degradation on HTV SR test samples were conducted every 15 minutes during the first hour of each test, again after 180 minutes, 300 minutes and at the end of the

test (i.e. 360 minutes). In addition to material degradation, electrical activity in the form of DBA was observed and is discussed. Due to the nature of the test setup, visual observations of electrode degradation could only be done at the end of the test. As the nature of the contaminant flow has a fundamental impact on the outcome of the test, this was carefully observed throughout the duration of the test and is reported on as well.

5.2.1.1 HTV SR Material Degradation

5.2.1.1.1 Tests with Steel Electrodes

Figure 5-1 shows a time-lapse photo of the test conducted using steel electrodes for both samples. Within 15 minutes of energisation, slight blackening of the material surface was observed close to the ground electrode (Figure 5-1 b). This blackening was located on either side of the contaminant flow path. This blackening intensified as the test progressed, with tracking being observed within 60 minutes (Figure 5-1 e). A slight brown residue was also observed alongside the blackened area as well as in the area of the ground electrode. Light erosion of the SR material was observed close to the ground electrode. Although the test ran for the full duration, both samples are considered to have failed the test as the length of the tracks observed exceeded the minimum pass criteria of 25 mm. The measured tracking distance was 30 mm for sample 1 and 34 mm for sample 2.

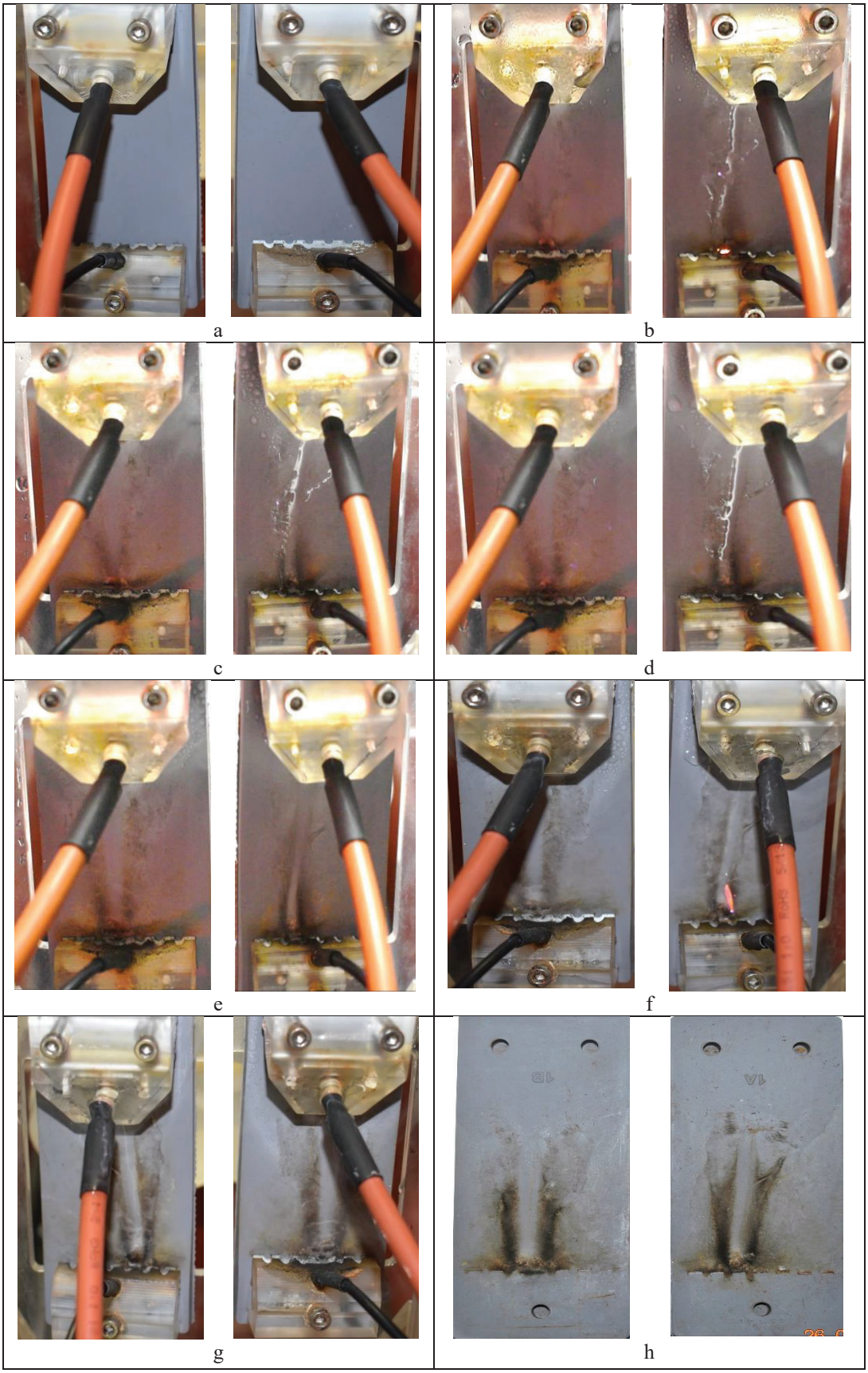

Figure 5-1: Time-lapse photo of the two HTV SR samples, i.e. Sample 1 (left) and Sample 2 (right) with AC voltage applied to the electrodes, which are both steel electrodes, at the following durations after the start of the test: (a) 0 minutes, (b) 15 minutes, (c) 30 minutes, (d) 45 minutes, (e) 60 minutes, (f) 180 minutes, (g) 300 minutes and (h) 360 minutes.

5.2.1.1.2 Tests with combination of Steel and Glass Electrodes

Figure 5-2 shows a time-lapse photo of the test conducted using steel electrodes for sample 1 and glass for sample 2. Slight blackening of both HTV SR test samples close the ground electrode was observed within the first 15 minutes of energisation, as can be seen in Figure 5-2 (b). This progressed to tracking on sample 1 within 60 minutes (Figure 5-2 (e)). Sample 2 continued to show blackening throughout the test period, however it did not progress to tracking. Sample 1 failed the test due to tracking in excess of 25 mm (33 mm), seen in Figure 5-2 (h), while sample 2 passed the test. Slight erosion was observed on sample 1. A brown residue was also observed on sample 1. No erosion or any other colour changes were noted on sample 2.

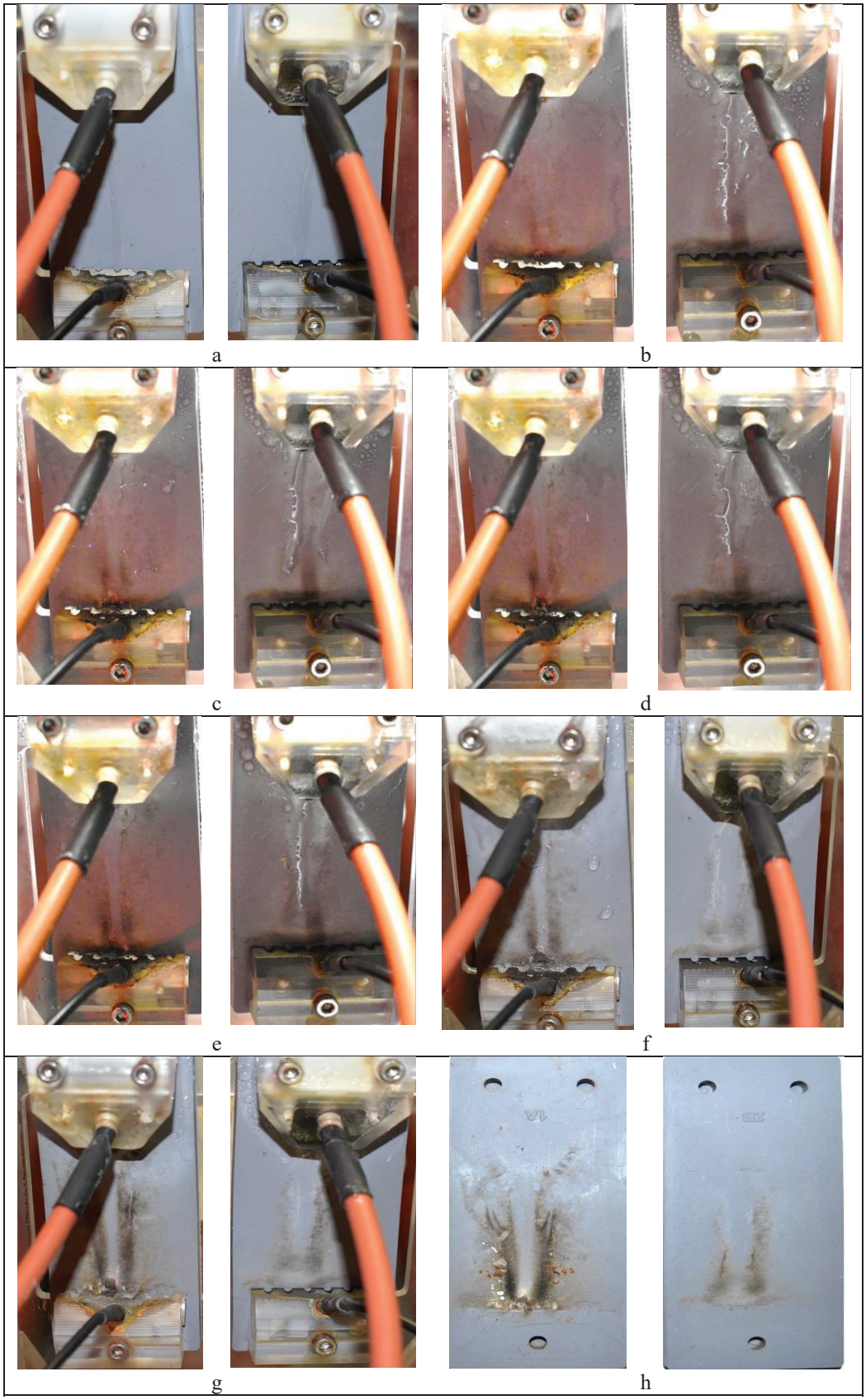

Figure 5-2: Time-lapse photo of the two HTV SR samples, i.e. Sample 1 (left) and Sample 2 (right) with AC voltage applied to the electrodes, sample 1 being steel and sample 2 glass, at the following durations after the start of the test: (a) 0 minutes, (b) 15 minutes, (c) 30 minutes, (d) 45 minutes, (e) 60 minutes, (f) 180 minutes, and (g) 300 minutes and (h) 360 minutes.

5.2.1.1.3 Test with Glass Electrodes

Figure 5-3 shows a time-lapse photo of the test conducted using glass electrodes for both samples. Slight blackening was observed on sample 1 within 30 minutes of energisation, with both samples exhibiting blackening within the first 60 minutes of the test (see Figure 5-3 (e)). At 300 minutes, tracking was observed on sample 1, with severe blackening noted on sample 2, shown in Figure 5-3 (g). Slight erosion was observed on sample 1.

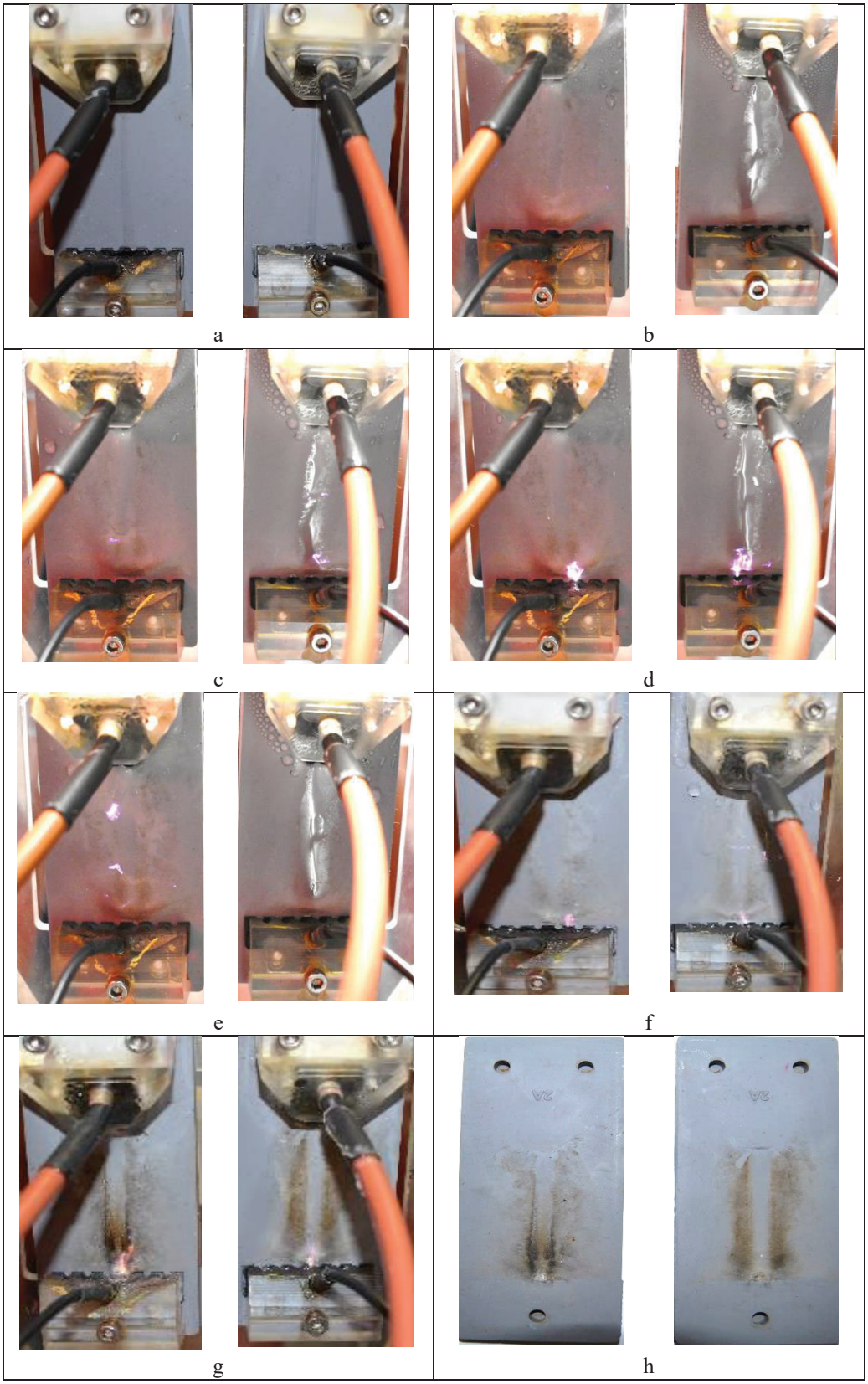

Figure 5-3: Time-lapse photo of the two HTV SR samples, i.e. Sample 1 (left) and Sample 2 (right) with AC voltage applied to the electrodes, which are both carbon glass electrodes, at the following durations after the start of the test: (a) 0 minutes, (b) 15 minutes, (c) 30 minutes, (d) 45 minutes, (e) 60 minutes, (f) 150 minutes, and (g) 300 minutes and (h) 360 minutes.

5.2.1.2 Electrode Degradation

5.2.1.2.1 Tests with Steel Electrodes

Figure 5-4 shows photos of both the live and ground steel electrodes for samples 1 and 2 taken at the end of the AC test. No visual degradation was observed on either of the two live steel electrodes (Figure 5-4 (a & b)). Slight blackening of the tip of the electrode on sample 2 was noted. A brown circle was noted at the point where the HV supply made contact with the electrode material on both live electrodes. The ground electrodes on both samples had a dark brown residue across the entire surface (Figure 5-4 (c & d)), with slight blackening in the areas where tracking and material erosion occurred. No other visible material loss or degradation was observed on the ground electrodes.

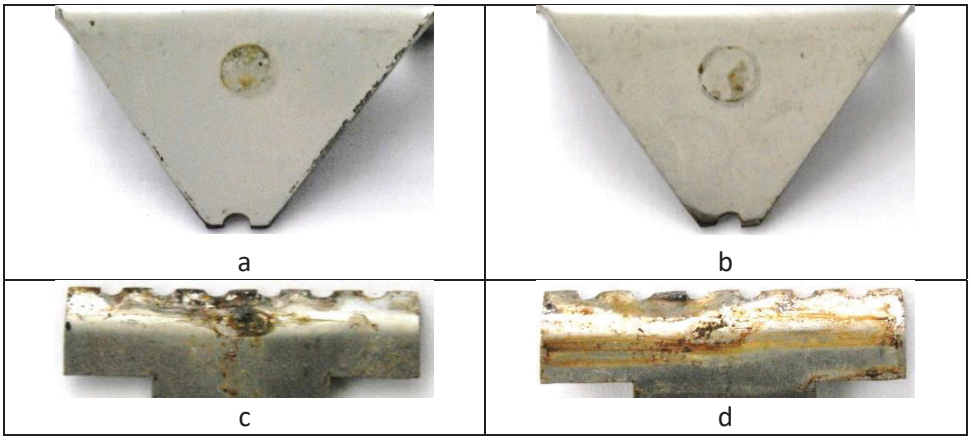

Figure 5-4: Photo of electrodes at end of test, i.e. Sample 1 live and ground steel electrode (left) and Sample 2 live and ground steel electrode (right), with AC voltage applied.

5.2.1.2.2 Tests with combination of Steel and Glass Electrodes

Figure 5-5 shows photos of both the live and ground electrodes for samples 1 (steel) and 2 (carbon glass) taken at the end of the AC test. No visible damage was observed on the live steel electrode of sample 1. The ground steel electrode had a dark brown residue, with blackening in areas where tracking and erosion of SR material took place (Figure 5-5 (c)). Both the live and ground carbon glass electrodes of sample 2 showed no signs of damage, with the ground electrode having a green residue in the area where the HV supply made contact with the electrode. Neither the tips nor the teeth of both the glass and steel electrodes showed any signs of wear.

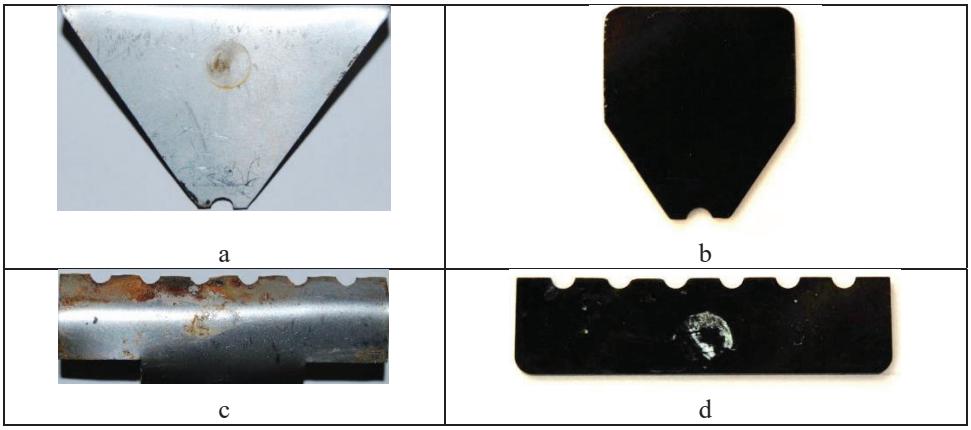

Figure 5-5: Photo of electrodes at end of test, i.e. Sample 1 live and ground steel electrode (left) and Sample 2 live and ground carbon glass electrode (right), with AC voltage applied.

5.2.1.2.3 Test with Glass Electrodes

Figure 5-6 shows photos of both the live and ground carbon glass electrodes for samples 1 and 2 taken at the end of the AC test. Both live glass electrodes showed no signs of damage. The ground electrode of sample 1 showed slight damage on one of the middle teeth (Figure 5-6 (c)), in the vicinity of the localised stable DBA that formed during the latter part of the test. Discolouration at the HV source point of contact was noted on all electrodes. Whitening and residue was observed on the ground electrode of sample 1.

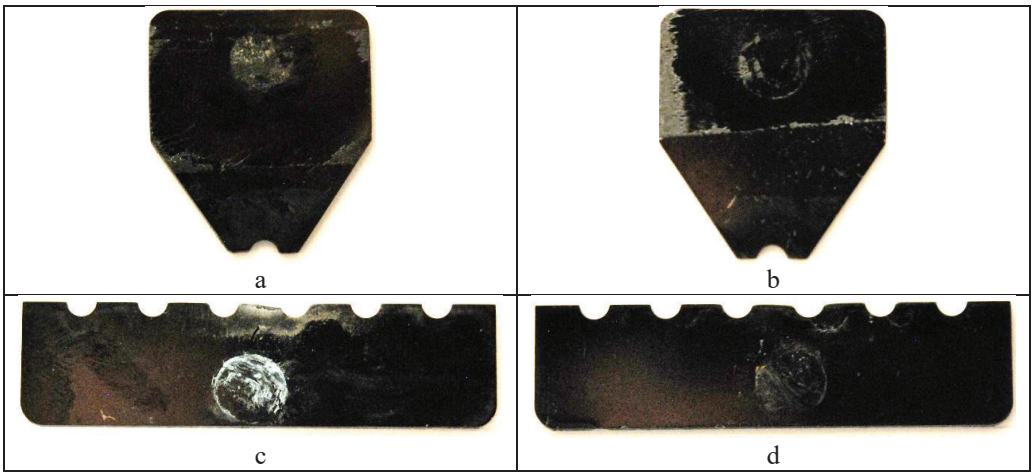

Figure 5-6: Photo of electrodes at end of test, i.e. Sample 1 live and ground carbon glass electrode (left) and Sample 2 live and ground carbon glass electrode (right), with AC voltage applied.

5.2.1.3 Contaminant Flow Observations

5.2.1.3.1 Tests with Steel Electrodes

At the beginning of the test, a steady consistent flow rate was established on both samples. The contaminant flow path on sample 1 tended to be more random early on in the test, as opposed to sample 2 which formed a direct steady stream from the live to the ground electrode, visible in Figure 5-7 below. Within 50 minutes of the test commencing, flow ceased on channel 2, and the test had to be suspended in order for the flow to be re-established. The establishment of a channel with blackening and tracking marks on either side on both samples, resulted in the consistent flow of contaminant in a steady stream from the live to the ground electrode, which continued for the remainder of the test.

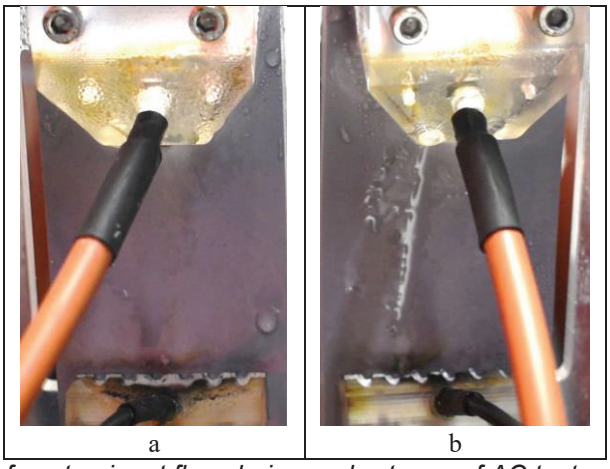

Figure 5-7: Photo of contaminant flow during early stages of AC test on samples 1 and 2 using steel electrodes.

5.2.1.3.2 Tests with combination of Steel and Carbon Glass Electrodes

The test commenced with consistent flow on both samples, as shown in Figure 5-8. Visually, the flow on sample 2 seemed to be slightly more than sample 1. The flow on sample 1 tended to be more random, as opposed to sample 2 which flowed in a more direct line. This was particularly evident within the first 10 minutes of energization. The commencement of blackening of the material close to the ground electrode resulted in a defined path for the contaminant to flow. A visible decrease in contaminant flow on sample 1 was noted roughly 50 minutes into the test, with flow ceasing after 70 minutes. Intermittent flow problems were experienced on sample 1 over a period of 30 minutes, where after normal flow was established until the end of the test.

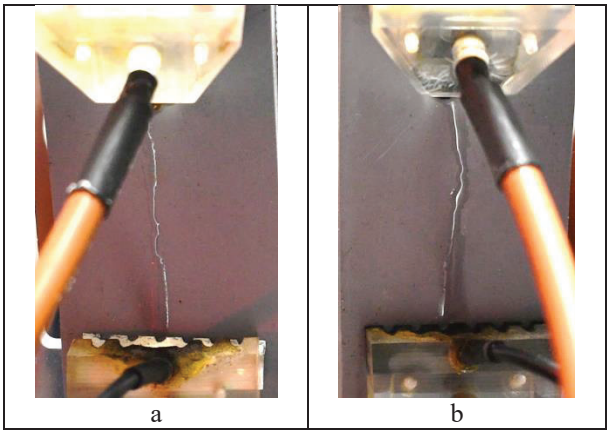

Figure 5-8: Photo of contaminant flow during early stages of AC test on samples 1 with steel electrodes and sample 2 with carbon glass electrodes.

5.2.1.3.3 Test with Carbon Glass Electrodes

Steady flow of contaminant was established on both samples as can be seen in Figure 5-9. The contaminant formed a steady stream until close to the ground electrode where random arcing resulted in dispersion of flow. Once steady DBA was established, as well as the commencement of blackening and tracking, contaminant flow followed a relatively straight path between the two electrodes. Consistent flow was maintained for the duration of this test.

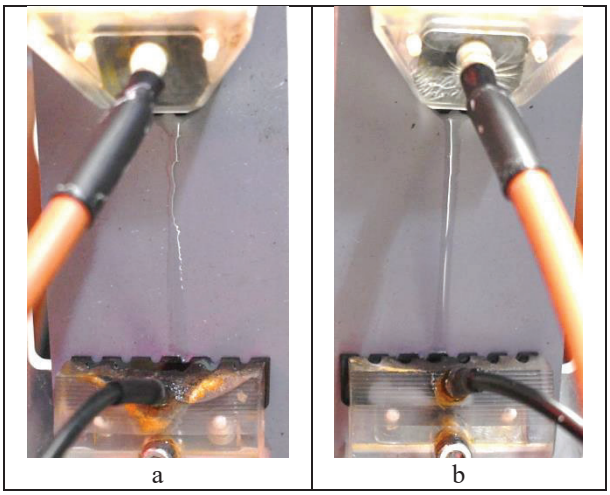

Figure 5-9: Photo of contaminant flow during early stages of AC test on samples 1 and 2 using carbon glass electrodes.

5.2.2 Leakage Current

5.2.2.1 Tests with Steel Electrodes

Figure 5-10 shows graphs of measured rms leakage currents for both samples with steel electrodes under AC voltage. Sample 1 exhibited slightly higher leakage current than sample 2 during the first

hour of the test. Measured currents were in the range from 10 mA to 15 mA. Contaminant flow ceased on sample 2 approximately 50 minutes into the test and resulted in a drop in leakage current. As the entire test rig had to be switched off, leakage current ceased on sample 1 as well for a period of approximately 10 minutes. On resumption of the test, the measured leakage current was generally slightly higher on sample 2, with a few current spikes observed on sample 1. For both samples, the measured leakage current was well below the failure threshold of 60 mA.

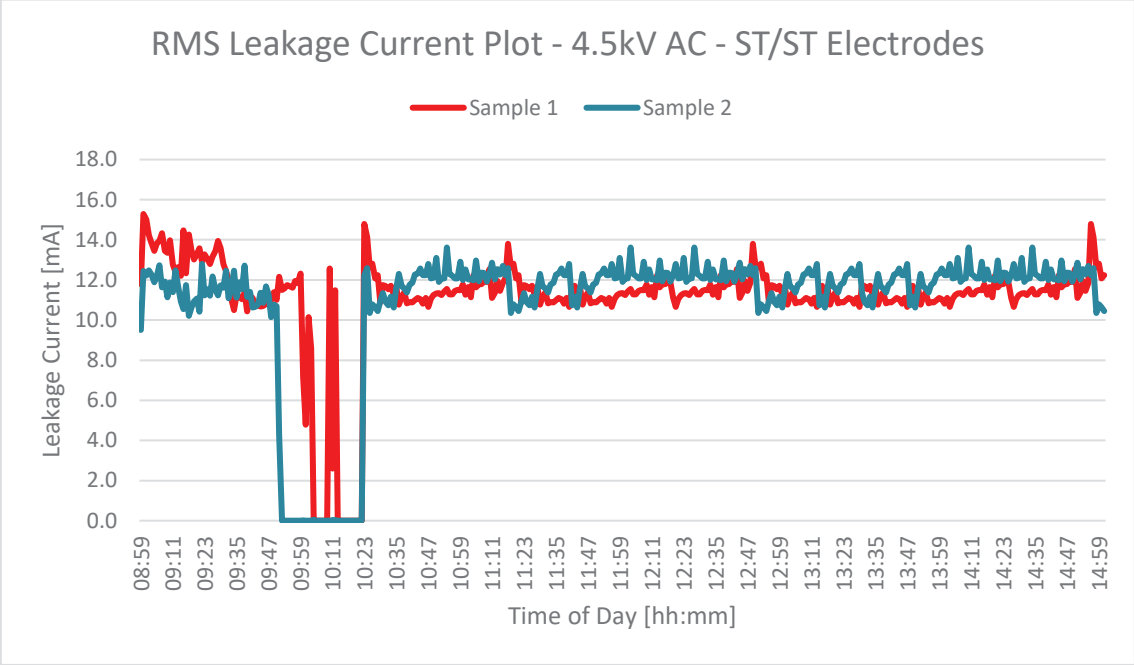

Figure 5-10: Graph of measured rms leakage current for samples 1 and 2, both with steel electrodes under AC voltage.

5.2.2.2 Tests with combination of Steel and Glass Electrodes

Figure 5-11 shows graphs of measured rms leakage currents for sample 1 using steel electrodes and sample 2 with carbon glass electrodes, under AC voltage. The leakage current of sample 1 was found to be consistently higher than that of sample 2. The current measured on sample 1 ranged between 12 and 14 mA and compares favourably to that measured with the previous test (figure 5-10), showing consistency in terms of leakage current with steel electrodes under AC energisation. The leakage current on sample 2 with glass electrodes ranged on average between 4 and 7 mA. Sample 1 showed a decrease in current levels 50 minutes into the test due to a drop in contaminant flow. Flow was problematic on this sample for a period of 30 minutes, whereafter modifications to the contaminant

reservoir resulted in normal contaminant flow, and consistent leakage current on both samples for the remainder of the test.

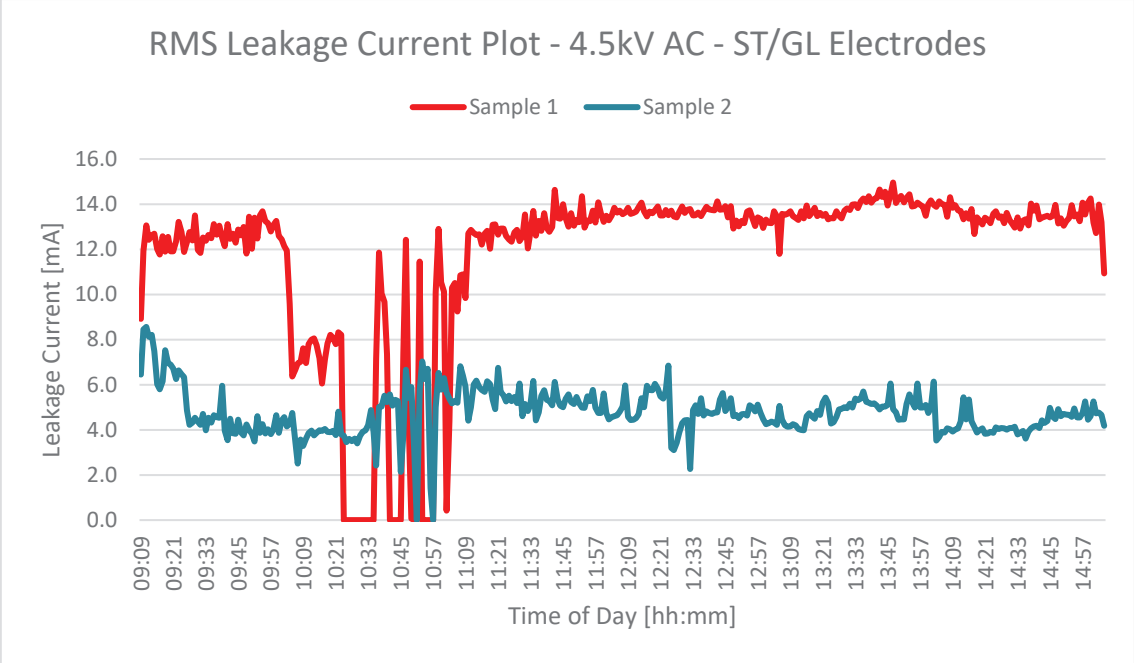

Figure 5-11: Graph of measured rms leakage current for sample 1 with steel electrodes and sample 2 with carbon glass electrodes under AC voltage.

5.2.2.3 Test with Glass Electrodes

Figure 5-12 shows graphs of measured rms leakage currents for both samples 1 and 2 using carbon glass electrodes under AC voltage. Sample 1 exhibited higher leakage currents at the beginning of the test, ranging from 10 to 14 mA. Sample 2 recorded leakage currents in the region of 6 to 10 mA, with two spike of 14 mA being recorded towards the latter part of the test. Both samples recorded leakage current well below the failure threshold of 60 mA.

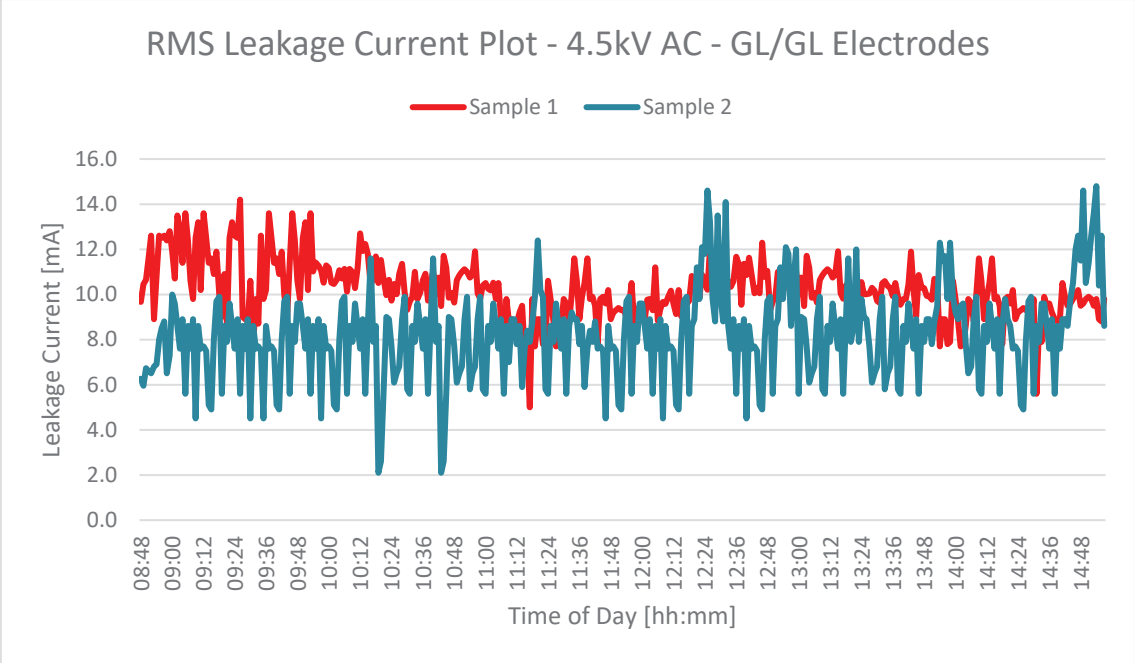

Figure 5-12: Graph of measured rms leakage current for samples 1 and 2, both with carbon glass electrodes under AC voltage.

5.2.3 Mass Loss on Electrodes and SR Samples

5.2.3.1 Tests with Steel Electrodes

Table 5-1 shows measured weight differences for the SR test samples and steel electrodes measured prior to and at the end of the AC test. The ground electrodes of both samples experienced a mass loss of 5 mg. The live electrode of sample 1 experienced a weight gain of 4.7 mg and that of sample 2 a weight gain of 3.2 mg. The HTV SR material of sample 1 exhibited a mass loss of 45.6 mg, with a measured erosion depth of 1 mm and erosion area of 4 mm^2. Sample 2 HTV SR material showed a mass loss of 21.2 mg, with an erosion depth of approximately 0.5 mm and erosion area of 2 mm^2.

Table 5-1 Mass loss on steel electrodes and HTV SR test samples under AC voltage.

	Sample 1 masses			Sample 2 masses		
	Top electrode (Steel)	Bottom electrode (Steel)	SR	Top electrode (Steel)	Bottom electrode (Steel)	SR
Before [g]	14.3135	4.4072	55.5456	14.2486	4.3815	57.4155
After [g]	14.3182	4.4022	55.5000	14.2518	4.3765	57.3943
Mass loss / (gain) [g]	(0.0047)	0.005	0.0456	(0.0032)	0.005	0.0212
Mass loss/(gain) [%]	(0.03)	0.11	0.08	(0.02)	0.11	0.04

5.2.3.2 Tests with combination of Steel and Glass Electrodes

Table 5-2 shows measured weight differences for the SR test samples as well as steel and carbon glass electrodes measured prior to and at the end of the AC test. The live steel electrode of sample 1

experienced a weight gain of 5.2 mg, whereas the live glass electrode of sample 2 showed a negligible weight loss of 0.2 mg. The ground steel electrode of sample 1 exhibited a weight loss of 2.4 mg, whereas the ground glass electrode showed a weight gain of 0.5 mg. Sample 1 HTV SR material showed a weight loss of 25.6 mg, with an erosion depth of 1 mm and an erosion area of 3 mm^2. Sample 2 has a measured weight loss of 9.8 g, with no signs of erosion.

Table 5-2: Mass loss on steel and carbon glass electrodes as well as HTV SR test samples under AC voltage.

	Sample 1 masses			Sample 2 masses		
	Top electrode (Steel)	Bottom electrode (Steel)	HTV SR	Top electrode (Glass)	Bottom electrode (Glass)	HTV SR
Before [g]	14.2771	4.3950	56.1262	0.5229	0.5207	55.2534
After [g]	14.2823	4.3926	56.1006	0.5227	0.5212	55.2436
Mass loss / (gain) [g]	(0.0052)	0.0024	0.0256	0.0002	(0.0005)	0.0098
Mass loss/(gain) [%]	(0.03)	0.05	0.05	0.04	(0.09)	0.11

5.2.3.3 Test with Glass Electrodes

Table 5-3 shows that miniscule weight differences occurred for both carbon glass live electrodes. The ground electrode on sample 1 showed a weight gain of 4.8 mg whereas sample 2 ground electrode showed negligible weight gain. Sample 1 showed a weight loss of 38.7 mg, as a result of the slight erosion that occurred. The measured depth of erosion on sample 1 was 0.5 mm with a 1 mm^2 erosion area. Sample two showed a weight loss of 22.2 mg with no visible erosion.

Table 5-3: Mass loss on carbon glass electrodes and HTV SR test samples under AC voltage.

	Sample 1 masses			Sample 2 masses		
	Top electrode (Glass)	Bottom electrode (Glass)	HTV SR	Top electrode (Glass)	Bottom electrode (Glass)	HTV SR
Before [g]	0.4950	0.5654	57.0515	0.5230	0.5641	56.5260
After [g]	0.4956	0.5702	57.0128	0.5229	0.5644	56.5038
Mass loss / (gain) [g]	(0.0006)	(0.0048)	0.0387	0.0001	(0.0003)	0.0222
Mass loss/(gain) [%]	(0.12)	(0.85)	0.07	0.02	(0.05)	0.04

5.3. DC + Test Results

5.3.1 Visual Observations

Similarly to the AC tests, visual observations of material degradation on HTV SR test samples were conducted every 15 minutes during the first hour of each DC + test, again after 180 minutes, 300 minutes and at the end of the test (i.e. 360 minutes). In certain instances, severe material degradation was noted within the first hour of the test. In those instances, 15-minute visual observations were continued after the first hour until failure occurred. Electrode degradation, contaminant flow and observed electrical activity over the surface of the test samples as the test progressed is also discussed.

5.3.1.1 SR Material Degradation

5.3.1.1.1 Tests with Steel Electrodes

Figure 5-13 shows a time-lapse photo of the test conducted using steel electrodes for both samples under DC + voltage. Extensive erosion was observed on both samples within the first hour. DBA was random within the first 15 minutes of the test, thereafter stabilizing close to the ground electrode. The first signs of erosion were observed at approximately 30 minutes on sample 1 and 33 minutes on sample 2. By 40 minutes, stable DBA was observed on both samples, leading to more aggressive erosion. Within 60 minutes, a burning smell, resembling burnt toast, was noted. Sample 1 began to exhibit severe erosion and had to be de-energized at 85 minutes due to severe burning (Figure 5-13 (f)). Sample 2 exhibited similar degradation and was de-energized at 105 minutes.

The surfaces of both test samples showed extensive whitening (shown in Figure 5-13 (g)), which is characteristic of HTV SR when exposed to high temperatures. This area is normally highly hydrophobic, resulting in the contaminant having a defined path across the surface, increased stable DBA and increased burning. Prior to whitening of the surface, a dark brown residue was visible on both samples (Figure 5-13 (c&d)).

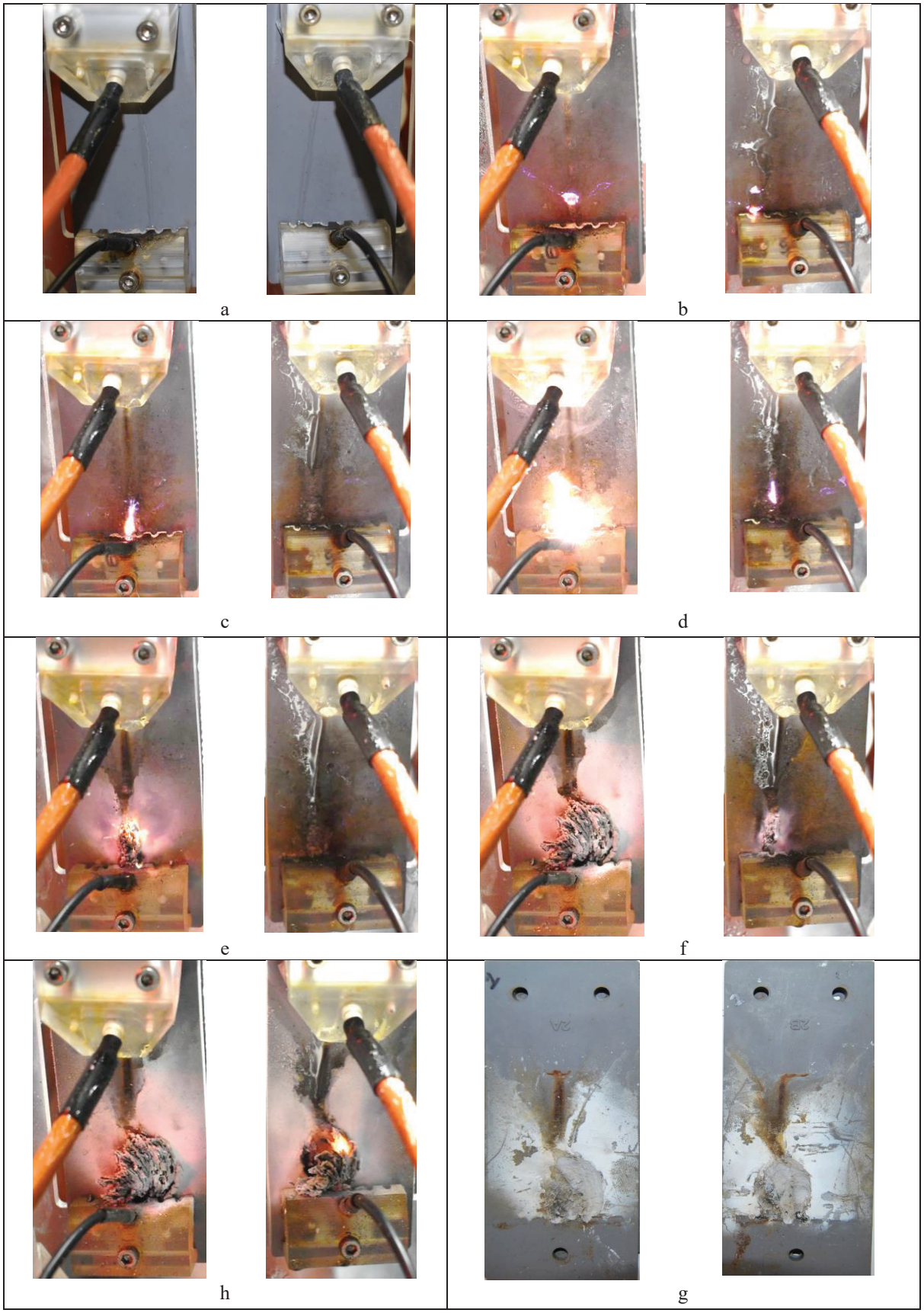

Figure 5-13: Time-lapse photo of the two SR samples, i.e. Sample 1 (left) and Sample 2 (right) with DC + voltage applied to the electrodes, which are both steel electrodes, at the following durations after the start of the test: (a) 0 minutes, (b) 15 minutes, (c) 30 minutes, (d) 45 minutes, (e) 60 minutes, (f) 75 minutes, (g) 90 minutes and (h) end of test for both samples.

5.3.1.1.2 Tests with combination of Steel and Glass Electrodes

Figure 5-14 shows a time-lapse photo of the test conducted using steel electrodes for sample 1 and carbon glass electrodes for sample 2 under DC + voltage. Within the first 15 minutes of the test, a brown residue was observed on the surface of sample 1, as well as stable DBA close to the ground electrodes of both samples. The brown residue on sample 1 intensified throughout the test period. Within 45 minutes, erosion was observed on sample 2, close to the ground electrode (Figure 5-14 (d)). DBA was found to be extremely consistent and localised to a specific point near the ground electrode on sample 2, resulting in ignition and failure at 75 minutes. DBA on sample 1 was found to be more random across a wider area of the ground electrode during the first hour of the test, stabilising closer to the middle part of the ground electrode for the remainder of the test. Sample 1 was tested for the full duration of 6 hours. Extensive tracking and erosion were observed on sample 1 at the end of the test. No tracking was observed on sample 2 prior to ignition. Figure 5-14 (h) shows the intense brown residue that remained on the surface of sample 1 after 6 hours of energisation, as well as intense whitening of the surface of sample 2 that was observed after ignition. The performance of sample 1 with steel electrodes during this test, having lasted the full 6 hours, is in stark contrast to the performance of the previous two samples with steel electrodes, which only lasted for 85 and 105 minutes.

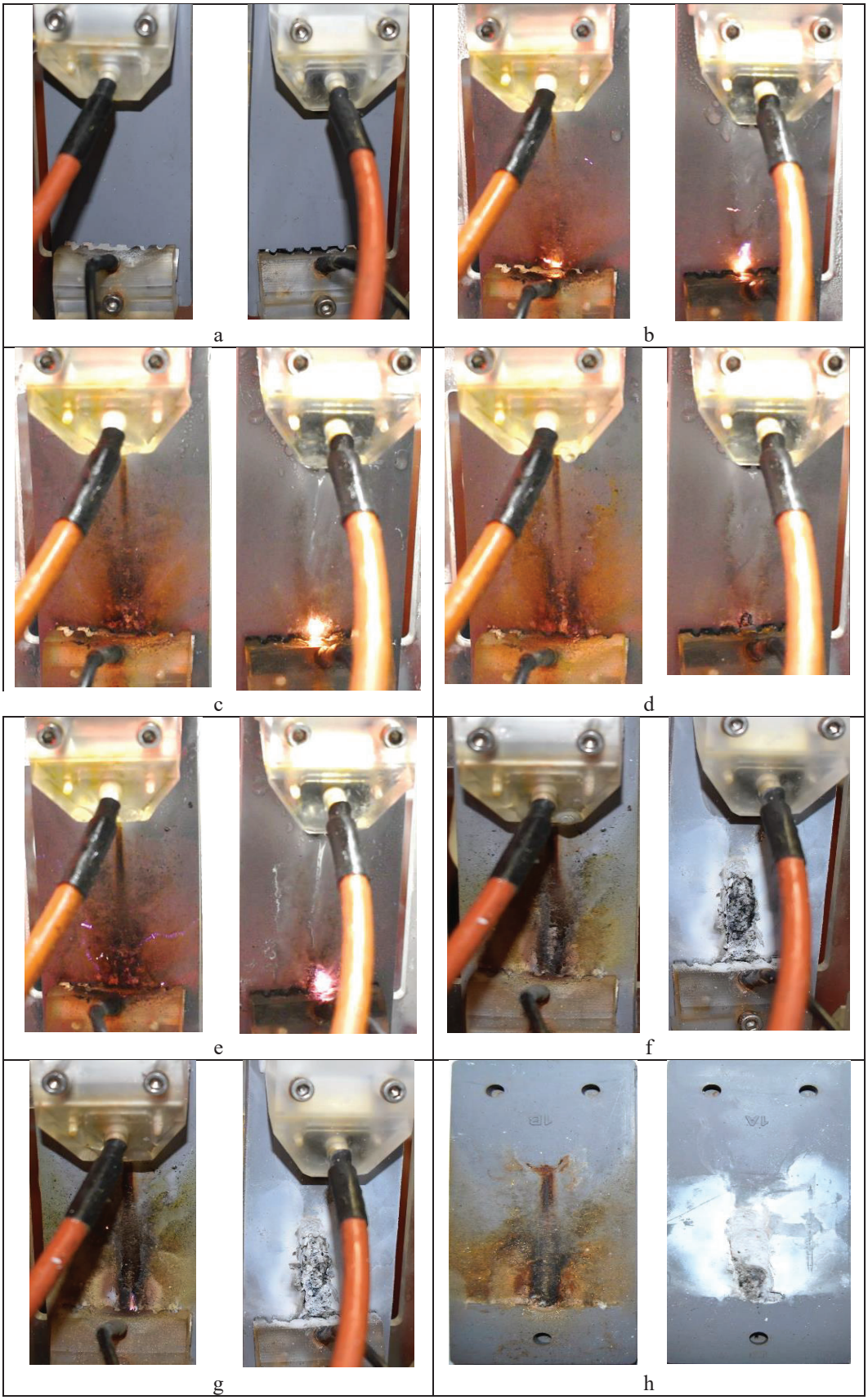

Figure 5-14: Time-lapse photo of the two SR samples, i.e. Sample 1 (left) and Sample 2 (right) with DC + voltage applied to the electrodes, sample 1 being steel and sample 2 glass, at the following durations after the start of the test: (a) 0 minutes, (b) 15 minutes, (c) 30 minutes, (d) 45 minutes, (e) 60 minutes, (f) 180 minutes, (g) 300 minutes and (h) 360 minutes.

5.3.1.1.3 Test with Glass Electrodes

Figure 5-15 shows a time-lapse photo of the test conducted using carbon glass electrodes for samples 1 and 2 under DC + voltage. Within the first 15 minutes of the test commencing, whitening and signs of erosion were observed on both samples close to the ground electrode (Figure 5-15 (b)), with sample 2 being slightly more severe. DBA was found to be random within the first 5 minutes of the test, becoming more concentrated near the ground electrode particularly on sample 2. Within 10 minutes, stable DBA was observed close to the ground electrode on both samples. At 31 minutes, sample 2 had ignited as can be seen in Figure 5-15 (c), and was thus classified as having failed. The burnt material ejected from the test sample on its own. This prevented the contaminant from flowing effectively over the test sample, causing it to drip from the top point of hole that was created by the burning. After 42 minutes of energisation, sample 1 ignited and was classified as having failed (Figure 5-15 (d)). Similarly, to sample 2, the burnt material was ejected from the test sample, preventing contaminant flow between electrodes. As with other samples that ignited, severe whitening of the material surrounding the burnt area was observed on both samples. The test was stopped within 1 hour.

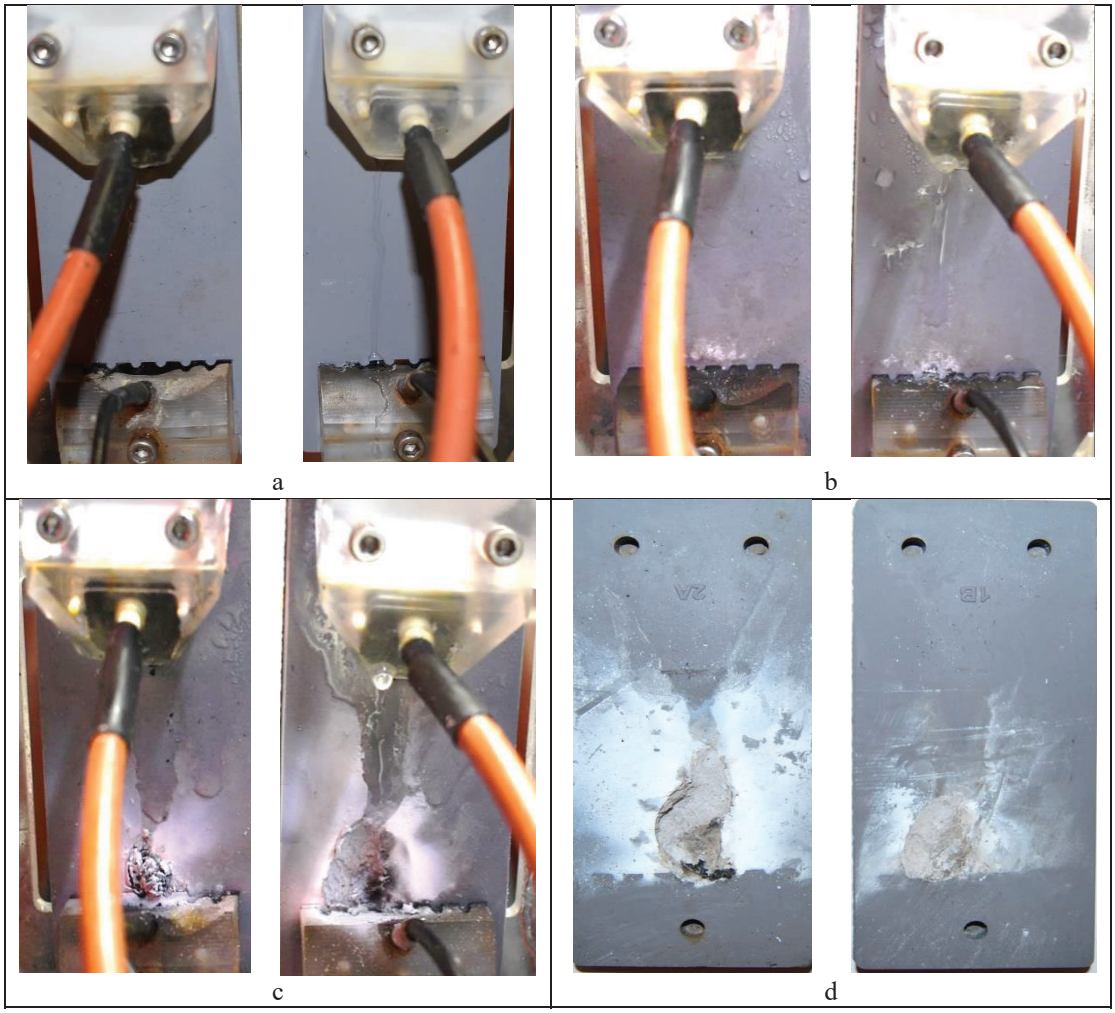

Figure 5-15: Time-lapse photo of the two HTV SR samples, i.e. Sample 1 (left) and Sample 2 (right) with DC + voltage applied to the electrodes, which are both carbon glass electrodes, at the following durations after the start of the test: (a) 0 minutes, (b) 15 minutes, (c) 30 minutes, (d) 45 minutes.

5.3.1.2 Electrode Degradation

5.3.1.2.1 Test with Steel Electrodes

Figure 5-16 shows photos of both the live and ground steel electrodes for samples 1 and 2 taken at the end of the DC+ test. Due to the short duration of this particular test, where failure happened within 45 minutes for both samples, very little degradation was noted on both live electrodes. A slight brown residue was noted on the ground electrode of sample 2 (Figure 5-16 (d)), and a brown residue together with blackening was observed on the centre teeth of the ground electrode on sample 1 (Figure 5-16 (c)).

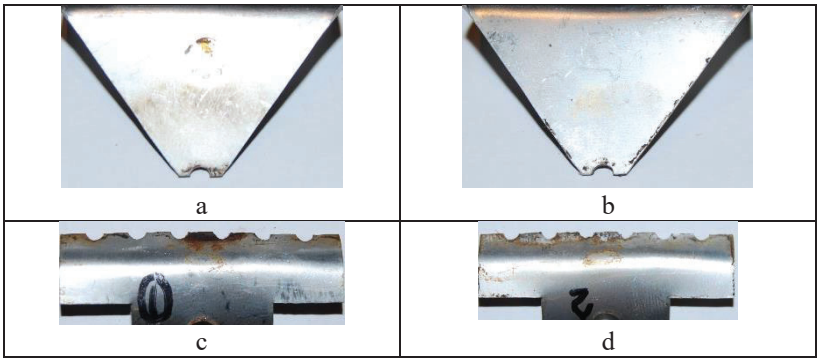

Figure 5-16: Photo of electrodes at end of test, i.e. Sample 1 live and ground steel electrode (left) and Sample 2 live and ground steel electrodes (right) with DC + voltage applied.

5.3.1.2.2 Test with combination of Steel and Glass Electrodes

Figure 5-17 shows photos of both the live and ground electrodes for samples 1 (steel) and 2 (carbon glass) taken at the end of the DC+ test. Figure 5-17 (a) shows substantial erosion at the tip of the live steel electrode on sample 1. When the live glass electrode on sample 2 was removed at the end of the test, it was found to have cracked near the top right side, as can be seen in Figure 5-17 (b). No other damage was noted. The steel ground electrode of sample 1 displayed a dark brown residue, but no signs of erosion. The carbon glass ground electrode of sample 2 showed no damage, except for slight whitening.

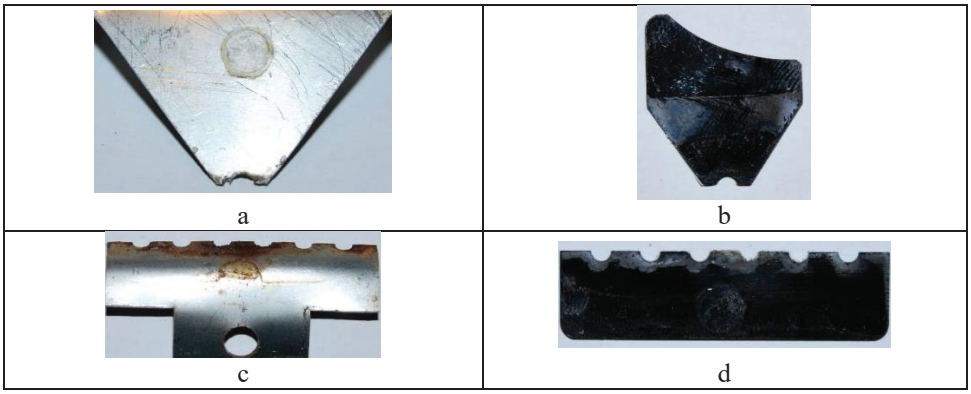

Figure 5-17: Photo of electrodes at end of test, i.e. Sample 1 live and ground steel electrode (left) and Sample 2 live and ground carbon glass (right) with DC + voltage applied.

5.3.1.2.3 Test with Glass Electrodes

Figure 5-18 shows photos of both the live and ground carbon glass electrodes for samples 1 and 2 taken at the end of the DC+ test. When the live glass electrode on sample 1 was removed at the end of the test, it was found to have cracked at the point where the HV supply makes contact with the electrode (Figure 5-18 (a)). A slight crack was also observed on the top right side of the sample 2 live

electrode. The ground electrode on sample 1 had an extensive white residue covering most of the teeth. This was evident on the ground electrode of sample 2 as well but to a lesser extent. No damage was observed on either of the ground electrodes.

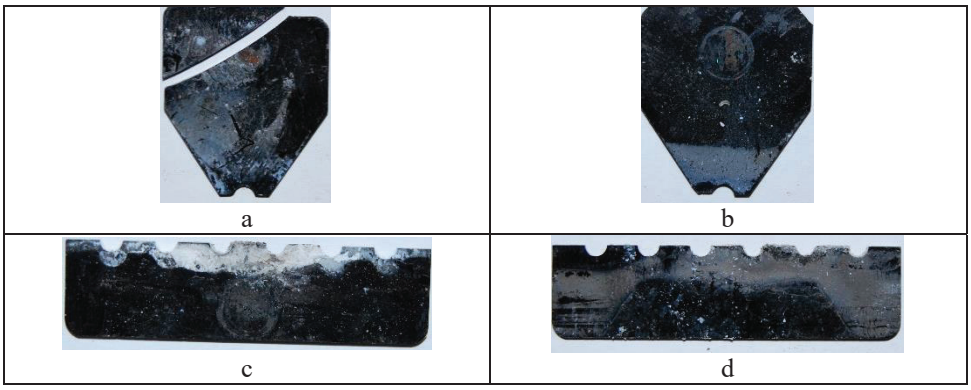

Figure 5-18: Photo of electrodes at end of test, i.e. Sample 1 live and ground carbon glass electrode (left) and Sample 2 live and ground carbon glass electrodes (right) with DC + voltage applied.

5.3.1.3 Contaminant Flow Observations

5.3.1.3.1 Tests with Steel Electrodes

Figure 5-19 shows the consistent contaminant flow that was established at the beginning of the test, with sample 1 having a flow slightly to the right of centre, and sample 2 having a flow substantially to the left. These flow paths would remain throughout the test period for both samples. Although the random DBA prevalent in the beginning of the test caused a dispersion in the path of the contaminant, the general area of flow for both samples remained similar to that in the beginning of the test. Consistent contaminant flow was observed for the full duration of the test.

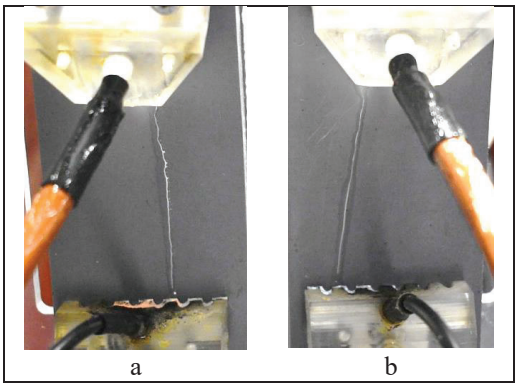

Figure 5-19: Photo of contaminant flow during early stages of DC + test on samples 1 and 2 using steel electrodes.

5.3.1.4 Tests with combination of Steel and Glass Electrodes

Figure 5-20 shows the good contaminant flow that was established early on with both samples, however after 3 minutes flow ceased on sample 2. This was corrected, however this occurred again on sample 2 after 40 minutes and was again corrected. In this instance, contaminant was passing through the filter paper reservoir to the live electrode holder and then dripping on to the drip tray below the test sample. Sample 1 displayed consistent contaminant flow throughout the test period.

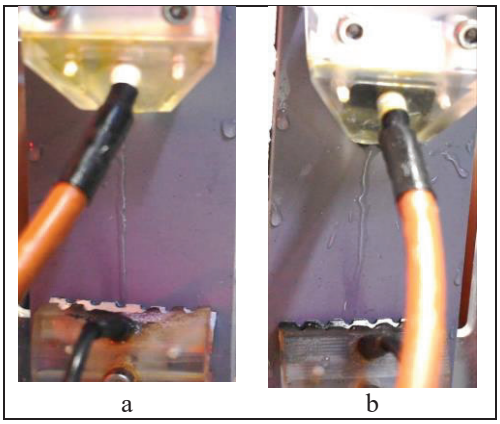

Figure 5-20: Photo of contaminant flow during early stages of DC + test on sample 1 with steel electrodes and sample 2 using carbon glass electrodes.

5.3.1.4.1 Test with Glass Electrodes

Slight difficulty was experienced at the beginning of the test in establishing a consistent flow on sample 1. Contaminant was consistently flowing via the reservoir to the electrode holder and dripping from there. Figure 5-21 shows the flow that was achieved after adjustments to the filter paper reservoir were made within the first 5 minutes. Flow remained consistent thereafter for the full duration of the test. Both samples on this test failed due to ignition within a very short period, less than 45 minutes. Once burning had taken place, the extreme hydrophobicity of the material resulted in reduced contaminant flow in the burnt area, with the contaminant dripping off the surface of the sample to the drip tray below.

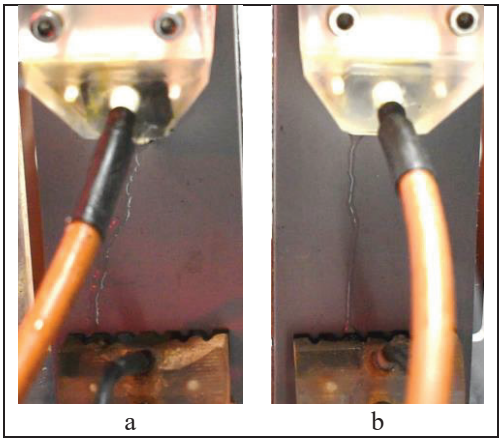

Figure 5-21: Photo of contaminant flow during early stages of DC + test on samples 1 and 2 using carbon glass electrodes.

5.3.2 Leakage Current

5.3.2.1 Tests with Steel Electrodes

Figure 5-22 shows graphs of measured leakage currents for both samples with steel electrodes under DC + voltage. Sample 1 exhibited slightly higher leakage currents than sample 2. Measured currents were in the region of 13 to 17 mA for the full duration of the test. Sample 1 experienced ignition and expulsion of the burnt material, resulting in reduced contaminant flow and reduced leakage current until it was de-energised at 85 minutes. Sample 2 experienced the same failure mode at 105 minutes and was de-energised. For both samples, the recorded leakage currents were well below the failure threshold of 60 mA.

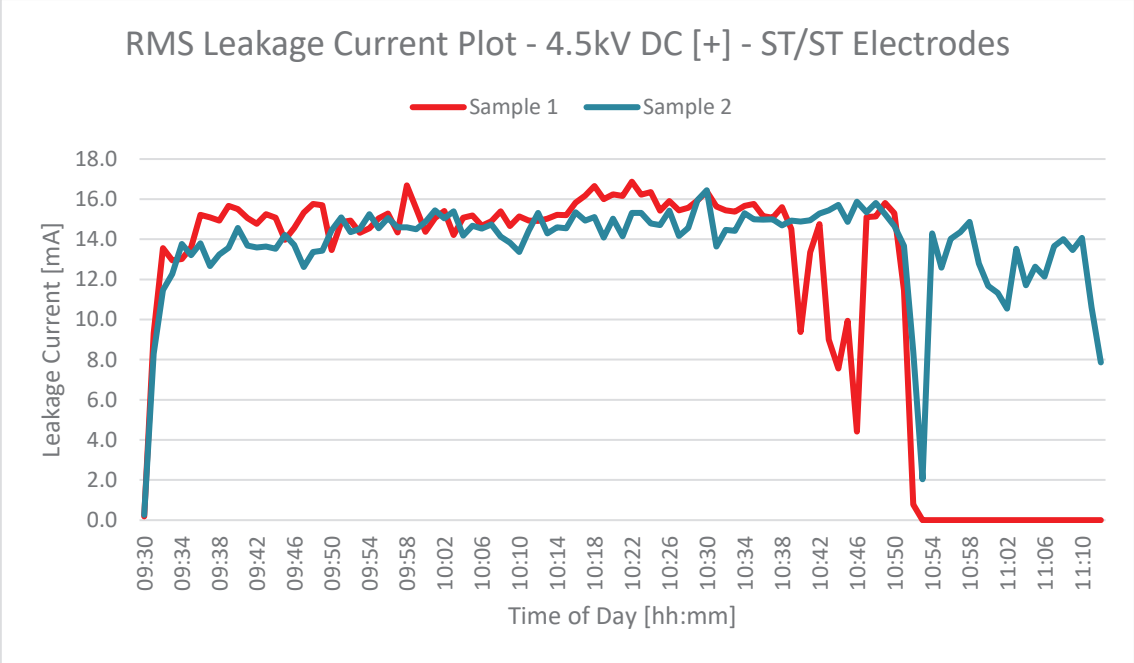

Figure 5-22: Graph of measured rms leakage current for samples 1 and 2, both with steel electrodes under DC + voltage.

5.3.2.2 Tests with combination of Steel and Glass Electrodes

Figure 5-23 shows graphs of measured leakage currents for sample 1 using steel electrodes and sample 2 using carbon glass electrodes under DC + voltage. The leakage current of sample 1 was consistently higher than that of sample 2. The current measured on sample 1 ranged between 15 and 20 mA and that of sample 2 in the region of 10 mA. Large current spikes close to 40 mA were observed on sample 2 prior to ignition and failure of the material. The measured values were still below the 60 mA threshold for failure. The current on sample 1 was consistently below 20 mA for the duration of the test.

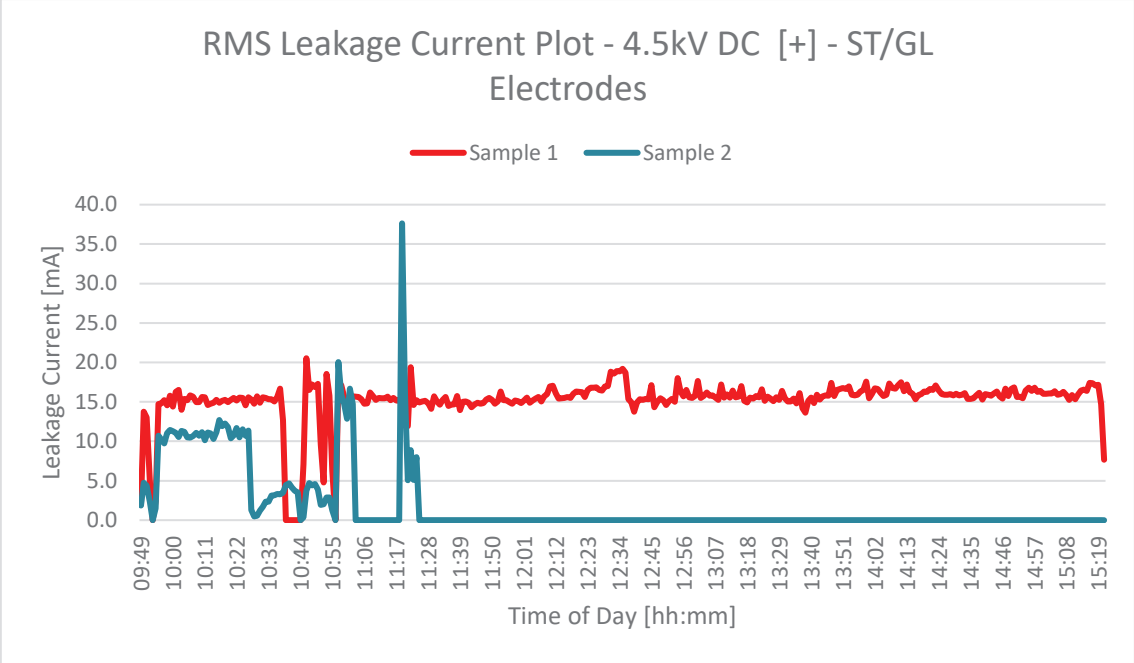

Figure 5-23: Graph of measured rms leakage current for sample 1 with steel electrodes and sample 2 with carbon glass electrodes under DC + voltage.

5.3.2.3 Test with Glass Electrodes

Figure 5-24 shows graphs of measured leakage currents for both samples with carbon glass electrodes under DC + voltage. Failure for both samples happened within the space of 1 hour. Leakage current was found to be erratic and intermittent as a result of ignition of both samples early in the test. The maximum recorded current was in the region of 20 mA.

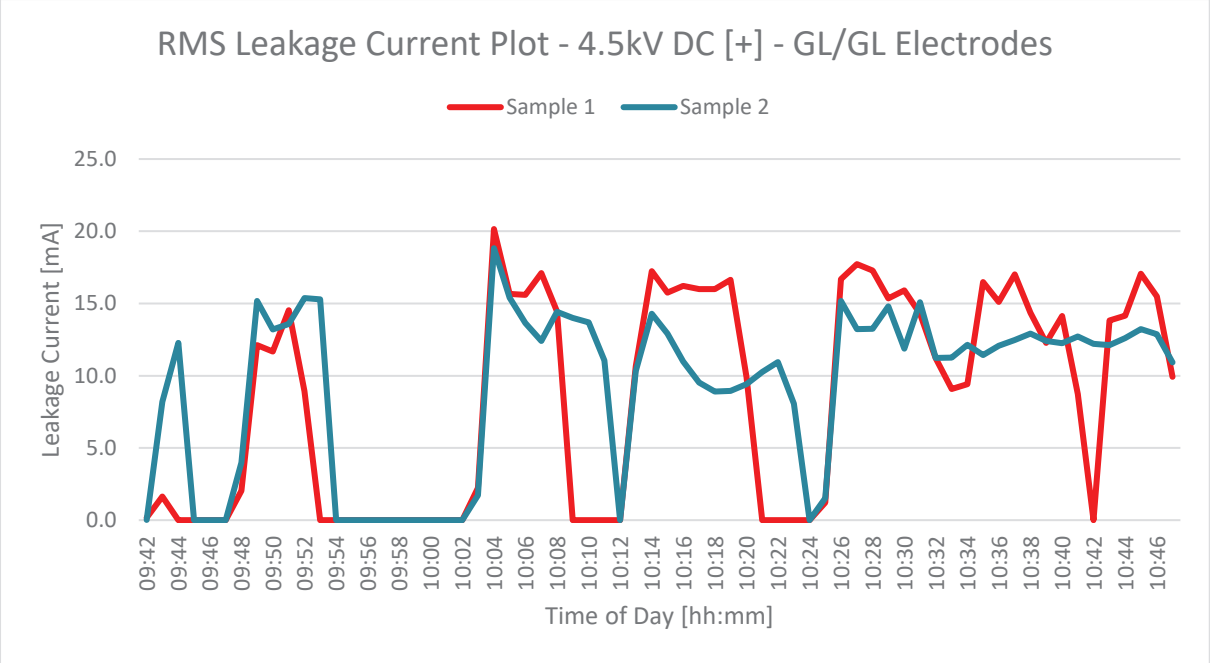

Figure 5-24: Graph of measured rms leakage current for samples 1 and 2, both with carbon glass electrodes under DC + voltage.

5.3.3 Mass Loss on Electrodes and SR Samples

5.3.3.1 Tests with Steel Electrodes

Table 5-4 shows that the live steel electrode of sample 1 experienced minor weight loss, however that of sample 2 had a weight loss of 7.6 mg. The ground steel electrodes of samples 1 and 2 showed weight gain of 2.4 mg and 6.2 mg respectively. Both samples 1 and 2 experienced severe material erosion and this is evident in the weight loss of 1.344 g and 1.2608 g, respectively. This represents a weight loss of over 2% for both samples. The depth of erosion for sample 1 was recorded as 6mm, with a total erosion area of 391 mm^2. The depth of erosion for sample 2 was measured as 5 mm, with a total erosion area of 352 mm^2.

Table 5-4: Mass loss on steel electrodes and HTV SR test samples under DC + voltage.

	Sample 1 masses			Sample 2 masses		
	Top electrode (Steel)	Bottom electrode (Steel)	SR	Top electrode (Steel)	Bottom electrode (Steel)	SR
Before [g]	14.2588	4.3898	57.7937	14.2758	4.3956	55.2530
After [g]	14.2580	4.3922	56.4497	14.2682	4.4018	53.9922
Mass loss / (gain) [g]	0.0008	(0.0024)	1.344	0.0076	(0.0062)	1.2608
Mass loss/(gain) [%]	0.01	(0.05)	2.33	0.05	(0.14)	2.28

5.3.3.2 Tests with combination of Steel and Glass Electrodes

Table 5-5 shows that the live steel electrode of sample 1 had a mass loss of 19.2 mg, with the sample 1 ground steel electrode showing a weight gain of 4.2 mg. The live glass electrode of sample 2 had a mass loss of 4 mg, due to a light crack at the top right corner. The ground glass electrode had a weight gain of 1.9 mg. Sample 1 showed a material weight loss of 96 mg, with sample 2 having a much larger weight loss of 807.5 mg. The erosion depth on sample 1 was measured as 2 mm with an erosion area of 66 mm^2. The erosion depth on sample 2 was measured at 4mm with an erosion area of 256 mm^2.

Table 5-5: Mass loss on steel and carbon glass electrodes as well as HTV SR test samples under DC + voltage.

	Sample 1 masses			Sample 2 masses		
	Top electrode (Steel)	Bottom electrode (Steel)	SR	Top electrode (Glass)	Bottom electrode (Glass)	SR
Before [g]	14.2515	4.3992	55.5153	0.5064	0.5751	56.5710
After [g]	14.2323	4.4034	55.4186	0.5024	0.5770	55.7635
Mass loss / (gain) [g]	0.0192	(0.0042)	0.0967	0.004	(0.0019)	0.8075
Mass loss/(gain) [%]	0.14	(0.1)	0.17	0.79	(0.33)	1.43

5.3.3.3 Test with Glass Electrodes

Table 5-6 shows that negligible mass difference was observed on the live glass electrode of sample 1. Sample 2 live electrode had a mass loss of 2.1 mg, with the ground electrode showing a mass gain of 2.3 mg. Sample 1 suffered extensive material loss due to burning, resulting in a drop in weight of 1.48 g. An erosion depth of 6 mm was measured, with an erosion area of 330 mm^2. Sample 2 had a weight loss of 0.513 g with an erosion depth of 3mm and an erosion area of 187 mm^2.

Table 5-6: Mass loss on carbon glass electrodes and HTV SR test samples under DC + voltage.

	Sample 1 masses			Sample 2 masses		
	Top electrode (Glass)	Bottom electrode (Glass)	SR	Top electrode (Glass)	Bottom electrode (Glass)	SR
Before [g]	0.5199	0.5582	57.2690	0.5048	0.5752	55.6844
After [g]	0.5196	0.5613	55.7854	0.5027	0.5775	55.1714
Mass loss / (gain) [g]	0.0003	(0.0031)	1.4836	0.0021	(0.0023)	0.513
Mass loss/(gain) [%]	0.06	(0.56)	2.59	0.42	(0.4)	0.92

5.4. DC – Test Results

5.4.1 Visual Observations

As with the AC and DC + tests, visual observations of material degradation on the HTV SR test samples were conducted every 15 minutes during the first hour of each test, again after 180 minutes, 300 minutes and at the end of the test (i.e. 360 minutes). Electrode degradation, contaminant flow and observed electrical activity over the surface of the test samples as the test progressed is also discussed.

5.4.1.1 HTV SR Material Degradation

5.4.1.1.1 Tests with Steel Electrodes

Figure 5-25 shows a time-lapse photo of the test conducted using steel electrodes for both samples under DC - voltage. Within 15 minutes of energisation, tracking was observed close to the ground electrode (Figure 5-25 (b)). A slight brown residue also formed alongside the tracked area. DBA was random within the first 10 minutes, but stabilised thereafter close to the ground electrode. Erosion was observed on sample 2 after approximately 4 hours (Figure 5-25 (g)). The test ran for the full duration of 6 hours. At the end of the test a brown residue was observed on the surface of the material but only in the vicinity of the ground electrode. Slight erosion was observed on sample 1 at the end of the test. Slight whitening of the material was observed predominately on sample 2, alongside areas that were exposed to sustained DBA activity at the ground electrode.

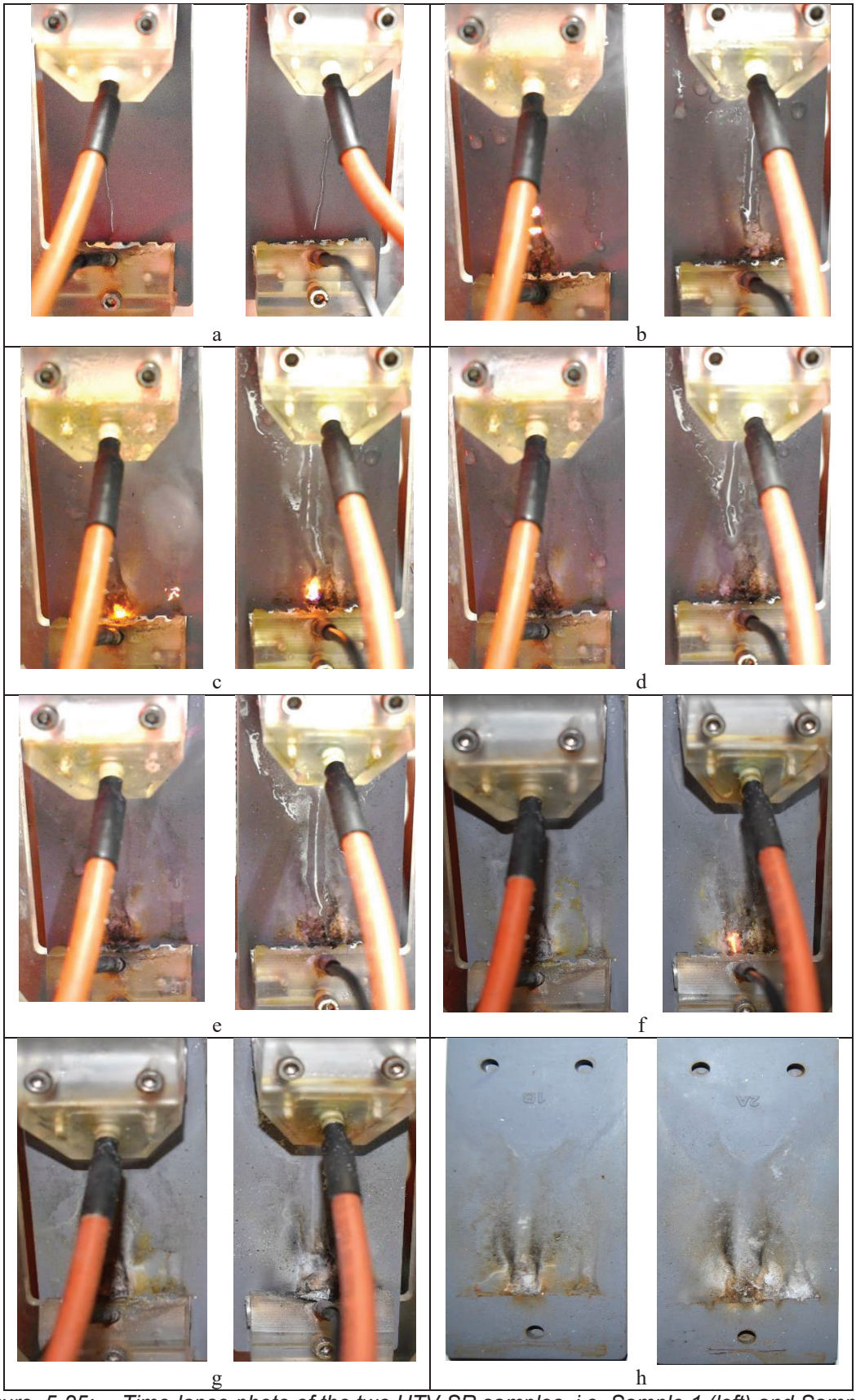

Figure 5-25: Time-lapse photo of the two HTV SR samples, i.e. Sample 1 (left) and Sample 2 (right) with DC - voltage applied to the electrodes, which are both steel electrodes, at the following durations after the start of the test: (a) 0 minutes, (b) 15 minutes, (c) 30 minutes, (d) 45 minutes, (e) 60 minutes, (f) 180 minutes, (g) 300 minutes and (h) 360 minutes.

5.4.1.1.2 Tests with combination of Steel and Glass Electrodes

Figure 5-26 shows a time-lapse photo of the test conducted using steel electrodes for sample 1 and carbon glass electrodes for sample 2 under DC - voltage. Within the first 15 minutes of the test, a brown residue was observed on the surface of sample 1. Slight erosion was observed on sample 1 after 20 minutes. Stable DBA was observed close to the ground electrode on sample 1, whereas sample 2 exhibited random DBA due to contaminant flow that was more random (figure 5-26 (d)), as opposed to a defined path which was observed with most of the tests. The brown residue on sample 1 became more pronounced as the test progressed, however it was only observed in the area close to the ground electrode. Sample 2 showed little signs of degradation up to 210 minutes, when ignition commenced, resulting in burning and extensive loss of material. Failure due to erosion was recorded at 220 minutes. Sample 1 lasted for the full test duration of the test, with slight erosion being observed.

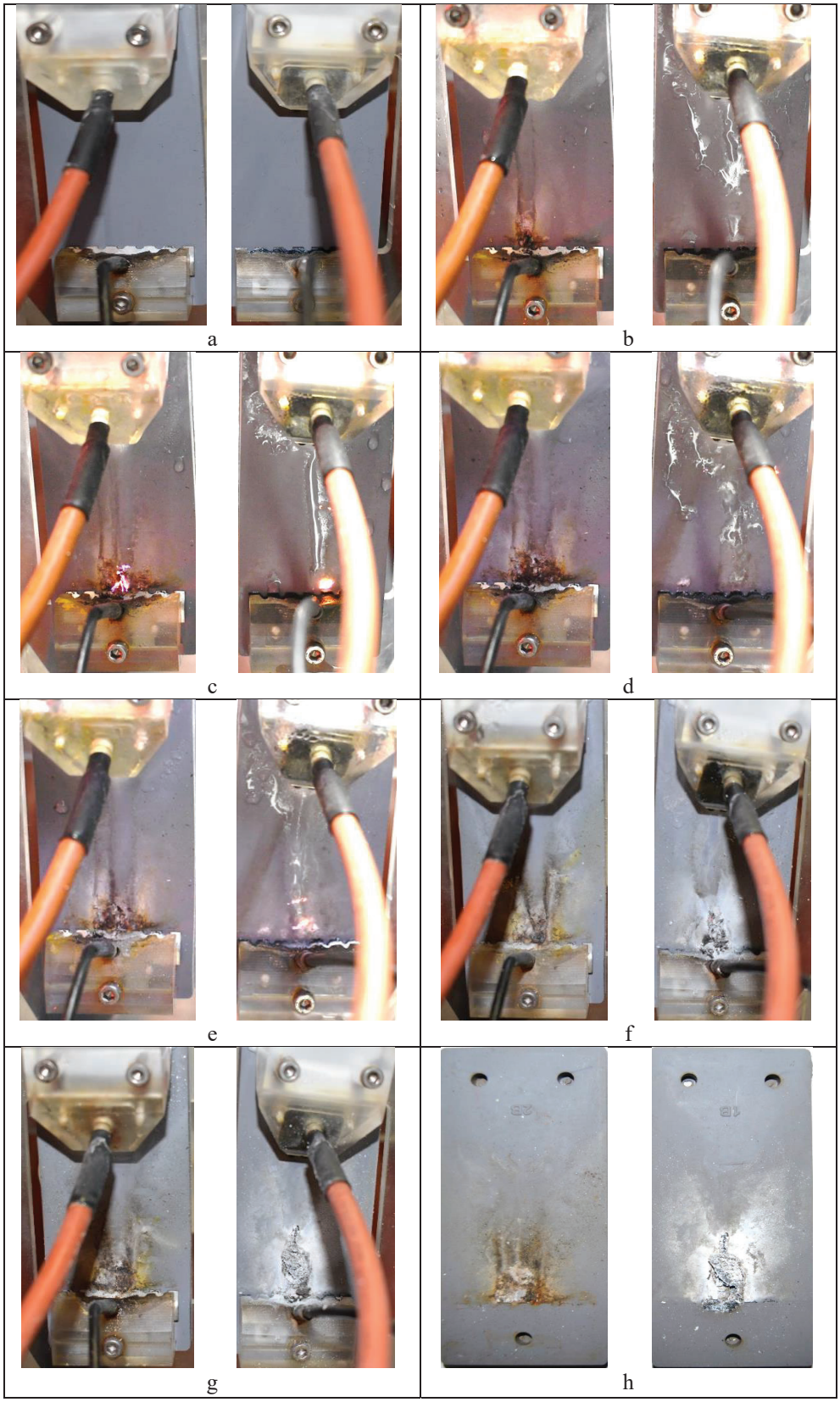

Figure 5-26: Time-lapse photo of the two HTV SR samples, i.e. Sample 1 (left) and Sample 2 (right) with AC voltage applied to the electrodes, sample 1 being steel and sample 2 glass, at the following durations after the start of the test: (a) 0 minutes, (b) 15 minutes, (c) 30 minutes, (d) 45 minutes, (e) 60 minutes, (f) 180 minutes, (g) 300 minutes and (h) 360 minutes.

5.4.1.1.3 Test with Glass Electrodes

Figure 5-27 shows a time-lapse photo of the test conducted using carbon glass electrodes for samples 1 and 2 under DC - voltage. Within the first 15 minutes of the test commencing, whitening of the SR material was observed on both samples close to the ground electrode. DBA was found to be random on sample 2 for a much longer period than sample 1, due mainly to a more random contaminant flow path for sample 2, as can be seen in Figure 5-27 (c), where the contaminant is flowing mainly on the left side sample 2. Stable DBA was observed on sample 1 from 30 minutes onwards. This led to ignition of sample 1 at approximately 165 minutes. Sample 1 was de-energised 10 minutes later having failed due to burning and severe erosion. Severe whitening of the material surrounding the burnt area was observed on sample 1. Sample 2 remained energised until 235 minutes, when it failed due to erosion.

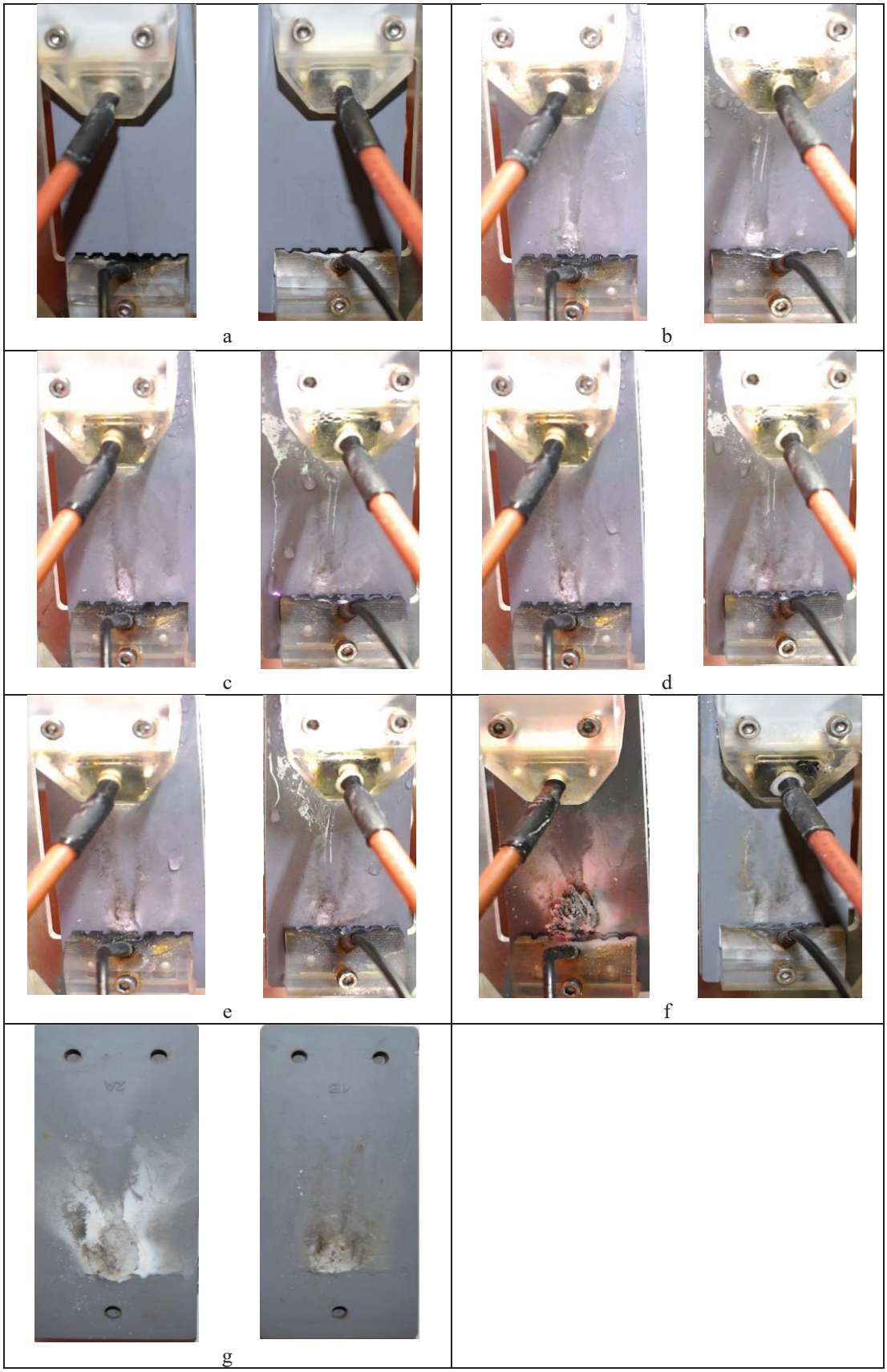

Figure 5-27: Time-lapse photo of the two HTV SR samples, i.e. Sample 1 (left) and Sample 2 (right) with AC voltage applied to the electrodes, which are both steel electrodes, at the following durations after the start of the test: (a) 0 minutes, (b) 15 minutes, (c) 30 minutes, (d) 45 minutes, (e) 60 minutes, (f) 180 minutes, (g) 235 minutes.

5.4.1.2 Electrode Degradation

5.4.1.2.1 Tests with Steel Electrodes

Figure 5-28 shows photos of both the live and ground steel electrodes for samples 1 and 2 taken at the end of the DC- test. No degradation was noted on either of the live electrodes. A slight brown residue was noted on the ground electrode of sample 1, and a brown residue together with blackening was observed on the centre teeth of ground electrode on sample 2. No other degradation was noted on either of the ground electrodes.

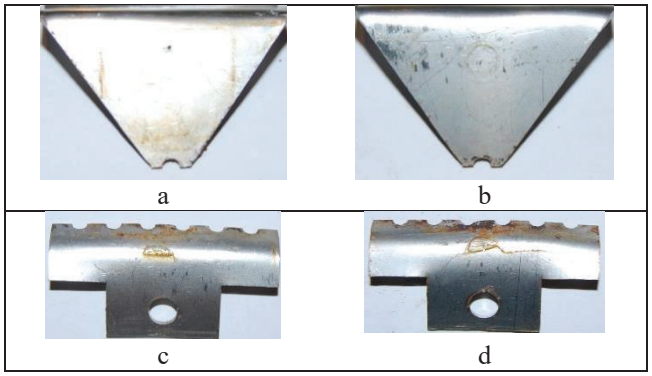

Figure 5-28: Photo of electrodes at end of test, i.e. Sample 1 live and ground steel electrode (left) and Sample 2 live and ground steel electrodes (right) with DC - voltage applied.

5.4.1.2.2 Tests with combination of Steel and Glass Electrodes

Figure 5-29 shows photos of both the live and ground electrodes for samples 1 (steel) and 2 (carbon glass) taken at the end of the DC- test. No degradation was noted on either of the two live electrodes. The steel electrode showed a brown residue at the point of contact with the HV supply. The tips of both electrodes showed no damage. The ground steel electrode has substantial brown discolouration, but no signs of damage to the teeth. The glass electrode showed substantial white and black residue towards the middle part of the electrode, however no damage to any of the teeth was observed.

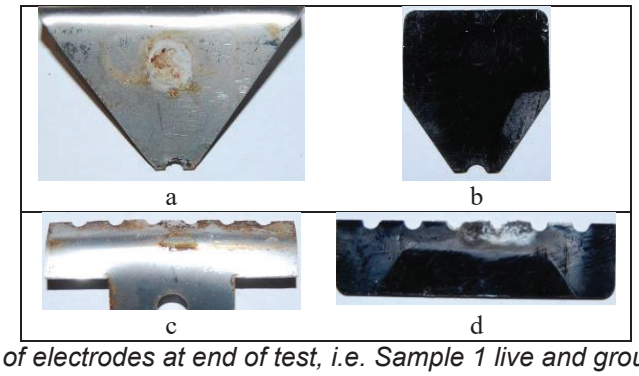

Figure 5-29: Photo of electrodes at end of test, i.e. Sample 1 live and ground steel electrode (left) and Sample 2 live and ground carbon glass (right) with DC - voltage applied.

5.4.1.2.3 Test with Glass Electrodes

Figure 5-30 shows photos of both the live and ground carbon glass electrodes for samples 1 and 2 taken at the end of the DC- test. The live electrode of sample 2 showed substantial colour change in the material itself. No colour change or damage was observed on the sample 1 live electrode. The ground electrodes of both samples showed a white residue in the areas close to where material degradation was noted. There was no damage to any of the teeth on the ground electrodes.

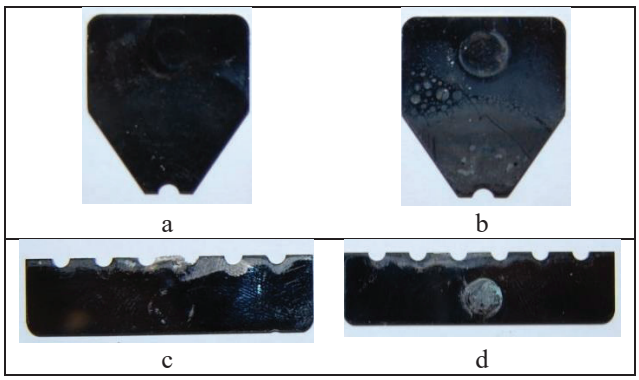

Figure 5-30: Photo of electrodes at end of test, i.e. Sample 1 (left) and Sample 2 (right) with AC voltage applied to the electrodes.

5.4.1.3 Contaminant Flow Observations

5.4.1.3.1 Tests with Steel Electrodes

Figure 5-31 shows that consistent contaminant flow was observed on both samples at the beginning of the test. Flow remained consistent for the full duration of the test.

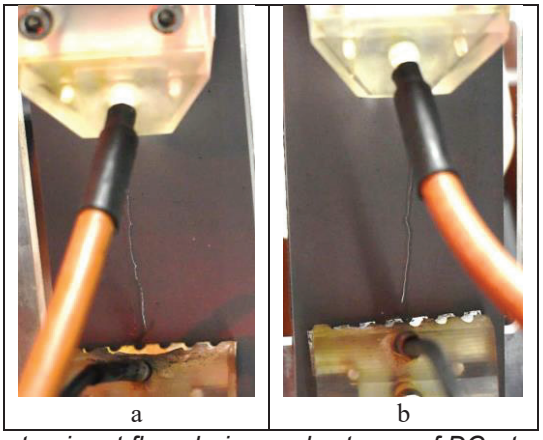

Figure 5-31: Photo of contaminant flow during early stages of DC - test on samples 1 and 2 using steel electrodes.

5.4.1.3.2 Tests with combination of Steel and Glass Electrodes

Figure 5-32 shows the steady flow of contaminant that was established on both samples. The flow on sample 2 was situated on the extreme left in the beginning, but migrated towards the middle of the sample within the first 3 minutes of the test. Flow, although generally centred around the middle of the samples, tended to be random in the beginning, resulting in random DBA. Within 10 minutes, a definite channel of contaminant flow had been formed resulting in more stable DBA as well. Steady flow continued on both samples for the duration of the test.

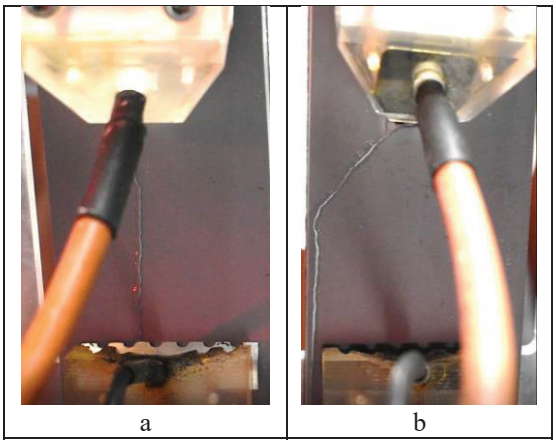

Figure 5-32: Photo of contaminant flow during early stages of DC - test on sample 1 with steel electrodes and sample 2 using carbon glass electrodes.

5.4.1.3.3 Test with Glass Electrodes

Figure 5-33 shows the steady contaminant flow was observed on both samples at the beginning of the test. Flow remained consistent for the full duration of the test.

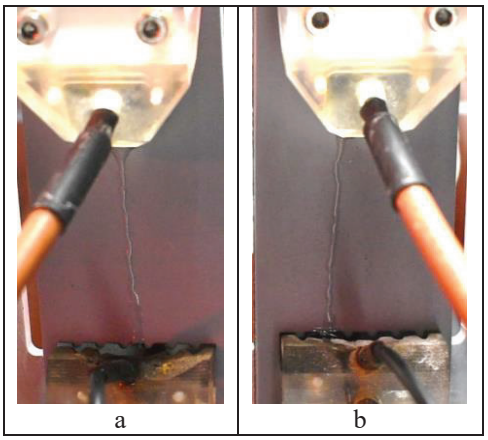

Figure 5-33: Photo of contaminant flow during early stages of DC - test on samples 1 and 2 using carbon glass electrodes.

5.4.2 Leakage Current

5.4.2.1 Tests with Steel Electrodes

Figure 5-34 shows graphs of measured leakage currents for both samples with steel electrodes under DC - voltage. In general, leakage currents ranged from 9 to 14 mA, with sample 2 showing slightly higher currents.

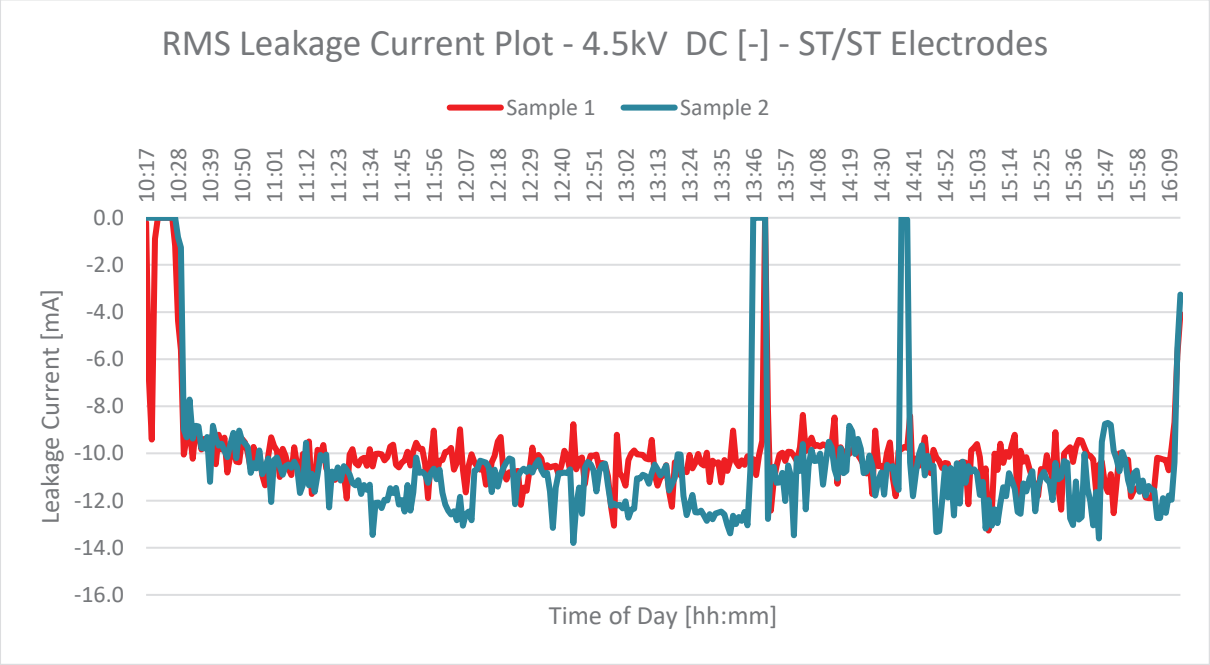

Figure 5-34: Graph of measured rms leakage current for samples 1 and 2, both with steel electrodes under DC – voltage.

5.4.2.2 Tests with combination of Steel and Glass Electrodes

Figure 5-35 shows graphs of measured leakage currents for sample 1 using steel electrodes and sample 2 using carbon glass electrodes under DC - voltage. Sample 1 exhibited leakage currents in the region of 12 to 16 mA early in the test, stabilising around 12 mA as the test progressed. Sample 2 showed lower leakage currents in the region of 8 to 12 mA. Sample 2 failed 210 minutes into the test, whereas sample 1 lasted for the full duration.

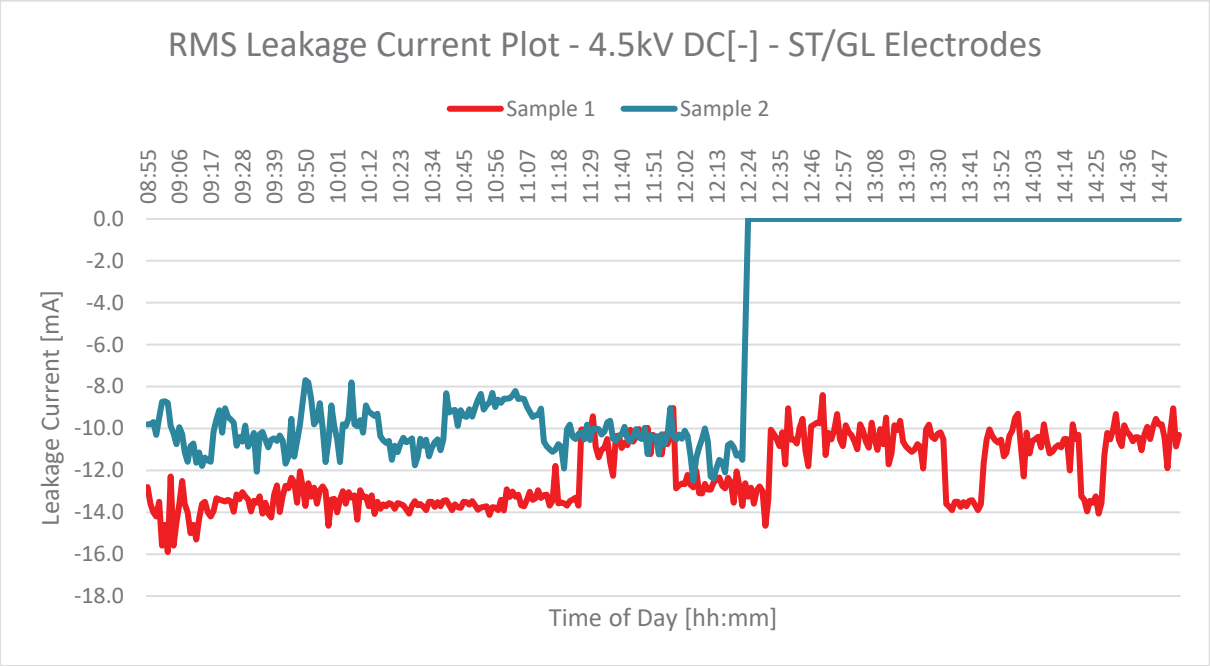

Figure 5-35: Graph of measured rms leakage current for sample 1 with steel electrodes and sample 2 with carbon glass electrodes under DC + voltage.

5.4.2.3 Test with Glass Electrodes

Figure 5-36 shows graphs of measured leakage currents for both samples with carbon glass electrodes under DC - voltage. Measured current was found to be consistent in the range from 8 to 12 mA for both samples. Both samples exhibited current well within the test threshold of 60 mA.

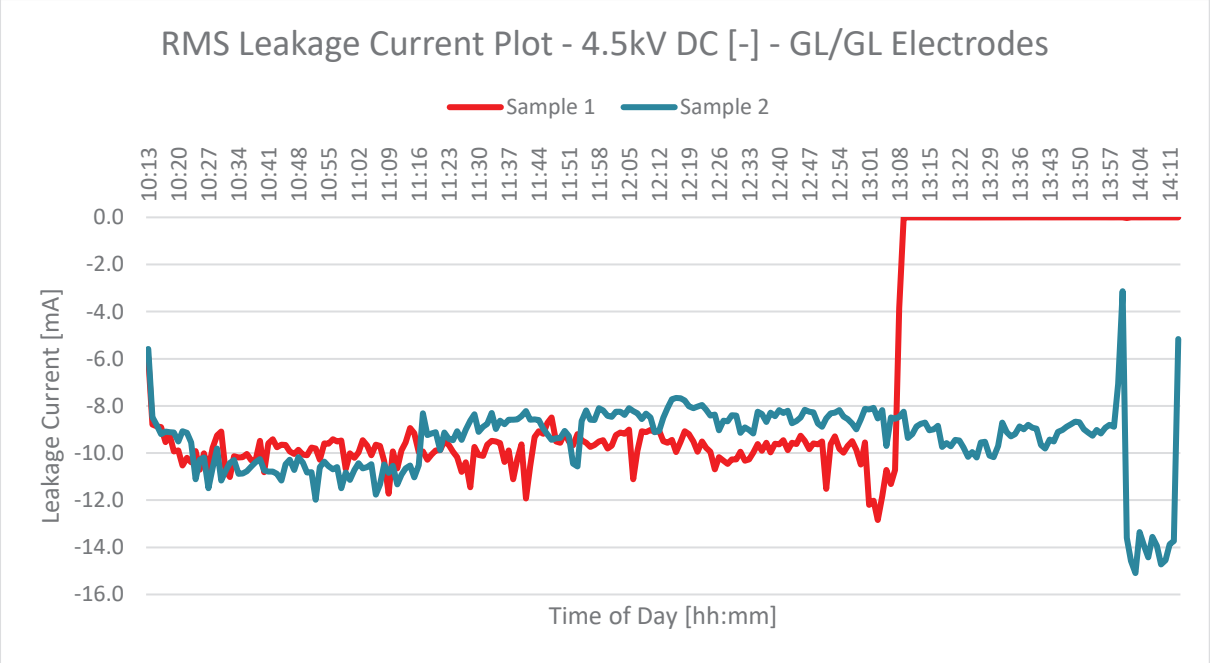

Figure 5-36: Graph of measured rms leakage current for samples 1 and 2, both with carbon glass electrodes under DC – voltage.

5.4.3 Mass Loss on Electrodes and SR Statistics

5.4.3.1 Tests with Steel Electrodes

Table 5-7 shows that the live steel electrodes of samples 1 and 2 experienced a mass gain of 5.6 mg and 7.6 mg respectively. The ground electrode both showed weight loss ranging from 2.8 mg for sample 1 and 4.9 mg for sample 2. Sample 1 had a SR material mass loss of 27.3 mg, exhibiting minor erosion with a depth of 1 mm and an erosion area of 20 mm^2. Sample 2 had a SR material mass loss of 154.2 mg, a larger erosion depth of 3 mm and an erosion area of 72 mm^2.

Table 5-7: Mass loss on carbon glass electrodes and HTV SR test samples under DC – voltage.

	Sample 1 masses			Sample 2 masses		
	Top electrode (Steel)	Bottom electrode (Steel)	SR	Top electrode (Steel)	Bottom electrode (Steel)	SR
Before [g]	14.2674	4.2981	55.5927	14.3204	4.3897	57.3157
After [g]	14.2730	4.2953	55.5654	14.3280	4.3848	57.1615
Mass loss / (gain) [g]	(0.0056)	0.0028	0.0273	(0.0076)	0.0049	0.1542
Mass loss/(gain) [%]	(0.04)	0.07	0.05	(0.05)	0.11	0.23

5.4.3.2 Tests with combination of Steel and Glass Electrodes

Table 5-8 shows that the sample 1 live steel electrode had a mass gain of 4.4 mg, with the ground steel electrode showing a mass loss of 1.4 mg. This equates to a 0.03 % mass gain and loss for the top and

bottom electrodes respectively. Both the live and ground glass electrodes showed a gain in mass, albeit very slight for the top electrode. The ground glass electrode showed a weight gain of 2.4 mg and this could be attributed to the substantial residue attached to the electrode as a result of the burning and erosion that took place. Sample 1 SR material loss was measured as 51 mg, with an erosion depth of 0.5 mm and an erosion area of 100 mm^2. Sample 2 SR material loss was far greater and measured 731.3 mg, with an erosion depth of 5 mm and erosion area of 135 mm^2.

Table 5-8: Mass loss on carbon glass electrodes and HTV SR test samples under DC – voltage.

	Sample 1 masses			Sample 2 masses		
	Top electrode (Steel)	Bottom electrode (Steel)	SR	Top electrode (Glass)	Bottom electrode (Glass)	SR
Before [g]	14.2635	4.3929	55.3191	0.5084	0.5509	56.2949
After [g]	14.2679	4.3915	55.2681	0.5086	0.5533	55.5636
Mass loss / (gain) [g]	(0.0044)	0.0014	0.051	(0.0002)	(0.0024)	0.7313
Mass loss/(gain) [%]	(0.03)	0.03	0.09	(0.04)	(0.44)	1.3

5.4.3.3 Test with Glass Electrodes

Table 5-9 shows that the glass electrodes of both samples exhibited minor weight differences before and after the test. The SR material of sample 1 had a weight loss of 769 mg, with a substantial erosion depth of 4 mm and an erosion area of 260 mm^2. Sample 2 SR material has a smaller mass loss of 85 mg, with erosion of 2 mm and an erosion area of 81 mm^2.

Table 5-9: Mass loss on carbon glass electrodes and HTV SR test samples under DC – voltage.

	Sample 1 masses			Sample 2 masses		
	Top electrode (Glass)	Bottom electrode (Glass)	SR	Top electrode (Glass)	Bottom electrode (Glass)	SR
Before [g]	0.5227	0.5554	56.1716	0.5169	0.5732	55.7266
After [g]	0.5230	0.5547	55.4025	0.5166	0.5719	55.6414
Mass loss / (gain) [g]	(0.0003)	0.0007	0.7691	0.0003	0.0013	0.0852
Mass loss/(gain) [%]	(0.06)	0.13	1.37	0.06	0.23	0.15

6 Discussion, Conclusions and Recommendations

6.1. Overview

The main objective of this research was to investigate whether an alternative electrode material, in the form of carbon glass, could assist in improving the repeatability of the IEC 60587 Inclined Plane Test (IPT), particularly under DC energisation. This objective was achieved by implementing the research methodology outlined in Chapter 3, utilising equipment that was either designed or procured specifically for the test programme, and described in detail in Chapter 4.

In this chapter, the results obtained in Chapter 5 are discussed in relation to the research questions posed in Chapter 1, with conclusions drawn and recommendations made. The specific research questions for this study were:

- What is the extent of electrode erosion under DC energisation during the IPT?
- What is the effect of electrode erosion on material performance under DC energisation during the IPT?
- How can electrode erosion in the IPT be eliminated?
- To what extent will the repeatability of the DC IPT improve if the electrode erosion is eliminated?
- What other test parameters influence repeatability of the DC IPT?

6.2. Discussion of Results in Relation to Research Questions

6.2.1 What is the Extent of Electrode Erosion Under DC Energisation During the IPT?

As discussed in section 2.4.6, erosion of the steel electrodes during the IPT is known to occur over the duration of a few AC tests, and must be replaced on a regular basis. Many researchers have however reported increased erosion under DC energisation, as a result of electrolysis. Bruce et al reported mass losses in the region of 10 to 35 mg for the live electrode, with an increase in mass for the ground electrode, under DC + energisation [17]. During similar DC – tests, the ground electrode exhibited mass loss as well, albeit less than under DC + with a maximum weight loss of 18 mg being measured. Gorur et al conducted DC tests in a fog chamber and observed a drop in electrode weight of between 1 and 5 % of total weight as a result of electrode erosion [26].

The extent of weight loss/gain for both the live and ground steel electrodes, for this study, is shown in Figure 6-1 and Figure 6-2, respectively.

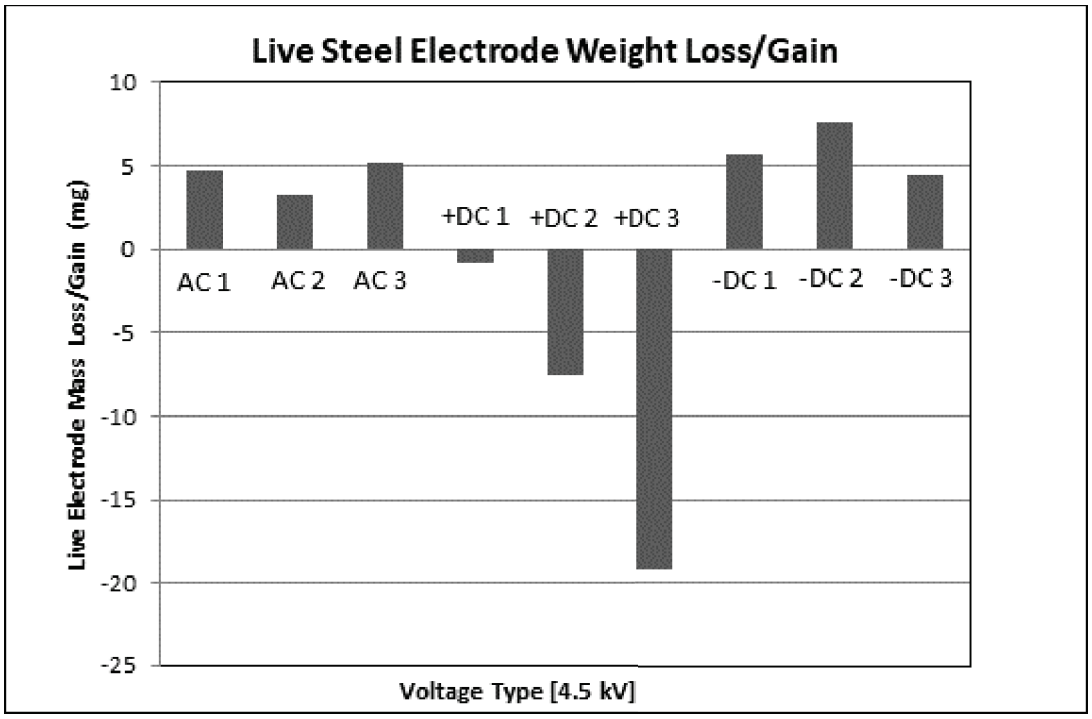

Figure 6-1: Graph showing live steel electrode weight loss/gain under AC and DC ± voltage.

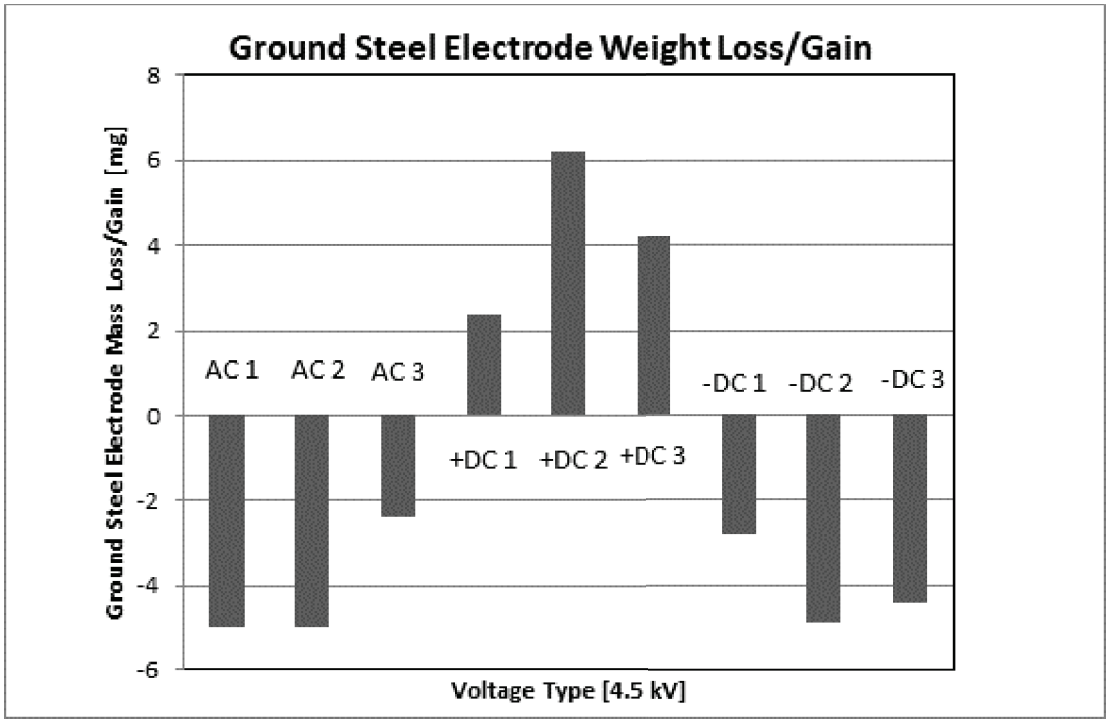

Figure 6-2: Graph showing ground steel electrode weight loss/gain under AC and DC ± voltage.

For each voltage type, 3 samples were tested using steel electrodes. It is important that these results be considered in conjunction with the length of time for each of the tests. Under AC energisation, all

3 samples lasted for the full duration of the test (i.e. 360 minutes). All 3 live electrodes exhibited weight gain in the region of 3 to 5 mg. The ground electrodes in turn showed weight loss of between 2.5 and 5 mg.

Under DC + energisation, all 3 live electrodes exhibited a weight loss. The first DC + sample was only energised for a period of 85 minutes, at which time the test had to be stopped due to burning of the SR test sample. This would explain the relatively small mass loss of 0.8 mg for the live electrode. The second test lasted slightly longer at 105 minutes and the extent of live electrode erosion was more evident, recording a mass loss of 7.6 mg. The third test was energised for the full 6 hours and a live electrode mass loss of 19.2 mg was recorded, which correlates to that observed in [16]. With the loss in weight of the live electrodes, the corresponding ground electrodes all displayed an increase in weight at the end of the test ranging from 2 to 6 mg.

Visually, the extent of electrode erosion during the third DC + test can be seen in Figure 6-3. Sample 1, which was tested using steel electrodes, displayed a dark brown residue covering the entire surface area where electrical activity was present. By contrast, sample 2, which was tested using carbon glass electrodes, shows no residue, except for whitening of the material as a result of burning.

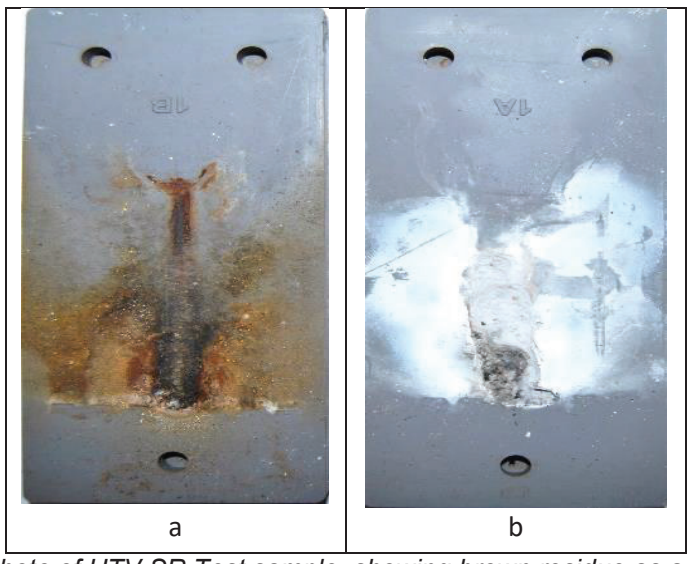

Figure 6-3: Photo of HTV SR Test sample, showing brown residue as a result of electrode erosion due to electrolysis (a) and whitening of SR material (b).

Under DC – energisation, the live steel electrodes showed a weight gain ranging from 4.4 to 7.6 mg, with the ground electrodes displaying weight losses in the region of 2.8 to 4.9 mg. All three DC - tests lasted for the full duration of 6 hours.

The effect of electrolysis on electrode degradation under DC + energisation is clearly shown by the results of the third DC test, which lasted the full 6 hours. The recorded mass loss of 19.2 mg for the live steel electrode is roughly 3 times that which was recorded for the other tests. It would thus be reasonable to assume that had the first two tests lasted for the full 6 hours, similar statistics in terms of mass loss for the live electrode would have been observed. For DC – tests, the measured mass loss of the ground electrodes, albeit to a lesser extent than during the DC + test, also confirms the effect of electrolysis on ground electrode degradation under DC – energisation. Interestingly, when comparing Figures 6-1 and 6-2, the pattern of mass gain/loss for AC and DC – tests show remarkable similarity.

6.2.2 What is the Effect of Electrode Erosion on HTV SR Material Performance Under DC Energisation During the IPT?

The assumption at the beginning of this research was that the erosion of steel electrodes during the DC IPT would have a marked effect on material performance and that substituting carbon glass for steel would result in the test being less severe, particularly under DC +. However, observing the material degradation in the form of erosion depth and area for the various tests, and the time taken for this to occur, shows this not to be the case.

Figure 6-4 and Figure 6-5 shows the extent of erosion depth and erosion area on the HTV SR samples for the various voltage types, using either steel or glass electrodes. Under AC voltage, very little erosion was observed with steel electrodes and close to zero was observed when testing with carbon glass.

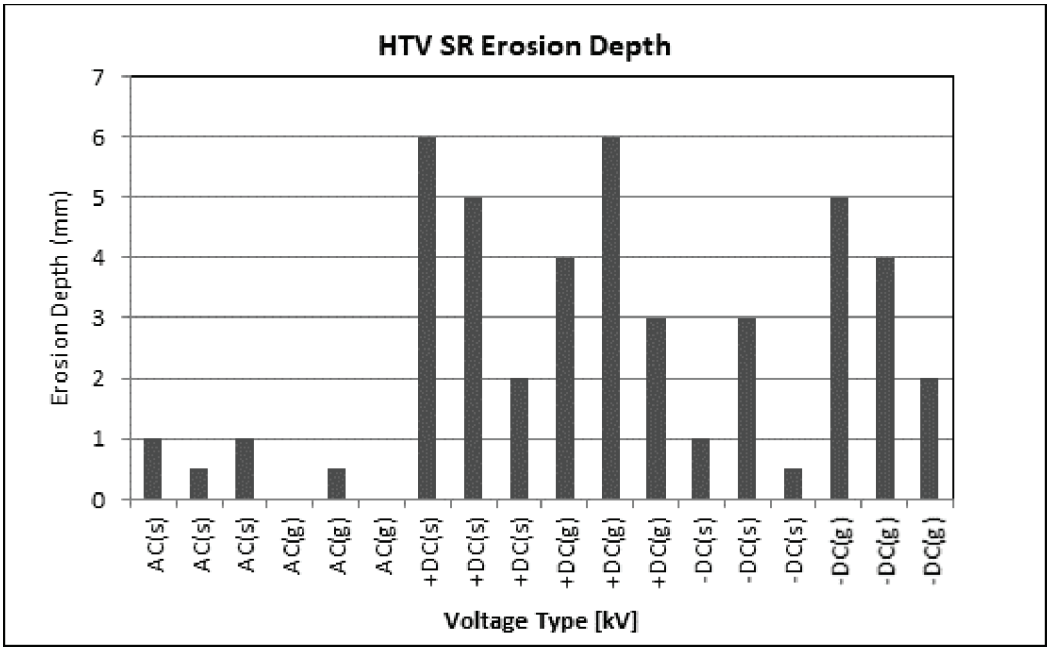

Figure 6-4: Graph showing HTV SR erosion depth under AC and DC ± voltage.

The DC + test was found to be harsh in terms of SR erosion with both steel as well as glass electrodes. Generally, the extent of erosion depth and area was found to be similar for both electrode materials.

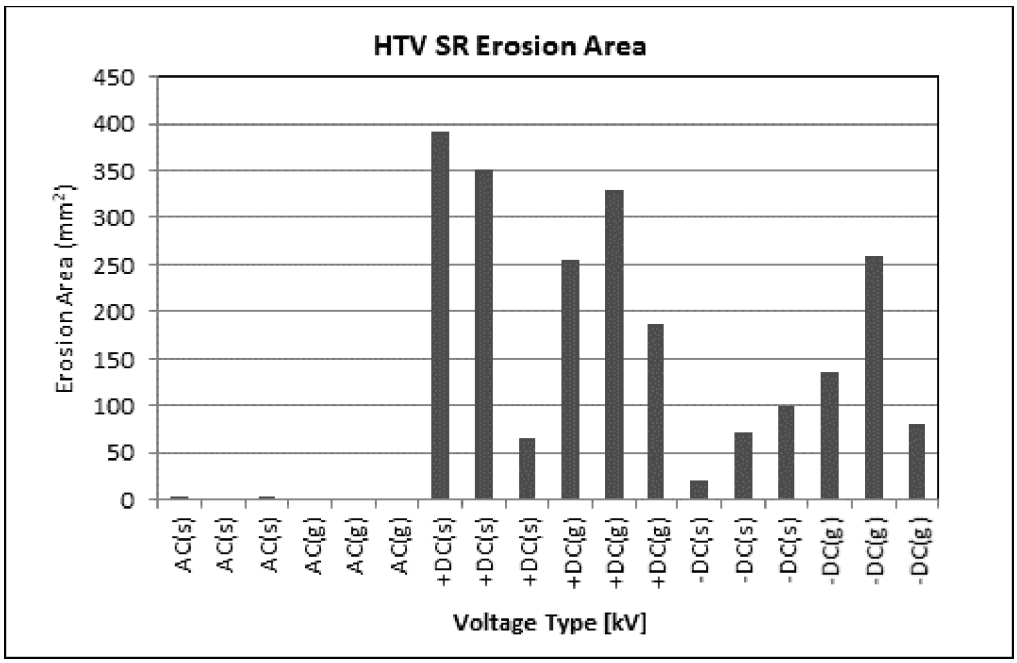

Figure 6-5: Graph showing HTV SR erosion area under AC and DC ± voltage.

The time to erosion, ignition and subsequent failure (shown in table 6-1) was found to be substantially shorter for tests with carbon glass electrodes as opposed to those with steel electrodes.

Under DC – energisation, erosion depth and area were found to be more severe for tests with carbon glass electrodes. All three tests with steel electrodes lasted the full duration of 6 hours, with steel electrodes under DC – voltage, whereas with carbon glass, failure occurred during the mid to latter part of the test.

The research question pertaining to the effect of electrode erosion on material performance could not be answered from these tests, as the substitution of carbon glass for steel, as an electrode material seems, to have introduced additional dynamics resulting in the test being even more aggressive.

6.2.3 How can Electrode Erosion in the IPT be Eliminated?

In order to eliminate electrode erosion during the IPT, particularly under DC energisation, testing, using an alternative electrode material in the form of carbon glass, was undertaken. At the end of these tests, visual examinations were conducted on the glass electrodes, as well as weights measured, to determine the extent of degradation. The visual observations are detailed in sections 5.2.1.2, 5.3.1.2 and 5.4.1.2 of Chapter 5, and in general, show that the carbon glass electrodes do not degrade under both AC and DC testing, except for instances where cracking of the live electrodes occurred under DC + energisation. The cracking of all three live electrodes during the DC + tests indicates a possible thermal inefficiency of the particular carbon glass material that was utilised. Figure 6-6 and Figure 6-7 show the measured weight differences for the glass electrodes at the end of both the AC and DC tests.

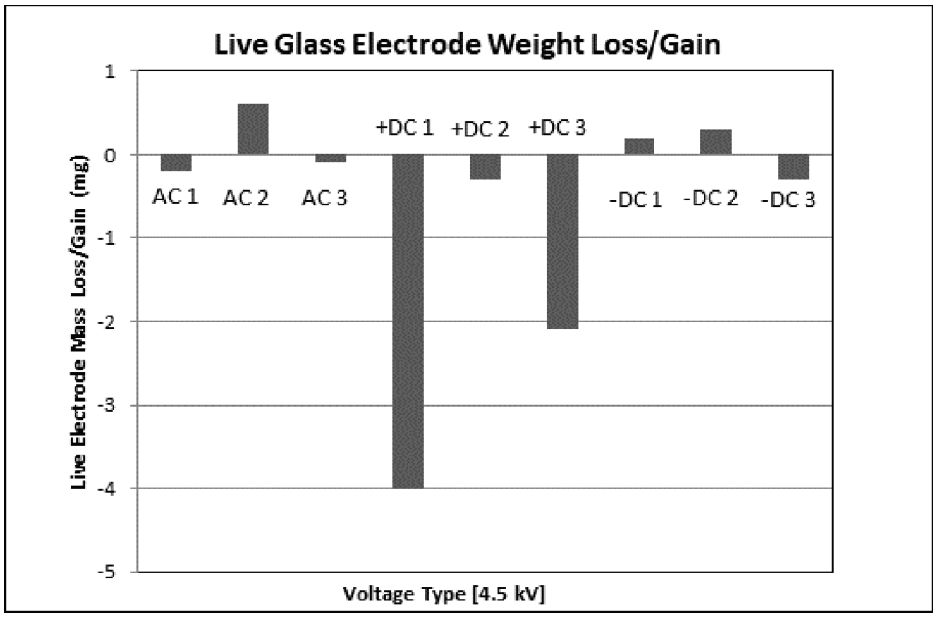

Figure 6-6: Graph showing live glass electrode weight loss/gain.

The larger weight loss at the end of the DC + tests could be attributed mainly to the cracking of the electrodes. Slight weight loss was also noted for two of the AC tests as well as the one DC -test. Visually, the live electrode from DC test 3 exhibited a colour change, which could indicate possible change in the material properties resulting in the weight loss observed.

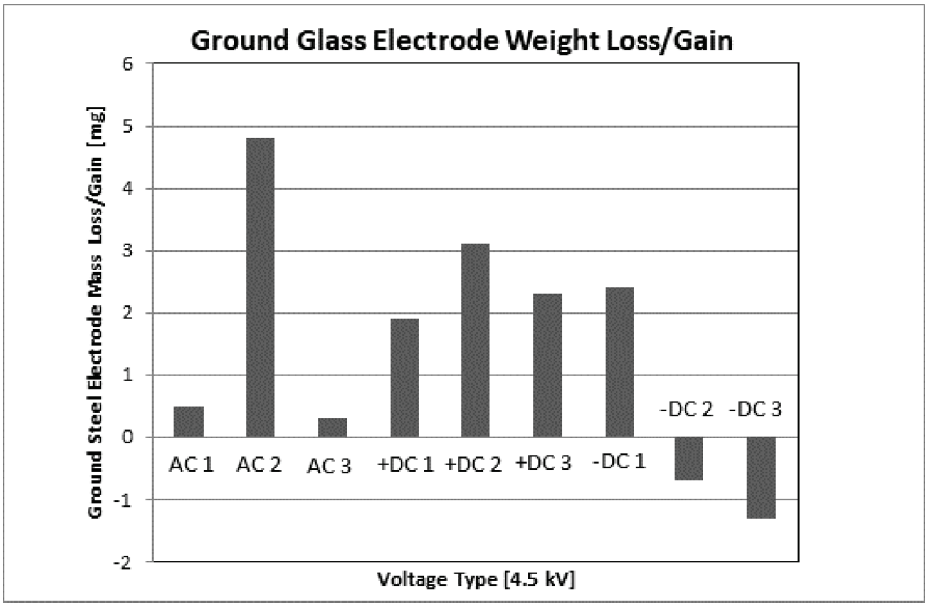

Figure 6-7: Graph showing ground glass electrode weight loss/gain.

All carbon glass ground electrodes exhibited weight gain, except for two subjected to DC -. The weight gain can be attributed, in part, to the residue that formed on most of the ground electrodes, particularly under DC + energisation, where burning of the SR material occurred.

By comparing HTV SR visual observations of the tests conducted with steel electrodes, to those utilising carbon glass, it is clearly seen that the dark brown residue evident on many of the tests using steel electrodes, has been eliminated by using carbon glass. This is particularly evident for the DC + tests. As such, these tests show that the use of an appropriate alternate electrode material, such as carbon glass, could provide a means to eliminate steel electrode erosion as a result of electrolysis during the DC IPT. It should be noted that for future work, carbon glass electrodes with a higher thermal conductivity, should be utilised.

6.2.4 To what Extent will the Repeatability of the DC IPT Improve if the Electrode Erosion is Eliminated?

Table 6-1 shows the time to failure (T_f) for samples tested with combinations of steel and glass electrodes under both polarities DC. Consistent with literature, the DC + test using steel electrodes was found to be severe in terms of material degradation, with failure in the form of burning occurring early in two of the three tests. For DC -, all three tests utilising steel electrodes ran for the full test period of 6 hours

Table 6-1: Time to failure (T_f) for samples with steel vs glass electrodes under DC ± voltage.

	Time to Failure (T_f) min	
Voltage Type	Steel Electrodes	Glass Electrodes
DC + 1	85	75
DC + 2	105	31
DC + 3	360	42
DC - 1	360	210
DC - 2	360	165
DC - 3	360	235

Although the use of carbon glass electrodes seems to have eliminated the problem of steel electrode erosion as a result of electrolysis during the DC test, a much higher failure rate was recorded using the glass electrodes. Of the six tests done with steel electrodes, two failed as a result of burning. Of the six tests done with glass electrodes, five failed as a result of burning. The T_f with glass electrodes was substantially shorter than what was recorded using steel. It is postulated that the carbon glass electrodes utilised in this study, do not have the same thermal conductivity as the steel electrodes, leading to increased surface temperature during static DBA and subsequent material breakdown. As such, the use of the carbon glass electrodes in this study did not improve the repeatability of the test. Even though the aspect of electrode erosion was seemingly removed with the use of glass electrodes, the effect on material performance was much more severe. For future work, the thermal properties of substitute electrodes need to be analysed in comparison to the standard steel electrodes.

6.2.5 What other Test Parameters Influence Repeatability of the DC IPT?

As discussed in section 2.4.5, the leakage current flowing across the surface of an insulator is largely determined by the resistance of the electrolytic pollution layer [1]. The resistance of the electrolytic pollution layer is a function of the resistivity of the contaminant solution as well as the area available for current flow as per equation 2.1 in section 2.5.5 and shown again below.

$$R_{pol} = \frac{\rho\, L_{CD}}{A} \qquad 5.1$$

In the context of the IPT, IEC 60587 specifies that standard samples measuring 50mm X 120 mm are utilized, hence the L_{CD} is always kept constant. Similarly, the contaminant is specified to have a resistivity of 3.95 Ωm at 23°C. Hence the only variable is the cross-sectional area of the electrolytic pollution layer, determined by the flow rate of the contaminant. Increasing the flow rate results in an increased cross-sectional area, leading to a decrease in surface resistance and subsequent increased surface leakage current.

As discussed in section 2.4.3, tracking and erosion occurs as a result of stable DBA and the associated heating effects thereof. For the IPT, there is an optimum flow rate that will result in the most tracking and erosion. A flow rate that is too high will result in high leakage current, leading to flashover, but will not allow for drying of the insulator surface and associated DBA. A flow rate that is too low will not be able to sustain the leakage current required to cause damage.

For the purposes of this research programme, the test apparatus was designed to provide a fixed contaminant flow rate of 0.6 ml/min. This flow was achieved using a peristaltic pump drawing contaminant from a 500 ml container and feeding it into a reservoir comprised of eight layers of filter paper placed between the test specimen and the live electrode holder. Prior to feeding the contaminant into the filter paper reservoir, the flow rate was confirmed by measuring the amount of contaminant deposited into a syringe over a period of 5 minutes. This equalled 3 ml, confirming a

contaminant flow rate of 0.6 ml/min. The electrode holders are attached to the test sample and a perspex backing plate via two sets of nuts and bolts as shown in Figure 6-8.

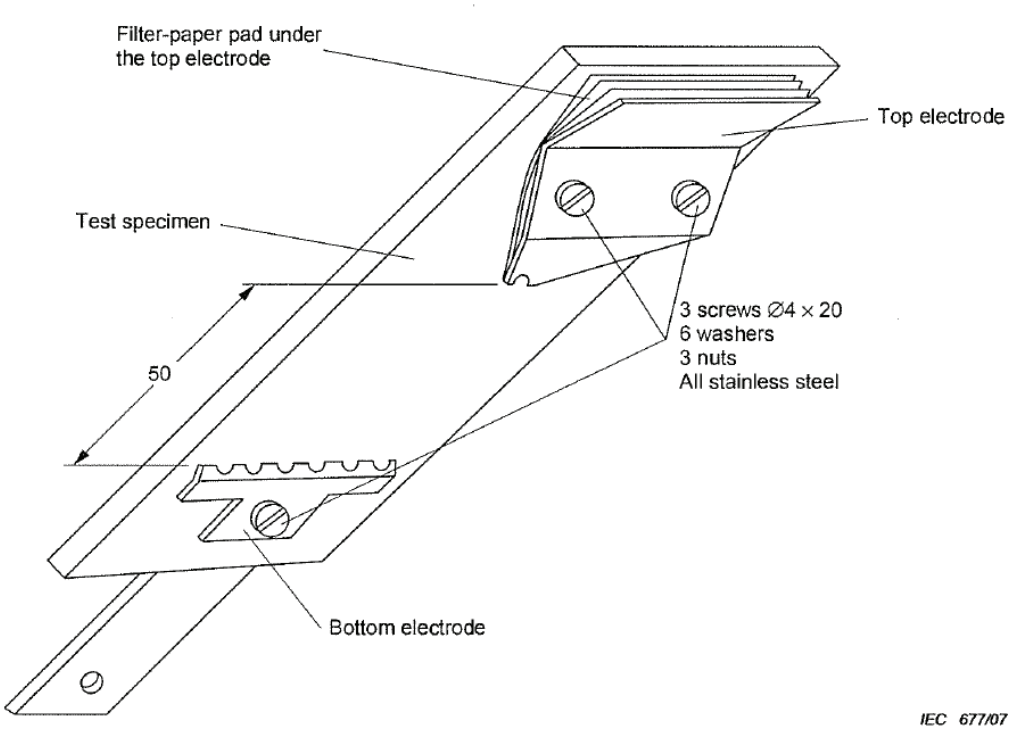

Figure 6-8: Attachment of live electrode to test sample with filter paper reservoir in-between [8].

The test procedure does not stipulate the extent to which these bolts must be tightened, except to state that uniform flow between the top and bottom electrodes shall occur before voltage application. The extent to which the bolts are tightened on the top electrode, affects the flow of contaminant from the filter paper reservoir. This test programme found that the resultant flow of contaminant across the test sample, was often difficult to control and was non-uniform when compared across the various tests that were done.

Figure 6-9 (shown in section 5.2.1.3.2 as well) shows the visual difference in contaminant flow rate for the AC test conducted with steel (a) and glass (b) electrodes. The flow on sample 1 decreased 50 minutes into the test and ceased at 70 minutes, necessitating suspension of the test so that the flow could be re-established.

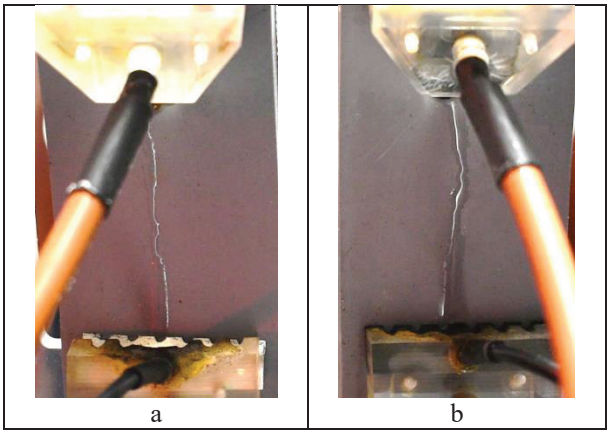

Figure 6-9: Photo of contaminant flow during early stages of AC test on sample 1 with steel electrodes and sample 2 using carbon glass electrodes.

A common difficulty with establishing continuous flow with many of the tests was the occurrence of the contaminant flowing from the filter paper reservoir onto the electrode holder and then dripping past the sample onto the drip tray below. This happened predominantly at the beginning of the tests, but was also found to occur during the latter stages as well, necessitating stoppage and realignment of the electrode holder and filter paper reservoir. It was observed that the dimensions of the filter paper had a huge impact on the flow of contaminant through the small hole at the tip of the electrode. If the paper was not properly aligned, flow would either cease or be diverted to the side of the electrode and onto the electrode holder. The result of this is that even though the contaminant flow rate is carefully controlled via the peristaltic pumps into the filter paper reservoir, it is very difficult to ensure that the same flow rate is delivered through the filter paper reservoir and onto the test sample in a consistent manner for each test that is conducted. As contaminant flow has a major impact on the dynamics of leakage current and DBA, which in turn affects material performance, the inability to accurately control contaminant flow is seen as a possible shortcoming with the current test setup, and a possible cause for lack of repeatability, not only with DC tests but AC as well.

6.3. Conclusions

From the test results it was shown that energisation under DC + voltage produced the most severe degradation and damage during the IPT. This was followed by DC – energisation, with AC voltage producing the least severe damage. This concurs with literature.

The results showed that under DC + energisation, substantial erosion of the top live electrodes took place as a result of electrolysis. This resulted in significant weight loss for the top electrodes as they become anodic and weight gain for the ground electrodes (cathode). With the process of electrolysis, Fe is expelled into the contaminant and becomes clearly visible on the surface of the test material. The cathodic reaction at the ground electrode gives rise to Fe_2O_3, commonly known as iron oxide or rust. As the molecular weight of iron ore is higher than that of steel, the formation of iron oxide on the ground electrode results in a slight weight gain. This process is reversed under DC – energisation, and the results obtained in terms of weight loss/gain confirm this.

In order to determine if electrode erosion in the IPT could be eliminated, an alternate electrode material in the form of carbon glass was utilised. The carbon glass electrode fulfilled this objective in that it proved to be inert and not subject to the effect of electrolysis. This was confirmed by visual observations of samples tested with glass electrodes which showed no residue on the surface during or after the tests. In addition, weight loss/gain measurements showed the carbon glass electrodes to be stable, with any weights changes being as a result of electrode breakage, or where SR material remained attached to the electrodes after the test.

The question of what the effect of steel electrode erosion is on material performance could not be answered from this research. Although the introduction of the carbon glass electrodes served the purpose of eliminating steel electrode erosion, it seemed to have introduced other dynamics which resulted in the test being radically more severe. Using the glass electrodes, the same pattern of DC + being the most severe, followed by DC – and then AC was observed. Erosion depth and erosion area was found to be in general greater with the glass electrodes and time to failure, where such occurred,

was much quicker with glass than with the steel electrodes. It is postulated that the carbon glass electrodes utilised in this study had lower thermal conductivity than the steel electrodes, leading to increased surface temperature on the HTV SR material during static DBA and subsequent material breakdown. Stainless steel roughly has a thermal conductivity of 14.4 W / m K, whereas standard glass and carbon have thermal conductivities of 1.05 and 1.7 W / m K respectively [48]. As such, the use of the carbon glass electrodes in this study did not improve the repeatability of the test. Even though the aspect of electrode erosion was removed with the use of glass electrodes, the effect on material performance was much more severe. For future work, the thermal properties of substitute electrodes need to be analysed in comparison to the standard steel electrodes.

One of the IEC failure criteria is leakage current in excess of 60 mA. None of the samples on test failed this criteria, however it was observed that samples tested with carbon glass electrodes exhibited lower leakage currents than those tested with steel electrodes. For DC + tests, the higher leakage currents with steel electrodes could possibly be explained as a result of the introduction of ions into the contaminant, resulting from steel electrode erosion caused by electrolysis. This would result in increased contaminant conductivity and subsequent increased leakage currents. However, the same phenomena of lower leakage currents for samples tested with carbon glass electrodes was observed for AC as well as DC – tests. This would indicate that the composition of the electrode material may have an influence on the level of leakage current.

What was observed during this work was that one of the biggest factors affecting the possible repeatability of the IPT, whether done under AC or DC, is the difficulty in ensuring a uniform and constant contaminant supply, according to the stipulated flow rate. The use of 8 layers of filter paper as a contaminant reservoir, wedged between the electrode holder and the test sample, presents challenges in ensuring repeatability of flow. It was difficult to establish flow at the beginning of most tests, with constant adjustments needed and this extended to flow issues being experience mid test as well.

6.4. Limitations of this study

Conclusions drawn from this work are done so bearing in mind certain limitations, and as such, these results pertain to this work and should not be generalized without extensive further testing and research. These limitations are:

- Only one type of HTV SR material, with a filler content of 51 %, was utilised for all the tests.
- There was a limited number of tests that could be performed within the research period.
- Tests were conducted at one voltage level of 4.5kV for both AC and DC, and at one flow rate of 0.6 ml/min.

6.5. Recommendations

The following recommendations are proposed for future work:

- The use of an alternate electrode material that is not susceptible to erosion and degradation under DC energisation, with identical thermal and electrical properties to that of the standard stainless steel electrodes.
- Electroplating or galvanizing of the standard steel electrodes to prevent electrolysis.
- Investigate alternative methods of introducing and controlling contaminant flow during the test.

References

[1] W. L. Vosloo, R. E. Macey and C. de Tourreil, The Practical Guide to Outdoor High Voltage Insulators, Johannesburg: Crown Publications, 2004.

[2] “IEC,” IEC, [Online]. Available: https://www.iec.ch/about/activities/?ref=menu. [Accessed 20 November 2020].

[3] “IEC TC 36,” IEC, [Online]. Available: https://www.iec.ch/public/miscfiles/sbp/36.pdf. [Accessed 20 November 2020].

[4] IEC 62217, “Polymeric HV insulators for indoor and outdoor use – General definitions, test methods and acceptance criteria,” IEC, Paris, 2012.

[5] IEC 60507, “Artificial pollution tests on high voltage insulators to be used on a.c. systems,” IEC, Paris, 1991.

[6] IEC 61109, “Composite insulators for a.c. overhead lines with a nominal voltage greater than 1000 V - Definitions, test methods and acceptance criteria,” IEC, Paris, 1992.

[7] IEC 61302, “Electrical insulating materials - Methods to evaluate the resistance to tracking and erosion - Rotating wheel dip test,” IEC, Paris, 1995.

[8] “IEC 60587 Electrical Insulating Materials used under sever ambient conditions – Test methods for evaluating resistance to tracking and erosion,,” IEC, 2007.

[9] P. Naidoo, R. D. Estment, D. Muftic and N. Ijumba, “Progress report on the investigations into the recycling of existing HVAC power transmission circuits for higher power transfers using HVDC technology,” in *IEE International Conference AC-DC Power Transmission*, Savoy Place, London, UK, 2006.

[10] J. M. Seifert, D. Stefanini and H. Janssen, “HTV Silicone Composite Insulators for HVDC Applications – Long Term Experience with Material and Design for 500kV and above,” in *16th International Symposium on High Voltage Engineering,*, Johannesburg, South Africa.

[11] Cigre WG 22 03, “Worldwide experience with HV composite insulators,” *Electra 130,* pp. 68-77, May 1990.

[12] R. A. Ghunem, S. H. Jayaram and E. A. Cherney, “Statistical Indicators of Silicone Rubber Erosion in the DC Inclined Plane Test,” in *Conference on Electrical Insulation and Dielectric Phenomena*, Montreal, Canada, 2012.

[13] R. A. Ghunem, S. H. Jayaram and E. A. Cherney, “Erosion of Silicone Rubber Composites in the AC and DC Inclined Plane Tests,” *IEEE Transactions on Dielectrics and Electrical Insulation,* vol. 20, no. 1, 2013.

[14] R. A. Ghunem, S. H. Jayaram and E. A. Cherney, “The DC Inclined-Plane Tracking and Erosion Test and the Role of Inorganic Fillers in Silicone Rubber for DC Insulation,” *IEEE Electrical Insulation Magazine,* pp. Vol 31, No 1, pages 12 – 21, January 2015.

[15] G. Heger, H. J. Vermeulen and W. L. Vosloo, “Evaluation of the performance of HTV Silicone Rubber exposed to AC & DC surface discharges using the Incline Plane Test,” in *16th International Symposium on High Voltage Engineering,*, Johannesburg, South Africa, 2009.

[16] G. P. Bruce, S. M. Rowland and A. Krivda, “DC Inclined-plane testing of silicone rubber formulations,” *Annual Report Conference on Electrical Insulation Dielectric Phenomena,* pp. 1-4, 2010.

[17] G. P. Bruce, S. M. Rowland and A. Krivda, “Performance of Silicone Rubber in DC Inclined Plane Tracking Tests,” *IEEE Transactions on Dielectrics and Electrical Insulation,* vol. 17, no. 2, 2010.

[18] D. Windmar, I. Gutman and J. Jonsson, “HVDC Pollution Testing of Insulation: Experience from Service, Laboratory and Test Station,” *IEEE Transactions on Dielectrics and Electrical INsulation,* vol. 21, no. 6, 2014.

[19] T. Sorqvist and A. E. Vlastos, “Outdoor Polymeric Insulators Long Terms Exposed to HVDC,” *IEEE,* 1996.

[20] T. G. Gustavsson, S. M. Gubanski, H. Hillborg, S. Karlsson and U. W. Gedde, “Ageing of Silicone Rubber under AC or DC Voltages in a Coastal Environment,” *IEEE Transactions on Dielectrics and Electrical Insulation,* vol. 8, p. 1029, 2001.

[21] G. N. .. Mouton, “An evaluation of different material line insulators under High Voltage AC and Bipolar DC Excitation in a marine polluted environment,” University of Stellenosch, 2012.

[22] W. L. Vosloo and R. L. Swinny, “Koeberg Insulator Pollution Test Station,” *Wattnow Magazine,* pp. 37-49, May 2013.

[23] A. I. Elombo, J. P. Holtzhausen, H. J. Vermeulen and P. J. Pieterse, “Comparitive evaluation of the leakage current and aging performance of HTV SR insulators of different creepage lengths when energised by AC, DC + or DC - in a severe marine environment,” *IEEE Transactions on Dielectrics and Electrical Insulation,* vol. 20, no. 2, 2013.

[24] W. L. Vosloo, R. L. Swinny and T. D. Mvayo, “Experience and lessons learned from testing composite insulators in South Africa,” *Insulator News and Markert Report (INMR),* 2007.

[25] R. S. Gorur, E. A. Cherney and R. Hackam, “The AC and DC performance of polymeric insulating materials under accelerated aging in a fog chamber,” *IEEE Transactions on Power Delivery,* vol. 3, no. 4, 1998.

[26] R. S. Gorur, E. A. Cherney and R. Hackam, “Polymer insulator profiles evaluated in a fog chamber,” *IEEE Transactions on Power Delivery,* vol. 5, no. 2, 1990.

[27] S. Bossi, A. Pigini, G. P. Fini, A. Porrino, Channakeshava, N. Vasudev, M. Ramamoorty and R. Reali, “Study of the performance of composite insulators in polluted conditions,” in *Cigre Conference paper 33-104*, 1994.

[28] A. Pigini, R. Cortina, M. Marzinotto and G. Lagrotteria, “Pollution tests on composite insulators: the Italian experience,” in *The 19th Symposium on High Voltage engineering*, Pilsen, Czech Republic, 2015.

[29] Y. Yu, L. Xidong, Z. Yuannxian and L. Xuesong, “Study of tracking wheel test method under DC voltage,” in *7th Internation conference on properties and applications of dielectric materials*, Nagoya, 2003.

[30] S. B. Limbo, H. J. Vermeulen, W. L. Vosloo, P. Pieterse and J. P. Holtzhausen, “Aging Performance of EPDM and HTV SR Insulators for HVAC and HVDC Excitation using the Tracking Wheel Test,” in *16th International Symposium on High Voltage Engineering*, Johannesburg, 2009.

[31] STRI Guide, “Hydrophobicity Classification Guide,” STRI LAB, Ludvika, Sweden, 1992.

[32] J. P. Holtzhausen, P. J. Pieterse, H. J. Vermeulen and S. Limbo, “Insulator aging tests with HVAC and HVDC excitation using the tracking wheel tester,” *IEEE Transactions on Dielectrics and Electrical insulation,* 2010.

[33] ASTM standard D2303-13, “Standard test methods for liquid contaminant, inclined plane tracking and erosion of insulating materials,” ASTM.

[34] R. A. Ghunem, S. H. Jayaram and E. A. Cherney, “Inclined Plane Initial Tracking Voltage for AC, +DC and –DC,” in *IEEE International Symposium on Electrical Insulation (ISEI)*, San Juan, 2012.

[35] R. A. Ghunem, S. H. Jayaram and E. A. Cherney, “Suppression of Erosion due to Dry-Band Arcing under DC by Alumina Tri-hydrate Filler in Silicone Rubber,” in *Annual Report Conference on Electrical Insulation and Dielectric Phenomena*, 2013.

[36] R. A. Ghunem, S. H. Jayaram and E. A. Cherney, “Dynamics of Dry-Band Arcing on Silicone Rubber in the Inclined Plane Test under AC, +DC and –DC Voltages,” in *IEEE 2014 Annual Report Conference on Electrical Insulation and Dielectric Phenomena.*.

[37] R. A. Ghunem, S. H. Jayaram and E. A. Cherney, “Suppression of Silicone Rubber Erosion by Alumina Tri-hydrate and Silica Fillers from Dry-Band Arcing under DC,” *IEEE Transactions on Dielectrics and Electrical Insulation,* vol. 22, no. 1, 2015.

[38] E. A. Cherney, R. A. Ghunem, S. H. Jayaram, R. S. Gorur, A. Krivda, S. M. Rowland, S. Li, M. Marzinotto and I. Ramirez, “DC Inclined-Plane Tracking and Erosion Test of Insulating Materials,” *IEEE Transactions on Dielectrics and Electrical Insulation,,* vol. 22, no. 1, 2015.

[39] G. Heger, H. J. Vermeulen, J. P. Holtzhausen and W. L. Vosloo, “A Comparative Study of Insulator Materials Exposed to High Voltage AC and DC Surface Discharges,” *IEEE Transactions on Dielectrics and Electrical Insulation,* vol. 17, no. 2, 2010.

[40] J. Crespo-Sandoval, A. Haddad, H. Griffiths and P. F. Coventry, “Rate of Energy Absorption as Indicator for the Tracking/Erosion Test of Silicone Rubber,” *IEEE Transactions on Dielectrics and Electrical Insulation,* vol. 17, no. 6, 2010.

[41] L. H. Meyer, E. A. Cherney and S. H. Jayaram, “The Role of Inorganic Fillers in Silicone Rubber for Outdoor Insulation – Alumina Tri-Hydrate or Silica,” *IEEE Electrical Insulation Magazine,* July 2004.

[42] L. Meyer, S. Jayaram and E. A. Cherney, “Thermal Conductivity of Filled Silicone Rubber and its Relationship to Erosion Resistance in the Inclined Plane Test,” *IEEE Transactions on Dielectrics and Electrical Insulation,* vol. 11, no. 4, 2004.

[43] S. Kumagai and N. Yoshimura, “Tracking and erosion of HTV Silcone Rubber and suppression mechanism of ATH,” *IEEE Transactions on Dielectrics and Electrical Insulation,* vol. 11, no. 4, 2001.

[44] R. A. Ghunem, S. H. Jayaram and E. A. Cherney, “Comparative Inclined Plane Tests on Silicone and EPDM Elastomers under DC,” in *Electrical Insulation Conference*, Ottawa, Ontario, Canada, 2013.

[45] DL/T 810-2002, “Electrical Power Industry Standard of the Peoples Republic of China, Technical Specification of +/- 500 kV D.C. Composite Long Rod Insulators”.

[46] Cigre WG D1.27, “Feasibility study for a DC tracking and erosion test,” Cigre, 2015.

[47] W. L. Vosloo, A comparison of the performance of High Voltage insulator materials in a severely polluted envkironment - PhD Thesis, Cape Town: University of Stellenbosch, 2002.

[48] “www.engineeringtoolbox.com,” [Online]. Available: https://www.engineeringtoolbox.com/thermal-conductivity-metals-d_858.html. [Accessed 7 December 2020].

[49] S. M. Rowland, G. P. Bruce, L. Yuting, A. Krivda and L. E. Schmidt, “Use of Image Analysis in DC Inclined Plane Tracking Tests of Nano and Micro Composites,” *IEEE Transactions on Dielectrics and Electrical Insulation,* vol. 18, no. 2, 2011.

[50] J. P. Holtzhausen, “A critical evaluation of AC pollution flashover models for HV insulators having hydrophilic surfaces - PhD Thesis,” University of Stellenbosch, 1977.

Annexure A: Inclined Plane Test Methodology followed

Date._____ Start Time_____ End Time_____

Contaminant Conductivity_____ Temp_____/_____ Humidity_____/_____

Test Voltage_____/_____ Electrode Configuration_____/_____

Video recording no_____ Electrode Mass (g) (1)_____ (2)_____

Sample Mass (g) (1)_____ (2)_____

Sample preparation.

1	Mark sample with unique test number (date and test position) on surface not subject to test.
2	Clean surface with ethyl alcohol to remove all debris.
3	Take photos of samples. Note photo numbers in table 1
4	Weigh the test sample and record in table 3.

Sample tests

1	Measure and note the relative humidity (% RH) Temperature (°C) and record above
2	Measure contaminant solution conductivity and record above.
3	Check which HV test is required. (Positive DC, Negative DC or AC) change the links in the supply transformer accordingly.
4	Determine electrode type to be used for each test channel and record above
5	Weigh live and ground electrode and record in table 4
6	Fit sample and electrodes into test position.
7	Check for uniform flow of contaminant over test specimen
8	Close test cabinet doors making sure door interlocks operating
9	Check earth removed from transformer supply
10	Open resistor earth capacitor discharge switch
11	Switch on supply and adjust variac output on control panel until correct test voltage is obtained.
12	Document test voltage at beginning of test period and record above
13	Start the timer and fill in start time above
14	Commence video recording of test samples and document video number
15	Check leakage current logger to ensure that data is being recorded
16	Monitor sample under test to be sure that it isn't flashing over burning etc. if anything is wrong
17	Switch off test supply by pressing emergency stop button on control panel

Test Run Completed

1	Note time of end of test
2	Turn down variac and switch off supply to control panel.

3	Close resistor switch to discharge capacitors
4	Earth transformers output supply.
5	Open cabinet door and remove test sample.
6	Reweigh the insulator test samples and record in table 3
7	Do visual inspections on test samples and record in table 3
8	Reweigh the electrodes and record in table 4
9	Do visual inspections on electrodes and record in table 4
10	Take photos of tested samples and electrodes and record in table 2

Table 1: Photo Records before test

Sample Number.	Material Type	Photo Numbers on Camera	
		Start Pic number	End Pic number
SR Sample 1			
SR Sample 2			
Electrode 1 Live			
Electrode 1 Earth			
Electrode 2 Live			
Electrode 2 Earth			

Table 2: Photo records after test

Sample Number.	Material Type	Photo Numbers on Camera	
		Start Pic number	End Pic number
SR Sample 1			
SR Sample 2			
Electrode 1 Live			
Electrode 1 Earth			
Electrode 2 Live			
Electrode 2 Earth			

Table 3: Observation on SR Test Samples

	Time to Tracking	Time to Erosion	Total time tested	Weight before test	Weight after test	Weight difference	Pass/Fail	Failure Mode	I_L end of test
SR Sample 1									
SR Sample 2									

Table 4: Observations on Steel and Glass Electrodes

	Material Type	Extent of Erosion	Weight before test	Weight after test	Weight difference
Electrode 1 Live					
Electrode 1 Earth					
Electrode 2 Live					
Electrode 2 Earth					

Notes / Comments etc.